

Pair condensation in the Bose-Hubbard Model: a path integral analysis

Agata Krzywicka

Ph.D. dissertation prepared under the advisorship of
prof. UAM dr hab. inż. Tomasz Polak

Condensed Matter Theory Division
Institute of Spintronics and Quantum Information, Faculty of Physics
Adam Mickiewicz University, Poznań, Poland



September 20, 2023

Abstract

Two bosonic pairing mechanisms with different sources are studied within the quantum rotor method of the path integral formulation. Firstly, interaction-based pairing is derived from density-induced tunnelling, the first-order correction to the Bose-Hubbard model, which stems from many body correlations and contributes significantly to hopping in bosonic systems especially. The pair condensate term is additionally transformed into dissipative in two approaches: assumed, where the pair fraction is treated as the environment and coupled harmonically to the single particle system, and derived, where the dissipation is internal. The second pairing mechanism is correlation-based, generated by the second order expansion of the standard Bose-Hubbard correlator. Both pair effective phase models take the form of an extended Quantum Phase model. The difference lies in the single and pair condensation coefficients, which depend nontrivially on the Bose-Hubbard parameters, as well as imaginary time. Imaginary time dependence emerges in different coefficients in the interaction-based and the correlation-based models. The properties of the pair condensate and its effect on single particle condensation in both effective phase models are compared. In both cases, the pair fraction strengthens the single particle condensate phase, increasing its critical temperature.

Contents

1	Introduction	9
1.1	The Bose-Hubbard model	12
1.1.1	General second quantisation Hamiltonian	13
1.1.2	Density-induced tunnelling	15
1.2	Methodology	17
1.2.1	Quantum rotor method	18
1.2.2	$S = 1$ pseudospin mapping	19
1.2.3	Self-consistent harmonic approximation	22
1.2.4	Quantum spherical mapping	24
1.3	Orbital magnetic effects	27
1.3.1	Phase models with bosonic pairing	28
2	Interaction-based pairing	31
2.1	Model	31
2.1.1	Effective phase model	34
2.2	$S = 1$ pseudospin mapping	38
2.3	Thermodynamics	39
2.4	Conclusions	43
3	Dissipative interaction-based pairing	45
3.1	Phase model	46
3.1.1	Coefficients	47
3.2	Dissipative models	49

3.3	Spherical mapping and critical line equation	50
3.4	Results	52
3.4.1	Analytical limits for parameter range	52
3.4.2	Analytical properties of the full correlator	53
3.4.3	Numerical comparison between the derived and assumed models	54
3.5	Conclusions	59
4	Correlation-based pairing	61
4.1	Model	62
4.2	Effective phase model	63
4.2.1	Self-consistent harmonic approximation	64
4.3	Thermodynamics of the effective model	66
4.4	Conclusions	69
5	Comparison of pairing mechanisms	71
5.1	Effective phase models	72
5.1.1	Correlation-based coefficients	72
5.1.2	Interaction-based coefficients	72
5.2	Results	74
5.3	Conclusions	79
5.3.1	Self-consistent harmonic approximation vs. $S = 1$ pseudospin	80
	Appendices	83
A	Interaction-based pairing: calculations	85
A.1	Quantum rotor derivation	88
A.1.1	Gauge transformation	91
A.1.2	Nambu-like matrix form	93
A.1.3	Trace calculations	96
A.1.4	Effective phase model	104
A.2	Pseudospin mapping	105

B	Dissipative interaction-based pairing: calculations	109
B.1	Coefficients	110
B.1.1	Derivation of imaginary time coefficients	111
B.2	Dissipative models	113
B.2.1	Preparing dissipative effective action	114
B.3	Quantum spherical mapping	116
B.4	Evaluating the correlator	123
B.4.1	Full correlator	125
B.5	Critical line equation	128
C	Correlation-based pairing: calculations	131
C.1	Quantum rotor derivation	131
C.1.1	Gauge transformation	133
C.1.2	Approximating the trace	136
C.2	Self-consistent harmonic approximation	140
C.2.1	Calculating the trial phase average	144
D	Magnetic density of states: analytical formulas	151
D.1	$f = 1/2$	151
D.2	$f = 1/3$	152
D.3	$f = 1/4$	152
D.4	$f = 1/6$	153
E	Related publications	155

Chapter 1

Introduction

It is common knowledge today that fermions form Cooper pairs in superconductors. The question naturally follows: do bosons form pairs of their own? Is there a condensate of bosonic pairs, lurking within or nearby the well-known single particle Bose-Einstein condensate (BEC)? If there is, how do the two phases interact? What effect would pairing have on the behaviour of strongly correlated bosonic systems in low temperatures?

The question of whether or not bosons forms pairs has been answered in the affirmative in experiments. Optical lattice experiments have allowed to observe single particle Bose-Einstein condensates using various methods, such as time-of-flight images [17], trap squeezing [51, 55], or multiband spectroscopy [9]. The condensed phase is identifiable as interference peaks, or a global compressibility of the atomic cloud. Bosonic pairs with anti-correlated momenta have been detected within optical lattices by Tenart et al. [60], in the depletion of an equilibrium interacting helium IV gas in the high density and strongly-interacting regime. The fraction of correlated particle pairs coexists with the macroscopically occupied condensate ground state. The probe was sensitive enough to detect quantum many body correlations (MBC). However, only large momenta were investigated, precluding detailed analysis of the effect of temperature on the pair condensate. It would also have been impossible in those experiments to increase a specific interaction, such as density-induced tunnelling. Observation of pair condensates is a new and challenging subject, as precise control is required over multiple parameters. There is much yet to be discovered about boson pairs.

Now that we know bosonic pairing can be measured, we wish to find out what physical phenomena it might stem from. Optical lattice-related studies tend to assume a Hamiltonian with chosen parameters and study its properties. The source and nature of the assumed interactions and coefficients are not a concern. This is possible due to the high customisability of optical lattices, which can act as quantum simulators. Our venture into the sources of bosonic pairing mechanisms goes beyond assumptions and strives to explicitly derive the relevant terms and their coefficients. The quantum rotor method [46] within the path integral formulation makes such derivations possible, albeit not simple.

In Chapter 2, we expand the standard Bose-Hubbard model (BHM) by adding the density-induced tunnelling term, the interaction with the biggest energy contribution, and the one most likely to significantly affect the total tunnelling [39]. An interaction-based bosonic pairing term appears in the effective phase model. The properties of this pair condensed phase are examined in relation to the single particle condensate.

Once a bosonic pairing mechanism has been derived, the next question is: how does the pair fraction affect the single particle condensate? In other words, what are we missing if we simplify a model past the point where many body correlations are allowed to contribute? Pair condensates seem to be in two minds, either strengthening or depleting the single particle superfluid depending on parameter range. Interestingly, in effective phase models, the terms responsible for pairing, when approximated to second order, are mathematically very similar to dissipative terms, as in Caldeira and Leggett, 1981 [6]. The similarity is especially clear if the pairing term coefficient contains imaginary time in the form $(\tau - \tau')^{-2}$.

Dissipative behaviour is usually generated by coupling the original system with external degrees of freedom. Driven-dissipative many body systems have been realised experimentally by coupling trapped ultra-cold atoms to the optical modes of a laser-driven dispersive cavity [49, 48, 29, 68, 15, 37]. An increase of interest in theoretical descriptions of such systems has followed. Counterintuitively, within the right parameter range, dissipation can enhance coherence and entanglement [44, 43, 2, 10, 24, 1, 59]. This stabilisation leads to a wealth of interesting phenomena, including emergent phase transitions, many body pair coherent states, and novel mode competition and symme-

try breaking. In two-photon driven bosonic lattice models, the dissipative steady states can be found exactly [50]. A two particle loss term can increase correlations to the point of effectively inhibiting dissipation altogether [28]. In high T_c superconductors, non-local dissipative bosonic mediators can act coherently and increase the superconducting critical temperature T_c [56]. The stabilising effect of dissipation can also facilitate experimental observation of non-equilibrium and exotic states, such as superfluid time crystals [27, 26, 8, 54]. Bosonic pairs, or doublons, have been studied in systems with loss, including three-body losses, which can be used to realise effective three-body interactions [40, 5]. The complex nature of driven-dissipative many body models means that it is not possible to fully describe them using methods that do not account for quantum fluctuations and information on the spatial distributions of individuals [57]. Therefore, up to now, the body of work has consisted mainly of relatively limited approaches, such as few body systems and one-dimensional studies [53, 20, 63]. Furthermore, for all the new and interesting phenomena that have already been observed, dissipation has consistently been treated as an external factor.

Chapter 3 is dedicated to exploring what the constructive effect of dissipation on correlations means for the relation between single and pair condensates. The $S = 1$ pseudospin mapping is exchanged for the more robust spherical model. The interaction-based pairing phase term is expanded to second order and treated as dissipative, in order to better understand the effect of the pair condensate on the standard BEC. This leads to a system where dissipation is not imposed by additional, external terms, but emerges from the intrinsic interactions themselves. We reveal a different facet of dissipative behaviour: one that is an implicit property of a strongly correlated model with extended interactions. It is known that dissipation can generate effective many body interactions. We show that the opposite is also possible: many body interactions can themselves be a source of dissipative behaviour. To verify the behaviour of this internal dissipation, results are compared to an assumed model, based on the same derivation but obtained in the standard way, in which the pair condensate is separated from the original system and treated as an external bath, coupled harmonically to the single particle condensate.

Even when systems of strongly interacting bosonic gases are forced into simple

interactions, many body correlations do still occur and affect their behaviour [12, 11, 58]. Any phenomena that might stem from MBCs warrant a closer look. In Chapter 4, therefore, we look for bosonic pairing within the correlations of the Bose-Hubbard model itself. We take a deeper look into the standard model and find a pair condensation term, which depends on imaginary time, in the second order series expansion of the correlator. The self-consistent harmonic approximation (SCHA) is used to study the effect of this correlation-based pair fraction on the single particle BEC.

Finally, the two derived pairing mechanisms are compared under the SCHA in Chapter 5. We show how orbital magnetic effects can be applied to facilitate differentiating between the two pairing mechanisms.

Chapters 2-5 focus on the physics and results rather than mathematical details. Detailed derivations of effective phase models and further approximations leading to the presented results are gathered in Appendices A-C.

1.1 The Bose-Hubbard model

The Hubbard model is a fundamental quantum many body model which represents an interacting gas trapped in an external potential. The interactions are short range, between nearest neighbouring lattice sites only. The model was originally intended for describing the behaviour of strongly correlated electrons in solids. However, conveniently, its bosonic counterpart turned out to be extremely well suited for the description of ultracold atoms in optical lattices [16]. A sinusoidal external potential represents an optical lattice framework, which means there is a direct relation between the amplitude, frequency and relative phases of the counterpropagating laser beams that constitute the lattice and the parameters of the model [13], as well as lattice geometry [65].

Optical lattices generate precisely controllable experimental conditions in simple geometries. The particles of a cooled gas are forced to only exhibit simple interactions, allowing their study in an essentially defect free environment using a plethora of methods and approximations [22, 31, 62, 7, 36, 14, 61, 41, 18, 3]. Among those, however, there has not been many studies focused on density dependent interactions [25, 42]. Density-induced tunnelling has been shown to contribute significantly to single particle

tunnelling and thus affect the condensate phase, especially in bosonic systems [14].

The Hamiltonian of the Bose-Hubbard model is

$$\hat{H} = \frac{U}{2} \sum_i \hat{n}_i (\hat{n}_i - 1) - t \sum_{\langle i,j \rangle} \hat{a}_i^\dagger \hat{a}_j - \mu \sum_i \hat{n}_i, \quad (1.1)$$

where $\langle i, j \rangle$ identifies a summation over nearest neighbouring sites and:

- $\hat{a}_i^\dagger, \hat{a}_i$ are the bosonic coherent creation and annihilation operators, respectively;
- $\hat{n}_i = \hat{a}_i^\dagger \hat{a}_i$ is the boson number operator on site i ;
- $U > 0$ is the on-site repulsive interaction between two particles;
- t is the exchange integral for single particle tunnelling between neighbouring lattice sites;
- μ is the chemical potential.

The BHM is an approximation of the general second quantisation model of a strongly interacting bosonic gas in a sinusoidal external potential, where only the two terms with the largest energy contributions are preserved. Extended BHMs are obtained by adding one or more of the omitted terms back into the Hamiltonian. [32]

1.1.1 General second quantisation Hamiltonian

The second quantisation many-body Hamiltonian describing a gas of N interacting bosons in an external potential V_{ext} is

$$\begin{aligned} \hat{H}(t) = & \int d\mathbf{r} \hat{\Psi}^\dagger(\mathbf{r}, t) \left[-\frac{\hbar^2}{2m} \nabla^2 + V_{ext} \right] \hat{\Psi}(\mathbf{r}, t) + \\ & + \frac{1}{2} \int d\mathbf{r} d\mathbf{r}' \hat{\Psi}^\dagger(\mathbf{r}, t) \hat{\Psi}^\dagger(\mathbf{r}', t) V(\mathbf{r} - \mathbf{r}') \hat{\Psi}(\mathbf{r}, t) \hat{\Psi}(\mathbf{r}', t), \end{aligned} \quad (1.2)$$

with bosonic creation and annihilation field operators $\hat{\Psi}^\dagger(\mathbf{r}, t)$ and $\hat{\Psi}(\mathbf{r}, t)$, respectively. We consider only on-site and nearest neighbour interactions. Three body interaction terms and higher can be added as additional potential terms as needed.

In the absence of long range interactions, the field operators can be expanded in a tight-binding approximation into a basis of orthonormal Wannier functions:

$$\hat{\Psi}(\mathbf{r}, t) = \sum_i \hat{a}_i w_i(\mathbf{r}), \quad (1.3)$$

where \hat{a}_i is the bosonic annihilation operator for the i -th lattice site. The Wannier functions w_i are orthonormal and localised around lattice sites, indicated by the minima of the external potential V_{ext} ; they decay exponentially outside of the i -th site [21].

Since interactions between particles in cold bosonic gases are dominated by s -wave scattering, the two-particle interaction potential can be treated as an isotropic contact pseudopotential with s -wave scattering length a_s [4]:

$$V(\mathbf{r} - \mathbf{r}') = \frac{4\pi\hbar^2 a_s}{m} \delta(\mathbf{r} - \mathbf{r}') = g \delta(\mathbf{r} - \mathbf{r}'), \quad (1.4)$$

where m is the atomic mass. In lattice coordinates $\mathbf{r} \rightarrow \mathbf{r}/a$, the interaction integral in Eq. (1.2) can be rewritten in the form

$$V_{ijkl} = \frac{8a_s}{\pi a} \int d\mathbf{r} w_i^*(\mathbf{r}) w_j^*(\mathbf{r}) w_k(\mathbf{r}) w_l(\mathbf{r}) \quad (1.5)$$

and then divided into specific interactions.

Thus, the on-site two-particle repulsive interaction for a contact potential is

$$U = gE_R \int d\mathbf{r} |w_i(\mathbf{r})|^4, \quad (1.6)$$

the nearest neighbour interaction is

$$V = E_R (V_{ijij} + V_{ijji}), \quad (1.7)$$

density-induced tunnelling, or the bond-charge interaction is

$$J_{BC} = -E_R \frac{(V_{iijj} + V_{ijji})}{2}, \quad (1.8)$$

and the nearest neighbour pair tunnelling is

$$J_{pair} = E_R V_{ijj}. \quad (1.9)$$

These amplitudes depend on nothing but the properties of Wannier functions and $E_R = \hbar^2/8ma^2$.

In the case of a sinusoidal potential V_{ext} , the full Hamiltonian in the Wannier function basis is

$$\begin{aligned} \hat{H} = & -J \sum_{\langle i,j \rangle} \hat{a}_i^\dagger \hat{a}_j + \frac{U}{2} \sum_i \hat{n}_i (\hat{n}_i - 1) + \frac{V}{2} \sum_{\langle i,j \rangle} \hat{n}_i \hat{n}_j + \\ & -J_{BC} \sum_{\langle i,j \rangle} \hat{a}_i^\dagger (\hat{n}_i + \hat{n}_j) \hat{a}_j + \frac{J_{pair}}{2} \sum_{\langle i,j \rangle} \hat{a}_i^{\dagger 2} \hat{a}_j^2, \end{aligned} \quad (1.10)$$

where additionally

$$J = - \int d\mathbf{r} w_i^*(\mathbf{r}) \left[-\frac{\hbar^2 \nabla^2}{2m} + V_{ext} \right] w_j(\mathbf{r}) \quad (1.11)$$

is the isotropic exchange integral for single particle tunnelling between adjacent sites, designated t in Eq. (1.1) and in further chapters. The significance of each of the terms in Eq. (1.10) has been illustrated in Fig. 1.1.

1.1.2 Density-induced tunnelling

It is clear in Fig. 1.1 that density-induced tunnelling, J_{BC} , is responsible for the largest energy contribution outside of the two standard Bose-Hubbard terms, U and J . The effects of DIT have been discussed in fermionic systems [19]; however, since bosons are not constrained by the Pauli principle, it follows that this interaction-assisted mobility will have more bearing on bosonic systems.

Exemplary zero-temperature phase diagrams between the two BHM ground states, superfluid and Mott insulator, are shown in Fig. 1.2 with and without DIT. The presence of density-induced tunnelling strengthens the superfluid, with the insulator-suppressing effects increasing with particle density. The variational method, however,

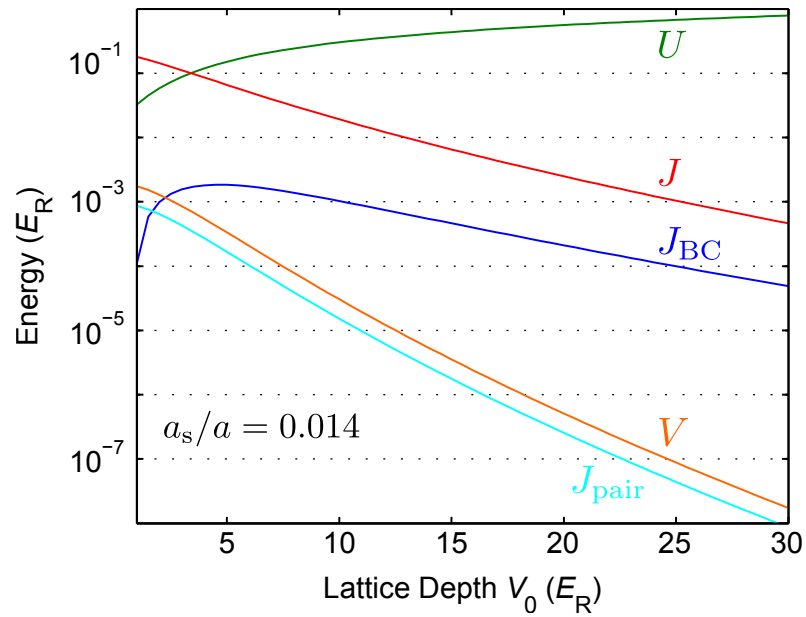


Figure 1.1: *Dependence on optical lattice depth of the lowest-band parameters of various terms of the extended Bose-Hubbard model: on-site interaction U , tunnelling J , bond-charge or density-induced tunnelling J_{BC} , correlated pair-tunnelling J_{pair} , density-density interaction V . Source: [39]*

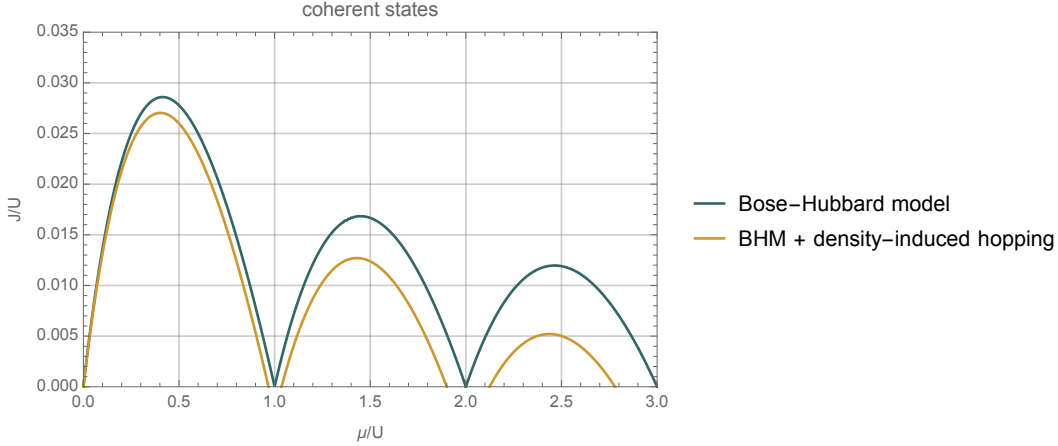


Figure 1.2: *Mean field zero-temperature Mott insulator-superfluid phase diagram without and with density-induced tunnelling ($J_{BC}/U = 0.004$), calculated in the coherent state basis using the variational method. Source: [32]*

is too oversimplified for analysing density-dependent processes. Only the three lowest energy states within the coherent state basis are taken into account; many body correlations (MBC) are not preserved whatsoever. While sufficient as a first glimpse at the density-induced tunnelling interaction, more accurate methods able to take into account MBCs are necessary to truly understand its effect on the standard system.

1.2 Methodology

In the path integral formulation, quantum operators are substituted by complex fields in the coherent state basis. This allows to introduce continuous effective statistical functions, starting with the partition function, which is defined by the effective action. Extremely precise analytical calculations can be carried out on microscopic models within this framework. In the particular case of quadratic models, the partition function takes the elegant form of a multi-dimensional Gaussian integral. The goal is thus usually to transform and, if necessary, approximate a given model to a quadratic form.

The coherent state basis in path integrals introduces overcompleteness. There is more information within the partition function than is needed to fully describe a system.

Therefore, there are two important steps to any path integral study: firstly, to recognise what in a chosen model is important information and what is clutter; secondly, to make sure any transformations carried out on the model preserve the former and decrease the latter. The choice of methods and approximations has great bearing on what results are possible to be obtained. Sometimes an approximation seems obviously helpful, but later on turns out to have barred access to correlations responsible for the very phenomena we were looking to analyse.

Below are listed the methods used in further chapters, along with short descriptions of the applications they were chosen for. Details on where and how exactly these methods were used are shown in Appendices A-C, which contain step by step calculations.

1.2.1 Quantum rotor method

The $U(1)$ quantum rotor method is the basis of all path integral calculations in this work, in Chapters 2-4. Since bosonic fields are complex, they are comprised of two factors: amplitude b and phase ϕ . The quantum rotor method relies on the assumption that the bosonic phase $\phi(\tau)$ provides all pertinent information about dynamics, while the amplitude is set as constant. In the case of the standard Bose-Hubbard model, the Quantum Phase Model can be derived [46].

We start with the partition function in the complex coherent state basis,

$$\mathcal{Z} = \int \{\mathcal{D}\bar{a}\mathcal{D}a\} e^{-\mathcal{S}[\bar{a},a]}, \quad (1.12)$$

where \mathcal{S} is the effective action,

$$\mathcal{S}[\bar{a}, a] = \int_0^\beta d\tau \left[\sum_i \bar{a}_i(\tau) \frac{\partial}{\partial \tau} a_i(\tau) + \mathcal{H}(\tau) \right], \quad (1.13)$$

which contains the complex field form of the Hamiltonian, \mathcal{H} . The strategy in any path integral study is to decouple any terms above quadratic in the effective action \mathcal{S} , Eq. (1.13). In the case of strongly correlated bosons, the first step is the Hubbard-

Stratonovich transformation, which decouples the on-site two particle interaction term,

$$e^{-\frac{U}{2} \sum_i \int d\tau n_i^2(\tau)} = \int \frac{dV}{2\pi} e^{-\sum_i \int d\tau \left[\frac{V_i^2(\tau)}{2U} - iV_i(\tau)n_i(\tau) \right]}. \quad (1.14)$$

This introduces an effective electrochemical potential field, V , which looks similar to a mean field. The potential V is dynamic and site-dependent, however, meaning the Hubbard-Stratonovich transformation is exact.

A gauge transformation,

$$a_i(\tau) = b_i(\tau) e^{i\phi_i(\tau)}, \quad (1.15)$$

is also performed, to separate phase from amplitude. The quadratic bosonic amplitude terms constitute a Gaussian integral, which carried out is equal to the trace of the logarithm of the model's correlator G :

$$\int \{ \mathcal{D}\bar{b}_i \mathcal{D}b_i \} e^{-\int_0^\beta d\tau \bar{b}_i G b_i} = \int_0^\beta d\tau \det G = e^{\int_0^\beta d\tau \text{Tr} \ln(G)^{-1}}. \quad (1.16)$$

At this point, ϕ is the only imaginary time-dependent variable in the partition function. The original model is thus replaced by an effective phase-only model, with the contribution from the bosonic amplitudes kept within the correlator G . The quantum rotor method preserves the same information on many body correlations and spatial distributions of individual particles as the original Hamiltonian, either in the phase fields or in the bosonic correlator.

The path integral formulation provides overcomplete systems. A model must be narrowed down to the areas of interest of a given study, within specific parameter ranges and limits. What information can be obtained depends on the methods and approximations chosen in further calculations, to analyse the effective phase model.

1.2.2 $S = 1$ pseudospin mapping

The $S = 1$ pseudospin model is relevant to phase ordering in granular superconductors [64] and systems of spin-charge separated stacks of condensates interacting via interplane Josephson coupling [30], which mathematically can be further related to

Josephson junction arrays. The quantum phase fields are transformed into classical spin operators. This allows to preserve some correlations under a mean field approximation of the pseudospin exchange term.

We start out with a phase-only Hamiltonian, such as the Quantum Phase Model (QPM):

$$H = U \sum_i N^2 - \sum_{\langle i,j \rangle} \varepsilon_1 \cos(\phi_i - \phi_j). \quad (1.17)$$

The eigenstates of the bosonic number operator,

$$\langle k | N(\phi) | m \rangle = \int_0^{2\pi} \frac{d\phi}{2\pi} e^{-ik\phi} \left(\frac{1}{i} \frac{\partial}{\partial \phi} \right) e^{im\phi} = m \delta_{k,m}, \quad (1.18)$$

can be used to define trigonometric functions of phase:

$$\langle k | \cos \phi | m \rangle = \int_0^{2\pi} \frac{d\phi}{2\pi} e^{-i(k-m)\phi} \cos \phi = \frac{1}{2} (\delta_{k-m-1,0} + \delta_{k-m+1,0}), \quad (1.19)$$

$$\langle k | \sin \phi | m \rangle = \frac{i}{2} (\delta_{k-m-1,0} - \delta_{k-m+1,0}). \quad (1.20)$$

The number operator basis is limited in this method to its lowest-energy states, in which $k, m \in \{-1, 0, 1\}$. The phase terms can then be rewritten as $S = 1$ pseudospin operators, assuming $k_B T / U < 1$:

$$N(\phi) = S_z, \quad (1.21)$$

$$\cos \phi = \frac{1}{\sqrt{2}} S_x, \quad (1.22)$$

$$\sin \phi = \frac{1}{\sqrt{2}} S_y. \quad (1.23)$$

This transforms the quantum phase Hamiltonian into a classical spin Hamiltonian. In the case of the QPM, Eq. (1.17), the transformation is as follows:

$$H = U \sum_i N^2 - \sum_{\langle i,j \rangle} \varepsilon_1 (\cos \phi_i \cos \phi_j + \sin \phi_i \sin \phi_j) \quad (1.24)$$

$$= U \sum_i (S_i^z)^2 - \frac{1}{2} \varepsilon_1 \sum_{\langle i,j \rangle} (S_i^x S_j^x + S_i^y S_j^y). \quad (1.25)$$

The pseudo exchange term is then treated with a mean field approximation:

$$S_i^x S_j^x \approx \langle S_i^x \rangle S_j^x + S_i^x \langle S_j^x \rangle - \langle S_i^x \rangle \langle S_j^x \rangle. \quad (1.26)$$

This introduces the order parameter $\Psi = \langle S_i^x \rangle$. The pseudospin mean field Hamiltonian is

$$H_{MF} = U (S_i^z)^2 - \frac{1}{2} \varepsilon_1 S_i^x \langle S_i^x \rangle = J \left(\frac{U}{J} (S_i^z)^2 - S_i^x \Psi \right), \quad (1.27)$$

where $J = \frac{1}{2} z \varepsilon_1$.

The next step is calculating the partition function, which is based on the eigenvalues of the spin model,

$$\mathcal{Z} = \text{Tr} \{ e^{-\beta H} \} = \sum_{n=1}^3 e^{-\beta E_n}. \quad (1.28)$$

From here, the free energy per lattice site, f , can be calculated and minimised in terms of the order parameter Ψ to obtain a self-consistent equation for Ψ . Other thermodynamic functions can be derived from f as temperature derivatives. Among those, specific heat is particularly interesting, since phase transitions are easily identifiable therein by a lambda-shaped peak. It is worth remembering, however, that the final step is a mean field approximation, which erases any correlations in the system which are not transferred from phase fields to pseudospin operators.

1.2.3 Self-consistent harmonic approximation

The self-consistent harmonic approximation (SCHA) [64] is based on the variational principle, which states that, for any system characterised by effective action \mathcal{S} and free energy \mathcal{F} ,

$$\mathcal{F} \leq \mathcal{F}_0 + \frac{1}{\hbar\beta} \langle \mathcal{S} - \mathcal{S}_0 \rangle_0 = \tilde{\mathcal{F}}, \quad (1.29)$$

where \mathcal{S}_0 is the action of any chosen trial system and \mathcal{F}_0 the corresponding trial free energy,

$$\mathcal{F}_0 = -\frac{1}{\beta} \ln \mathcal{Z}_0 = -\frac{1}{\beta} \ln \int \{\mathcal{D}\phi\} e^{-\mathcal{S}_0[\phi]}. \quad (1.30)$$

The average $\langle \mathcal{S} - \mathcal{S}_0 \rangle_0$ is calculated over the trial model. For a phase model in the path integral framework, it takes the form

$$\langle \mathcal{S} - \mathcal{S}_0 \rangle_0 = \frac{1}{\mathcal{Z}_0} \int \{\mathcal{D}\phi\} \exp\left(-\frac{1}{\hbar}\mathcal{S}_0[\phi]\right) (\mathcal{S}[\phi] - \mathcal{S}_0[\phi]), \quad (1.31)$$

with the trial partition function

$$\mathcal{Z}_0 = \int \{\mathcal{D}\phi\} \exp\left(-\frac{1}{\hbar}\mathcal{S}_0[\phi]\right). \quad (1.32)$$

The strategy of variational approximations is to choose a well known trial effective action and minimise the combined free energy, $\tilde{\mathcal{F}}$, by demanding that its variation $\delta\tilde{\mathcal{F}} = 0$. The trial coefficients are calculated based on this condition and depend on the parameters of the actual system. Thus, the properties of any model can be analysed by considering the trial system in its stead.

The trial action used in the SCHA is harmonic, with stiffness K :

$$\mathcal{S}_0[\phi] = \int_0^\beta d\tau \left[\frac{1}{U} \sum_i \left(\frac{\partial\phi_i}{\partial\tau} \right)^2 + \frac{K}{2} \sum_{\langle i,j \rangle} \phi_{ij}^2 \right]. \quad (1.33)$$

The free energy variation,

$$\delta\tilde{\mathcal{F}} = \delta \left(\mathcal{F}_0 + \frac{1}{\beta} \langle \mathcal{S} - \mathcal{S}_0 \rangle_0 \right) = 0, \quad (1.34)$$

consists of two partial derivatives:

$$\left(\frac{\partial \tilde{\mathcal{F}}}{\partial K} \right)_{D_{ij}} + \left(\frac{\partial \tilde{\mathcal{F}}}{\partial D_{ij}} \right)_K \left(\frac{\partial D_{ij}}{\partial K} \right) = 0, \quad (1.35)$$

where D_{ij} the trial nearest neighbour phase-phase average, which can be derived with use of the Fourier transform, replacing the inverse lattice dependence with the density of states $\rho(\xi)$,

$$D_{ij} = \langle (\phi_i - \phi_j)^2 \rangle_0 = \frac{1}{z} \int d\xi \rho(\xi) \sqrt{\frac{(z-\xi)U}{2K}} \coth \left(\frac{\beta}{2} \sqrt{\frac{(z-\xi)KU}{2}} \right). \quad (1.36)$$

The order parameters are defined as

$$\Psi_1 = \langle \cos \phi_i \rangle = e^{-\frac{1}{2} \langle \phi_i^2 \rangle}, \quad (1.37)$$

$$\Psi_2 = \langle \cos 2\phi_i \rangle = e^{-2 \langle \phi_i^2 \rangle}. \quad (1.38)$$

The averages in Eqs. (1.37-1.38)

$$\langle \phi_i^2 \rangle = \frac{1}{2} \int d\xi \rho(\xi) \sqrt{\frac{U}{K(z-\xi)}} \coth \left(\frac{\beta}{2} \sqrt{(z-\xi)KU} \right). \quad (1.39)$$

The result of variation minimisation, Eq. (1.34), is a self-consistent equation for the trial stiffness K . Since K is a function of the coefficients of the original system, the trial system can be analysed in its stead. The density of states function $\rho(\xi)$ can be inserted in analytical form for any chosen geometry.

Much like the $S = 1$ pseudospin mapping method in Section 1.2.2, the self-consistent harmonic approximation operates on analytical formulas for free energy. As such, any

thermodynamic function can be derived from the trial free energy \mathcal{F}_0 and studied. However, the SCHA preserves specific correlations within the condensate phase. It cannot be reliably applied beyond the critical region, as it struggles to reproduce the mutable characteristics of the critical point. The ordering of the system is different in the normal phase, so the SCHA cannot be recreated using the same parameters therein. Nonetheless, the critical temperature itself is easily identifiable as the point where thermodynamic functions rapidly cut off. Instead of specific heat, we can focus on entropy, to understand how the order within the condensate changes in the presence of pairing.

1.2.4 Quantum spherical mapping

The spherical model is a spin model, characterised by the variability of the direction and absolute value of the spins. The only condition is that the latter average to 1 over the entire lattice. To ensure that, the spherical condition requires that the sum of all spins σ squared be equal the total number of spins N :

$$\sum_i \sigma_i^2 = N. \quad (1.40)$$

1.2.4.1 Quantum spherical model

The unconstrained quantum spherical model partition function is

$$\mathcal{Z} = \int_{-\infty}^{+\infty} \left[\prod_i D\sigma_i \right] \left[\frac{1}{2\pi\hbar} \prod_i D\pi_i \right] e^{-S[\sigma_i, \pi_i]/\hbar} \quad (1.41)$$

$$= \int_{-\infty}^{+\infty} \left[\prod_i D\sigma_i \right] \left[\frac{1}{2\pi\hbar} \prod_i D\pi_i \right] e^{-\frac{1}{\hbar} \int_0^{\hbar\beta} d\tau \mathcal{L}[\sigma_i, \pi_i]}, \quad (1.42)$$

with Lagrangian

$$\mathcal{L}[\sigma_i(\tau), \pi_i(\tau)] = i \sum_i \pi_i \frac{d}{d\tau} \sigma_i + U \sum_i \pi_i^2 - \sum_{\langle i,j \rangle} J_{ij} \sigma_i \sigma_j - h \sum_i \sigma_i. \quad (1.43)$$

The spherical condition, Eq. (1.40), is introduced into \mathcal{Z} by means of a Dirac delta function, which can be expanded into an integral as

$$\delta[x(\tau)] = \frac{1}{2\pi i} \int_{c-i\infty}^{c+i\infty} d\lambda e^{\int_0^{\hbar\beta} d\tau \lambda x(\tau)}. \quad (1.44)$$

This introduces a new parameter into the system: the spherical constraint λ .

The independent π term can be integrated over and the partition function takes the form

$$\begin{aligned} \mathcal{Z} = & \frac{1}{2\pi i} \sqrt{\frac{\pi^N \hbar}{U}} \int_{c-i\infty}^{c+i\infty} d\lambda e^{\hbar\beta\lambda N} \int_{-\infty}^{+\infty} \left[\prod_i D\sigma_i \right] \\ & \times e^{-\frac{1}{\hbar} \int_0^{\hbar\beta} d\tau \left[\frac{\hbar}{4U} \sum_i \left(\frac{d\sigma_i}{d\tau} \right)^2 - \sum_{\langle i,j \rangle} J_{ij} \sigma_i \sigma_j - \hbar \sum_i \sigma_i + \hbar \lambda \sum_{\langle i,j \rangle} \sigma_i \sigma_j \delta_{ij} \right]}. \end{aligned} \quad (1.45)$$

After Fourier and Matsubara transforms, the spin-dependent part of the partition function is Gaussian; the spin dependence can be integrated out. The final product is a partition function in which the single variable is the spherical constraint λ :

$$\mathcal{Z} = \frac{1}{2\pi i} e^C \int_{c-i\infty}^{c+i\infty} d\lambda e^{N\phi(\lambda)}, \quad (1.46)$$

where

$$\phi(\lambda) = \hbar\beta\lambda + \frac{1}{2N} \sum_{k,m} \ln \frac{\hbar}{\frac{\hbar}{4U} \omega_m^2 - J_k + \hbar\lambda} + \frac{1}{4\hbar^2\beta} \frac{\hbar^2}{\hbar\lambda - J_0}. \quad (1.47)$$

The partition function can be approximated at saddlepoint in terms of the spherical constraint λ .

1.2.4.2 Saddlepoint approximation

The saddlepoint approximation method is a complex plane extension of Laplace's method of approximating integrals of the form

$$\int_a^b e^{Mf(x)} dx, \quad (1.48)$$

where $f(x)$ is a twice-differentiable function and M is large. In the complex case, the integral is defined over a contour C . The approximation assumes that the neighbourhood of the maximum of the function f makes the most significant contributions to the integral.

For sufficiently large $M \rightarrow \infty$, the integral is approximated by

$$\int_a^b e^{Mf(x)} dx \approx \sqrt{\frac{2\pi}{Mf''(x_0)}} e^{Mf(x_0)}. \quad (1.49)$$

The stationary point x_0 can be found by minimising f :

$$\left[\frac{df}{dx} \right]_{x=x_0} = 0. \quad (1.50)$$

In the quantum spherical model, the integral approximation Eq. (1.49) is

$$\mathcal{Z} = \frac{1}{2\pi i} (\pi^N N)^{\frac{N}{2}} \sqrt{\frac{2\pi}{N\phi''(\lambda_0)}} \exp[N\phi(\lambda_0)], \quad (1.51)$$

where λ_0 can be calculated from

$$\frac{d\phi}{d\lambda} = 0. \quad (1.52)$$

Since free energy per site is defined as

$$\mathcal{F} = -\frac{1}{\beta N} \ln \mathcal{Z} = -\frac{1}{\beta} \phi(\lambda_0), \quad (1.53)$$

finding the stationary point λ_0 is equivalent to minimising the free energy. For λ_0 to

be the critical point, $\mathcal{F}'(\lambda)$ must be equal zero at $\lambda = \lambda_0$. This condition leads to the critical line equation, which after summation over Matsubara frequencies is

$$1 = \frac{1}{2N} \sum_k \sqrt{\frac{U}{J_0 - J_k}} \coth\left(\beta\sqrt{U(J_0 - J_k)}\right). \quad (1.54)$$

Any thermodynamic function can also be calculated along the critical line from temperature derivatives of the free energy \mathcal{F} in Eq. (1.53).

1.2.4.3 Mapping phase models

This model can be mapped onto, much like in the case of $S = 1$ pseudospin, Sec. 1.2.2. The phase terms are transformed into spin operators by the same rules, Eqs. (1.21-1.23). The quantum spherical model is more robust than the $S = 1$ case, which only considers the three lowest-energy states. To make use of the additional available information, the mean field utilised in $S = 1$ pseudospin in Eq. (1.26) is in this case replaced by a saddlepoint approximation of the spherical constraint λ , introduced in Eq. (1.44).

1.3 Orbital magnetic effects

The Peierls phase factor shifts the single particle hopping by

$$t_{ij} \rightarrow t_{ij} \exp\left(\frac{2\pi i}{\Phi_0} \int_{\mathbf{r}_j}^{\mathbf{r}_i} \mathbf{A} \cdot d\mathbf{l}\right), \quad (1.55)$$

with flux quantum $\Phi_0 = hc/e$ and elementary charge e . This corresponds to synthetic magnetic fields $\mathbf{B} = \nabla \times \mathbf{A}(\mathbf{r})$, the vector potential of which, $\mathbf{A}(\mathbf{r})$, determines the phase shift [38, 23]. Moving the phase factor from the constant hopping coefficient t into the lattice factor ξ_k allows us to introduce magnetic fields within the density of states (DOS) functions themselves. [47, 45]

These effective fields correspond mathematically to angular velocity, meaning a rapidly rotating frame can be effectively treated as an external magnetic field. Those

fields can be distinguished by their rotation period, f , known within this context as the rotation frustration parameter. Neither the sign of f nor its integer part have bearing on the properties of the system. The relevant range for f thus consists of rational values within $0 < f < 1/2$, that is $f = 1/2, 1/3, 1/4, \dots$. Within that range, analytical expressions for the magnetic density of states functions can be obtained using Harper's equation [47].

1.3.1 Phase models with bosonic pairing

In effective phase models, bosonic condensates are represented by exponents of $\phi_i - \phi_j$ for neighbouring sites i, j . If such terms contain a factor of 2, they correspond to pair condensation. Since orbital magnetic effects correspond to phase shifts and affect the density of states, a specific vector potential $\mathbf{A}(\mathbf{r})$ affects single and pair condensates differently. Two separate DOS functions must be introduced, with two frustration parameters: the single f and the pair f_2 . The relation between the two is $f_2 = 2f$, due to the factor of 2 in pairing terms.

Orbital magnetic effects are nontrivial and difficult to describe analytically. The density of states functions change; the bandwidth increases and van Hove singularities appear within. Analytical formulas for DOS functions in various magnetic fields are complex and can be found in Appendix D. Diagrams of magnetic DOS functions are shown in Fig. 1.3.

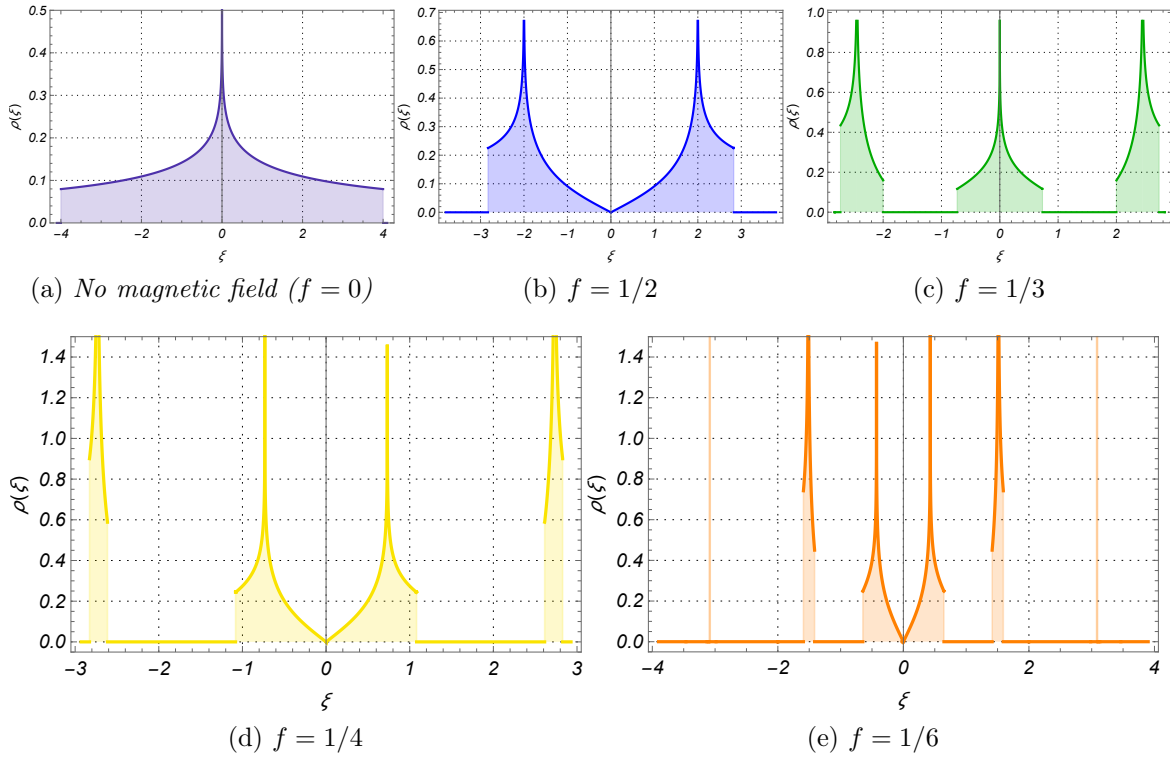


Figure 1.3: *Density of states diagrams on square lattice with various orbital magnetic effects.*

Chapter 2

Interaction-based pairing

Following the reasoning in [39], our attention turns towards density-induced tunnelling (DIT), as the interaction most likely to contribute significant alterations to hopping and bosonic condensation of all the terms not considered in the standard Bose-Hubbard model (BHM). We carry out a quantum rotor derivation to see how the DIT term changes the effective phase model compared to the standard BHM case [46]. We know that DIT strengthens the single particle superfluid in zero temperature, as shown in Section 1.1.2. We are now interested in the effect it has on Bose-Einstein condensation at non-zero temperatures, as well as whether it generates additional phase terms.

To avoid clutter, detailed calculations for this chapter can be found in Chapter A.

2.1 Model

We start with the extended Bose-Hubbard model Hamiltonian with density-induced tunnelling:

$$\begin{aligned} \hat{H} = & \frac{U}{2} \sum_i \hat{n}_i (\hat{n}_i - 1) - \frac{t}{2} \sum_{\langle i,j \rangle} \left(\hat{a}_i^\dagger \hat{a}_j + \hat{a}_j^\dagger \hat{a}_i \right) - \mu \sum_i \hat{n}_i + \\ & - J_{DIT} \sum_{\langle i,j \rangle} \left[\hat{a}_i^\dagger (\hat{n}_i + \hat{n}_j) \hat{a}_j + \hat{a}_j^\dagger (\hat{n}_i + \hat{n}_j) \hat{a}_i \right], \end{aligned} \quad (2.1)$$

where

- $U > 0$ is the on-site repulsion,
- t is the isotropic hopping integral,
- μ is the chemical potential,
- J_{DIT} is the density-induced tunnelling amplitude, designated J_{BC} in Section 1.1.

The Hamiltonian is rewritten to resemble the standard BHM, Eq. (1.1), as follows:

$$\hat{H} = \frac{U}{2} \sum_i \hat{n}_i^2 - J \sum_{\langle i,j \rangle} \hat{a}_i^\dagger \hat{a}_j - \sum_{\langle i,j \rangle} \tilde{\mu}_{ij} \hat{n}_i, \quad (2.2)$$

with the coefficients

$$J = t - 2J_{DIT}, \quad (2.3)$$

$$\tilde{\mu}_{ij} = \bar{\mu} + 4J_{DIT} \hat{a}_i^\dagger \hat{a}_j, \quad (2.4)$$

$$\bar{\mu} = \frac{U}{2} + \mu - 2J_{DIT}. \quad (2.5)$$

At this point, the path integral formalism is introduced. After Hubbard-Stratonovich and gauge transformations, the path integral partition function is

$$\mathcal{Z} = \int \{\mathcal{D}\bar{b}\mathcal{D}b\} \int \mathcal{D}\phi e^{-\mathcal{S}_b[\bar{b},b]} e^{-\mathcal{S}_\phi[n,\phi]}, \quad (2.6)$$

where the bosonic amplitude and phase effective action terms are, respectively,

$$\mathcal{S}_b = \int_0^\beta d\tau \sum_{\langle i,j \rangle} \left\{ \bar{b}_i(\tau) g_{ij}^1 b_j(\tau) + g_{ij}^2 [\bar{b}_i(\tau) b_j(\tau)]^2 \right\}, \quad (2.7)$$

$$\mathcal{S}_\phi = \sum_i \int_0^\beta d\tau \left\{ \frac{1}{2U} [\dot{\phi}_i(\tau)]^2 - \frac{\tilde{\mu}}{iU} \dot{\phi}_i(\tau) \right\}, \quad (2.8)$$

where the bosonic coefficients in Eq. (2.7) are

$$g_{ij}^1 = \delta_{ij} \frac{\partial}{\partial \tau} - (t - 2J_{DIT}) e^{-i\phi_{ij}(\tau)} - \frac{4\beta\bar{\mu}}{U} J_{DIT} e^{-i\phi_{ij}(\tau)}, \quad (2.9)$$

$$g_{ij}^2 = -\frac{8\beta}{U} J_{DIT}^2 e^{-i2\phi_{ij}(\tau)}, \quad (2.10)$$

and $\phi_{ij}(\tau) = \phi_i(\tau) - \phi_j(\tau)$.

The similarity to an extended Quantum Phase Model (QPM),

$$\mathcal{H} = J_1 \sum_{\langle i,j \rangle} \cos(\phi_{ij}) + J_2 \sum_{\langle i,j \rangle} \cos(2\phi_{ij}), \quad (2.11)$$

is identifiable in terms dependent on both $e^{-i\phi_{ij}(\tau)}$ in the linear coefficient in Eq. (2.9) and $e^{-i2\phi_{ij}(\tau)}$ in the quadratic coefficient in Eq. (2.10). The exponents can be rewritten respectively as cosine and double cosine terms. The single cosine term appears in the standard QPM, Eq. (1.17), and describes the superfluid phase. The double cosine term corresponds to pair condensation. In contrast to the single hopping, t , which contributes linearly to the single particle condensation term, the double phase exponent in Eq. (2.10) is proportional to the second power of the density-induced amplitude J_{DIT} : $g_{ij}^2 \sim J_{DIT}^2$.

The impact of density-induced tunnelling on the single particle condensate is already visible in the bosonic linear coefficient, g_{ij}^1 , Eq. (2.9), which contains two parts dependent on the DIT amplitude J_{DIT} . These two terms generate two contrasting effects on the Bose-Einstein condensate. On the one hand, density-induced tunnelling reduces single particle condensation with an amplitude $2J_{DIT}$, which shifts the single hopping t . On the other hand, however, is the last term in g_{ij}^1 , which strengthens the BEC at low temperatures and high densities. In the whole range of temperatures, DIT tends to have a dissipative effect on the original system, an effect similar to the presence of three-body correlations in optical lattice systems [25]. At high densities and low temperatures, however, DIT works in favour of the superfluid phase.

The pair-extended Quantum Phase model is assumed to consist of two independent parts with constant single and pair amplitudes J_1 and J_2 . However, as it turns out,

J_1 and J_2 are neither constant nor independent. They can even depend on imaginary time, or temperature. With the proper derivation of coefficients in QPM-related studies, the convenience of assumed models can be grounded in the actuality of a microscopic model.¹

Up to this point, the transformations are exact. The next steps require applying approximations that will lead to a phase-only effective model.

2.1.1 Effective phase model

To obtain a quadratic form in the bosonic action \mathcal{S}_b , Eq. (2.7), we make use of Wick's theorem, splitting the quadruple term into quadratic terms which contain bosonic averages:

$$\sum_{\langle i,j \rangle} b_i^\dagger b_i^\dagger b_j b_j \simeq \sum_{\langle i,j \rangle} \left[\langle b_j b_j \rangle b_i^\dagger b_i^\dagger + \langle b_i^\dagger b_i^\dagger \rangle b_j b_j + \left(4 \langle b_i^\dagger b_j \rangle + \delta_{ij} \right) b_i^\dagger b_j \right]. \quad (2.12)$$

At this point, the bosonic field terms in \mathcal{S}_b can be brought together as a quadratic Gaussian integral:

$$I = \int \{ \mathcal{D}\bar{b}_i \mathcal{D}b_i \} \exp \left\{ - \int_0^\beta d\tau \sum_{\langle i,j \rangle} [\bar{b}_i(\tau) S_{ij} b_j(\tau) - \Delta_j \bar{b}_i \bar{b}_i - \bar{\Delta}_i b_j b_j] \right\} \quad (2.13)$$

$$= \int \{ \mathcal{D}\bar{b}_i \mathcal{D}b_i \} \exp \{ -\mathcal{S}_{eff} \}, \quad (2.14)$$

¹Cf. A. Krzywicka, T. P. Polak, Coexistence of two kinds of superfluidity at finite temperatures in optical lattices, *Annals of Physics* 443:168973, 2022 [34].

where

$$S_{ij} = G_0 + S'_{ij}, \quad (2.15)$$

$$G_0^{-1} = \delta_{ij} \left(\frac{\partial}{\partial \tau} + \bar{\mu} \right), \quad (2.16)$$

$$S'_{ij} = -J e^{-i\phi_{ij}(\tau)} - \frac{4\bar{\mu}}{U} J_{DIT} e^{-i\phi_{ij}(\tau)} - \frac{8}{U} J_{DIT}^2 e^{-i2\phi_{ij}(\tau)} \cdot (4 \langle \bar{b}_i b_j \rangle + \delta_{ij}), \quad (2.17)$$

$$\Delta_i = -\frac{8}{U} J_{DIT}^2 e^{-i2\phi_{ij}(\tau)} \langle b_i b_i \rangle, \quad (2.18)$$

$$\bar{\Delta}_i = -\frac{8}{U} J_{DIT}^2 e^{-i2\phi_{ij}(\tau)} \langle \bar{b}_i \bar{b}_i \rangle. \quad (2.19)$$

In order to carry out the integration, we rewrite \mathcal{S}_{eff} in Eq. (2.14) in matrix form, introducing a Nambu-like space. The effective action then takes the form

$$S_{eff} = \bar{B} \Gamma B, \quad (2.20)$$

where the bosonic Nambu-like vectors are defined as

$$B = \begin{pmatrix} b_i \\ \bar{b}_i \\ b_j \\ \bar{b}_j \end{pmatrix}, \quad (2.21)$$

$$\bar{B} = \begin{pmatrix} \bar{b}_i & b_i & \bar{b}_j & b_j \end{pmatrix}, \quad (2.22)$$

and the correlation matrix is

$$\Gamma = \begin{pmatrix} 0 & \frac{1}{2} \delta_{ij} \Delta_i & \frac{1}{2} S_{ij} & 0 \\ \frac{1}{2} \delta_{ij} \bar{\Delta}_i & 0 & 0 & 0 \\ 0 & 0 & 0 & \frac{1}{2} \delta_{ij} \Delta_i \\ 0 & \frac{1}{2} S_{ij} & \frac{1}{2} \delta_{ij} \bar{\Delta}_i & 0 \end{pmatrix}. \quad (2.23)$$

After bosonic integration, the partition function is

$$\mathcal{Z} = \int \{\mathcal{D}\phi\} e^{-\sum_i \int_0^\beta d\tau \left[\frac{1}{2U} (\dot{\phi}_i(\tau))^2 + \frac{\mu}{iU} \dot{\phi}_i(\tau) \right]} \cdot e^{\int_0^\beta d\tau \text{Tr} \ln \Gamma^{-1}}. \quad (2.24)$$

Next, we approximate G_0 , Eq. (2.16) by b_0^2 , which is obtained by minimising the Hamiltonian [46, 47]:

$$\frac{\partial}{\partial b_0} \mathcal{H}|_{b=b_0} = 0. \quad (2.25)$$

In the case of the DIT BHM Hamiltonian,

$$b_0^2 = \frac{z(t - 4J_{DIT}) + \left(\frac{U}{2} + \mu\right)}{U - 8zJ_{DIT}}. \quad (2.26)$$

This approximation has been deemed sufficient to study low-temperature effects. It can be extended to account for correlations in \mathbf{k} space, e.g. with the Bogoliubov approach [67], providing a single framework to study both atom-atom correlations and time of flight images in optical lattice systems.

The trace in Eq. (2.24) is calculated as the sum of the eigenvalues of the correlation matrix Γ , Eq. (2.23), after its diagonalisation:

$$\text{Tr} \ln \Gamma'^{-1} = G_0^2 \left[\bar{\Delta}_i \Delta_i - \left(S'_{ij} \right)^2 \right] + 2S'_{ij} G_0. \quad (2.27)$$

At this point, we assume the on-site two-particle interaction U is strong. This simplification cannot accurately describe chemical potential variation; instead, μ is treated as a constant parameter. Once all averages in Eq. (2.27) are supplemented, the effective phase partition function is

$$\mathcal{Z} = \int \{\mathcal{D}\phi\} e^{-\sum_i \int_0^\beta d\tau \frac{1}{2U} [\dot{\phi}_i(\tau)]^2 + \sum_{\langle i,j \rangle} \int_0^\beta d\tau \{g_1 \cos[\phi_{ij}(\tau)] + g_2 \cos[2\phi_{ij}(\tau)]\}}. \quad (2.28)$$

where

$$g_1 = \left[\frac{z(t - 4J_{DIT}) + \left(\frac{U}{2} + \mu\right)}{U - 8zJ_{DIT}} \right]^2 \left[\frac{64\bar{\mu}}{U^2} J_{DIT}^3 - \frac{16}{U} (t - 2J_{DIT}) J_{DIT}^2 \right] \\ \times \left\{ 2 \left[\coth \frac{\beta\mu}{2} + \coth \frac{\beta(\mu + U)}{2} \right] + 1 \right\} + \\ + \frac{z(t - 4J_{DIT}) + \left(\frac{U}{2} + \mu\right)}{U - 8zJ_{DIT}} \left[\frac{8\bar{\mu}}{U} J_{DIT} - 2(t - 2J_{DIT}) \right], \quad (2.29)$$

$$g_2 = \left[\frac{z(t - 4J_{DIT}) + \left(\frac{U}{2} + \mu\right)}{U - 8zJ_{DIT}} \right]^2 \\ \times \left[(t - 2J_{DIT})^2 + \left(\frac{4\bar{\mu}}{U} J_{DIT} \right)^2 - 2(t - 2J_{DIT}) \frac{8\bar{\mu}}{U} J_{DIT} \right]. \quad (2.30)$$

We can also rewrite exponential phase terms as trigonometric functions. Our effective phase action is then

$$\mathcal{S}[\phi] = \int_0^\beta d\tau \frac{1}{U} \sum_i \left(\frac{\partial \phi_i}{\partial \tau} \right)^2 + \int_0^\beta d\tau \left(-g_1 \sum_{\langle i,j \rangle} \cos \phi_{ij} - g_2 \sum_{\langle i,j \rangle} \cos 2\phi_{ij} \right). \quad (2.31)$$

We have thus obtained a form equivalent to the extended Quantum Phase Model, with coefficients derived from the microscopic DIT BHM, Eq. (2.1). Our effective phase model is now ready for analysis. First, the phase terms in Eq. (2.31) are transformed into spin and their values limited to $S = 1$. The mapping transfers some of the correlations into the pseudospin operators themselves. Afterwards, a mean field approximation is applied. To observe the two condensate phases of single particles and pairs, which stem from the single and double cosine terms, we look at their respective order parameters, which minimise the free energy.

2.2 $S = 1$ pseudospin mapping

To map the partition function, Eq. (2.28), onto the $S = 1$ pseudospin model, at $k_B T/U < 1$, the phase terms are transformed as shown in Section 1.2.2:

$$N(\phi) = S_z, \quad (2.32)$$

$$\cos \phi_i = \frac{1}{\sqrt{2}} S_i^x, \quad (2.33)$$

$$\sin \phi_i = \frac{1}{\sqrt{2}} S_i^y. \quad (2.34)$$

Quadrupolar pseudo-superexchange operators are also introduced for the double cosine pair term:

$$Q_i = (S_i^x)^2 - (S_i^y)^2, \quad (2.35)$$

$$Q_i^{xy} = 2S_i^x S_i^y. \quad (2.36)$$

The mean field approximated pseudospin hamiltonian [30] is

$$\mathcal{H}_{MF} = J \left(\frac{U}{J} (S_i^z)^2 - S_i^x \Psi_\phi - \frac{J_2}{J} Q_i \Psi_{2\phi} \right), \quad (2.37)$$

with new condensate coefficients

$$J = \frac{1}{2} z g_1, \quad (2.38)$$

$$J_2 = \frac{1}{4} z g_2. \quad (2.39)$$

The single Ψ_ϕ and pair $\Psi_{2\phi}$ condensate order parameters are defined as

$$\Psi_\phi = \langle S_i^x \rangle, \quad (2.40)$$

$$\Psi_{2\phi} = \langle Q_i \rangle. \quad (2.41)$$

The free energy per site of the pseudospin system is defined as

$$f = \frac{1}{2} (J\Psi_\phi^2 + J_2\Psi_{2\phi}^2) - \frac{1}{\beta} \ln Z, \quad (2.42)$$

where the partition function can be calculated from the $S = 1$ energy eigenvalues. The two order parameters, single condensate Ψ_ϕ and pair condensate $\Psi_{2\phi}$, minimise the free energy:

$$\frac{\partial f}{\partial \Psi_\phi} = 0, \quad \frac{\partial f}{\partial \Psi_{2\phi}} = 0. \quad (2.43)$$

These conditions lead to the following self-consistent equations:

$$1 = \frac{4J \tanh \left[\frac{\beta}{2} \sqrt{(U - J_2\Psi_{2\phi})^2 + 4J^2\Psi_\phi^2} \right]}{\sqrt{(U - J_2\Psi_{2\phi})^2 + 4J^2\Psi_\phi^2} [X + 2]}, \quad (2.44)$$

$$\Psi_{2\phi} = \frac{U}{J_2 - 4J} + \frac{4J}{4J - J_2} \cdot \frac{1 - X}{2 + X}, \quad (2.45)$$

where

$$X = \frac{e^{-\frac{\beta}{2}(U + 3J_2\Psi_{2\phi})}}{\cosh \left[\frac{\beta}{2} \sqrt{(U - J_2\Psi_{2\phi})^2 + 4J^2\Psi_\phi^2} \right]}. \quad (2.46)$$

Based on the free energy f , any thermodynamic functions can be studied.

2.3 Thermodynamics

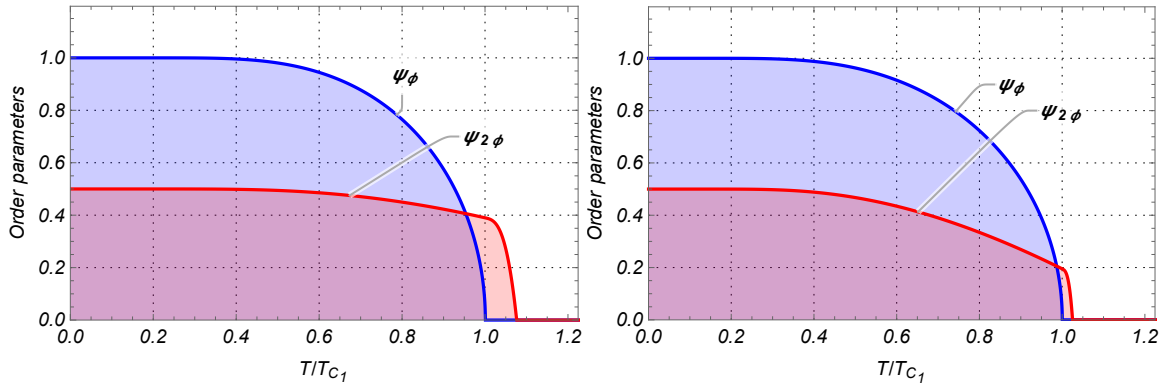
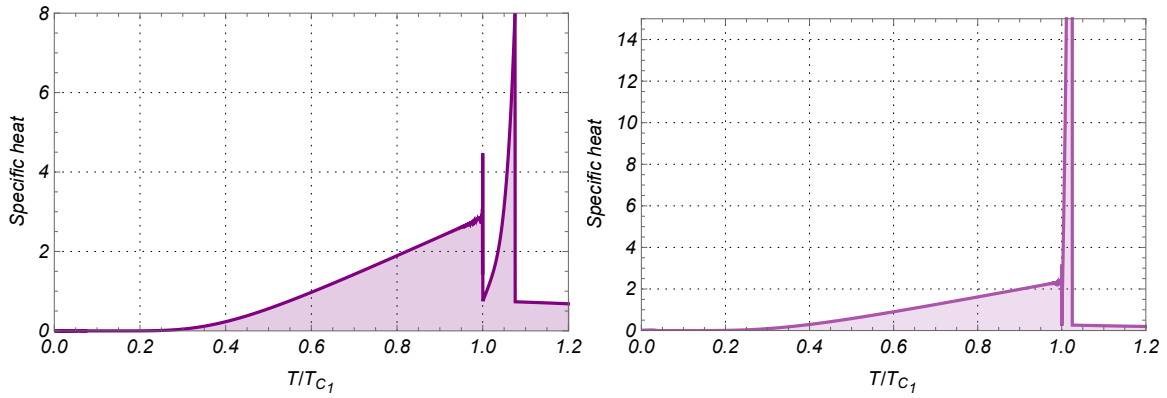
“Below are some exemplary diagrams obtained with use of Eqs. (2.44) and (2.45). Fig. (2.45) shows the dependence of the single and pair order parameters on a normalized temperature, T/T_{C_1} . Parameter values have been selected to ensure that phase separation can be seen clearly. The temperature is normalized to highlight the amplitude of the energy calculations.

T_{C_1} is the critical temperature of the single Bose-Einstein condensate phase transition, which separates the single Ψ_ϕ and pair $\Psi_{2\phi}$ superfluid phases.

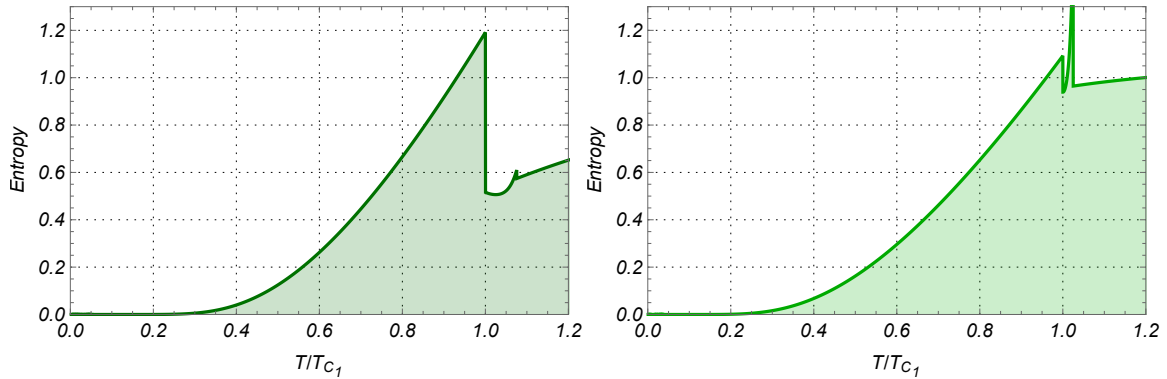
“Even though a mean-field approximation was used in the later stages of this analysis, the system clearly retained enough information to expose phenomena that elude approaches based exclusively on mean-fields. Not only are there two separate, coexisting superfluid phases in this model; pair condensation occurs independently of single-particle condensation. What’s more, pair condensation always survives at higher temperatures than single BEC, even as particle density and energy scales are changed. In the range of parameters where $t/J_{DIT} < 1$ (pair energy is higher), single particle condensation is almost suppressed and energy fluctuations are enormous, but pretty narrow in the temperature range. This is contrary to the opposite case, $t/J_{DIT} > 1$, where a strong single superfluid phase and a well-established and separated pair condensed fraction can be observed. No region has been observed with only single BEC present ($\Psi_\phi \neq 0$ and $\Psi_{2\phi} = 0$). The phase transitions are lambda-like, in accordance with those already observed experimentally.

“The actual temperature dependence of the specific heat is shown in Fig. (2.2), where opposite energy scales of the single hopping t and the density-induced tunnelling amplitude J_{DIT} are compared. Increasing J_{DIT} increases the BEC critical temperature T_{C_1} . However, the superfluid phase is simultaneously suppressed and a strong response in the pair sector is generated. In the opposite regime, the pair condensate phase disappears entirely. DIT instead provides support for the single BEC, while also increasing the BEC critical temperature T_{C_1}/U . For a DIT amplitude of $J_{DIT}/U = 0.009$, the critical temperature T_{C_1} of single-particle condensation becomes approximately seven times larger than when $J_{DIT} = 0$. Even at the smaller value of $J_{DIT}/U = 0.003$, T_{C_1} is still almost twice as large.”²

²Source: A. Krzywicka, T. P. Polak, Coexistence of two kinds of superfluidity at finite temperatures in optical lattices, *Annals of Physics* 443:168973, 2022 [34].

(a) Single Ψ_ϕ and pair $\Psi_{2\phi}$ order parameters.

(b) Specific heat.



(c) Entropy.

Figure 2.1: Temperature dependence of various functions for chosen parameter values: $t/U = 0.01$ and $J_{DIT}/U = 0.004$ on the left; $t/U = 0.001$ and $J_{DIT}/U = 0.0075$ on the right. ($\mu/U = 1.42$)

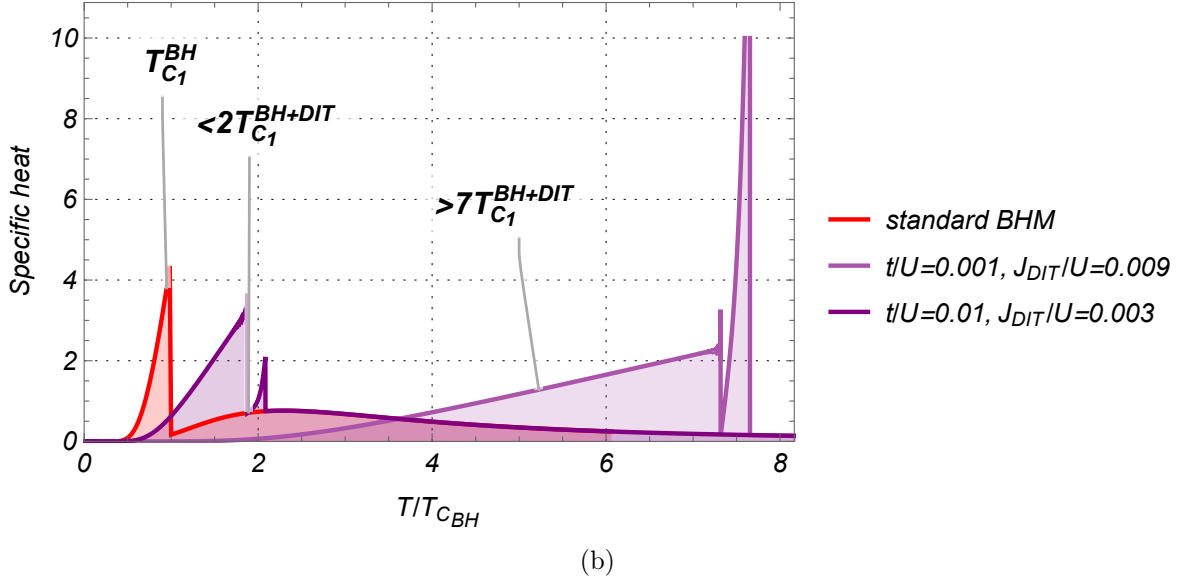
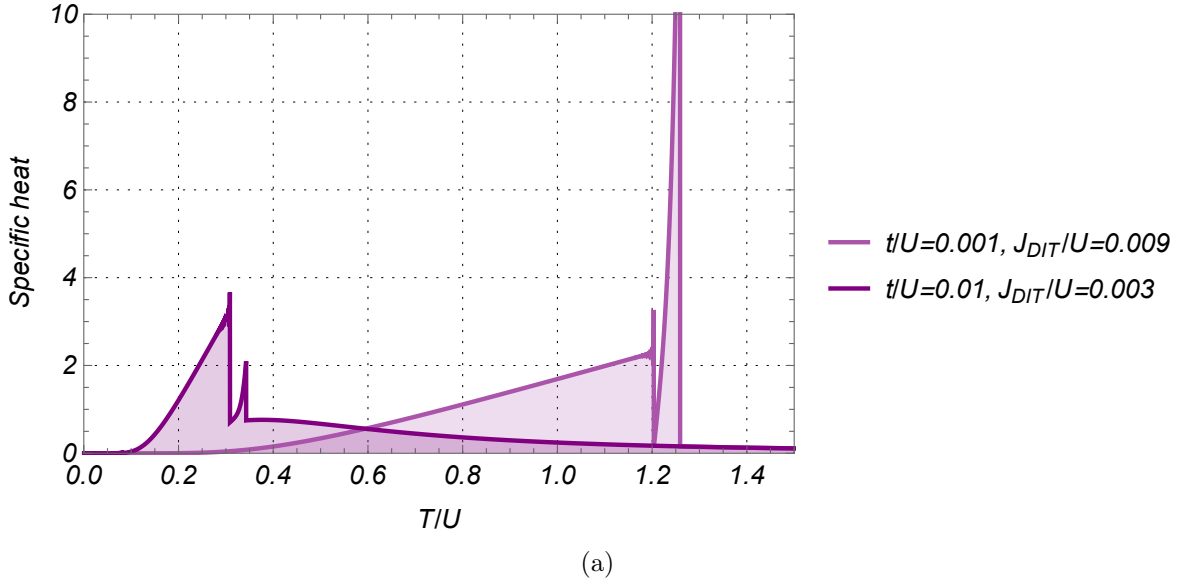


Figure 2.2: (a): Specific heat temperature dependence at opposite single and pair energy scales. (Left peak $t/J_{DIT} > 1$, right peak $J_{DIT}/t < 1$.) (b): Effect of density-induced tunnelling on the single boson condensation critical temperature, T_{C_1} , for opposite energy scales. ($\mu/U = 1.42$). Source: adapted from [34].

2.4 Conclusions

The first question posited in the Introduction thus receives an answer: bosons do form pairs. In fact, due to spin dependence being much less important than in the case of fermions, the phenomenon of bosonic pairing seems a much more frequent possibility. In terms of the effective action in the path integral formulation, any multi-index quadruple term could potentially be a source thereof. One might assume, then, that bosons both enter and leave the pair condensate phase without much consequence to the system. If that were the case, there would be little point in studying the mechanisms and properties of bosonic pairing. However, the single particle Bose-Einstein condensate, which is of primary interest in bosonic systems, clearly reacts to and interacts with the pair condensate phase.

To find out more about the effect a pairing mechanism might have on the standard BEC, we take another look at the effective phase model in Eq. (2.28). We are interested in a recontextualisation of the pair action term, strictly in terms of its effect on the single particle condensate.

Chapter 3

Dissipative interaction-based pairing

We now know that bosons do form pairs and that the pairing mechanism is responsible for the emergence of a new phase of bosonic pair condensation. Depending on the range of parameters, this phenomenon might compete with the single condensate phase, but might also strengthen it instead, as seen in Eq. (2.9). There is another mechanism which at certain ranges of parameters increases correlations rather than depleting them: dissipation in open systems. Pair condensates have indeed been shown to exhibit dissipative behaviour in experiments [60, 52, 66], causing single condensate depletion.

Keeping in mind the Taylor series expansion for a cosine, we speculate that the double cosine term responsible for bosonic pairing in the effective phase model, Eq. (2.28), might be reinterpreted as dissipative after Caldeira and Leggett, 1981 [6]. The simplest approach to this idea is one often adopted for studying open system dissipation: to separate the pair fraction from the single particle condensate and treat the former as an external reservoir, coupled harmonically to the original system of the latter. We entertain another idea, however. Since the trace in Eq. (2.27) contains the second power of the correlator G_0 , Eq. (2.16), which in turn depends on imaginary time τ , we might expect terms proportional to $(\tau - \tau')^{-2}$ to emerge if we keep the original form of the correlator instead of approximating it with the constant amplitude b_0^2 , as in Eq. (2.26). In that case, the artificial process of separating and then coupling back together in a different manner would become unnecessary. This would mean that the original

system itself supplies correlations which are dissipative in nature, without interacting with the environment; a very unintuitive, and therefore exciting, proposition. In order to ascertain whether such behaviour would make any sense, we set out to both look for implicit dissipation and compare it with the known harmonic coupling of the single particle condensate with an external reservoir, which in our case consists of the pair fraction. The pseudospin mapping is expanded from $S = 1$ to the sturdier quantum spherical model, shown in Section 1.2.4. The mean field approximation is replaced with a saddlepoint value of the spherical constraint, λ .

As in the previous chapter, detailed calculations are available in Appendix B.

3.1 Phase model

We return to the effective phase model with interaction-based pairing, Eq. (2.28):

$$\mathcal{S}[\phi] = \mathcal{S}_U[\phi] + \mathcal{S}_1[\phi] + \mathcal{S}_2[\phi], \quad (3.1)$$

which is comprised of three parts: an interaction part,

$$\mathcal{S}_U[\phi] = \frac{1}{2U} \sum_{\langle i,j \rangle} \int_0^\beta d\tau \left(\frac{\partial \phi_i}{\partial \tau} \right)^2 + \frac{\bar{\mu}}{iU} \dot{\phi}_i(\tau), \quad (3.2)$$

a single condensation part,

$$\mathcal{S}_1[\phi] = g_1 \sum_{\langle i,j \rangle} \int_0^\beta d\tau \cos[\phi_i(\tau) - \phi_j(\tau)], \quad (3.3)$$

and a pair condensation part,

$$\mathcal{S}_2[\phi] = g_2 \sum_{\langle i,j \rangle} \int_0^\beta d\tau d\tau' \cos 2 \left[\phi_i(\tau) - \phi_j(\tau') \right]. \quad (3.4)$$

The condensate coefficients, single g_1 and pair g_2 , depend on the treatment of the phase-phase correlator, G_0 , Eq. (2.16).

3.1.1 Coefficients

We consider two possible approaches. The simpler option is to approximate the correlator G_0 by a constant value. Deriving the coefficients explicitly is more complicated, but we find that doing so reveals implicit dissipative behaviour contained within the model.

3.1.1.1 Effective amplitudes

The traditional approach is to approximate the correlator G_0 , Eq. (2.16), by the bosonic amplitude b_0^2 , as in Eq. (2.26) in Chapter 2:

$$b_0^2 = \frac{z(t - 4J_{DIT}) + \left(\frac{U}{2} + \mu\right)}{U - 8zJ_{DIT}}. \quad (3.5)$$

The single and pair condensation coefficients, respectively, are as in Eqs. (A.125) and (A.126):

$$\begin{aligned} g_1 = & - \frac{z(t - 4J_{DIT}) + \left(\frac{U}{2} + \mu\right)}{U - 8zJ_{DIT}} \left[2(t - 2J_{DIT}) + \frac{8\bar{\mu}}{U} J_{DIT} \right] + \\ & + \left[\frac{z(t - 4J_{DIT}) + \left(\frac{U}{2} + \mu\right)}{U - 8zJ_{DIT}} \right]^2 \left(\frac{64\bar{\mu}}{U^2} J_{DIT}^3 + \frac{16}{U} J J_{DIT}^2 \right) \\ & \times \left\{ 2 \left[\coth \left(-\frac{\beta\mu}{2} \right) + \coth \left(\frac{\beta(\mu + U)}{2} \right) \right] + 1 \right\}, \end{aligned} \quad (3.6)$$

$$\begin{aligned} g_2 = & \left[\frac{z(t - 4J_{DIT}) + \left(\frac{U}{2} + \mu\right)}{U - 8zJ_{DIT}} \right]^2 \\ & \times \left[(t - 2J_{DIT})^2 + \left(\frac{4\bar{\mu}}{U} J_{DIT} \right)^2 + 2(t - 2J_{DIT}) \frac{8\bar{\mu}}{U} J_{DIT} \right]. \end{aligned} \quad (3.7)$$

These amplitudes are known to provide adequate results at low temperatures, e.g., to recover the well known λ -shaped peaks in the specific heat, which indicate single and pair condensation phase transitions [34].

3.1.1.2 Derived amplitudes

We introduce an alternative, more robust approach: keeping the original, imaginary time–dependent form of G_0 , Eq. (2.16), which after Fourier transform takes the form of

$$G_0 = \frac{-i\omega_m + \bar{\mu}}{\omega_m^2 + \bar{\mu}^2}. \quad (3.8)$$

The condensate coefficients depend on imaginary time, providing new physical effects:

$$g'_1(\omega_m) = -\frac{-i\omega_m + \bar{\mu}}{\omega_m^2 + \bar{\mu}^2} \left[2(t - 2J_{DIT}) + \frac{8\bar{\mu}}{U} J_{DIT} \right] + \quad (3.9)$$

$$+ \frac{1}{(-i\omega_m + \bar{\mu})^2} \left(\frac{64\bar{\mu}}{U^2} J_{DIT}^3 + \frac{16}{U} J J_{DIT}^2 \right) \quad (3.10)$$

$$\times \left\{ 2 \left[\coth \left(-\frac{\beta\mu}{2} \right) + \coth \left(\frac{\beta(\mu + U)}{2} \right) \right] + 1 \right\}, \quad (3.11)$$

$$g'_2(\omega_m) = \frac{1}{(-i\omega_m + \bar{\mu})^2} \times \left[(t - 2J_{DIT})^2 + \left(\frac{4\bar{\mu}}{U} J_{DIT} \right)^2 + 2(t - 2J_{DIT}) \frac{8\bar{\mu}}{U} J_{DIT} \right]. \quad (3.12)$$

In this version, imaginary time–dependent terms are present in both condensation parts of the effective phase model, \mathcal{S}_1 and \mathcal{S}_2 . The single coefficient g'_1 generates two contributions. The first, Eq. (3.9), is negligible in low temperatures after Matsubara summation. The second has an additional dissipation-like impact, Eq. (3.10). However, this latter term depends on higher orders of J_{DIT}/U than g'_2 , Eq. (3.12), so at $J_{DIT}/U \ll 1$ the pair dissipation is much stronger. Therefore, in this work, we forgo the marginally relevant contributions introduced by the single condensation coefficient g'_1 and replace it with the approximated g_1 of Eq. (3.6), focusing on the properties of the pair term, Eq. (3.4), in low temperatures.

The pair action term, \mathcal{S}'_2 , can be rewritten to separate the imaginary time dependency from the pair coefficient g'_2 :

$$\mathcal{S}'_2[\phi] = g'_2 \sum_{\langle i,j \rangle} \int_0^\beta d\tau d\tau' \frac{1}{(\tau - \tau')^2} \cos 2 \left[\phi_i(\tau) - \phi_j(\tau') \right], \quad (3.13)$$

where the derived pair condensate coefficient is now

$$g'_2 = (t - 2J_{DIT})^2 + \left(\frac{4\bar{\mu}}{U} J_{DIT} \right)^2 + 2(t - 2J_{DIT}) \frac{8\bar{\mu}}{U} J_{DIT}. \quad (3.14)$$

Other than the imaginary time dependence in the pair action \mathcal{S}'_2 , Eq. (3.13), the effective action remains the same, Eq. (3.1).

3.2 Dissipative models

Both versions of the pair condensation part of the effective action can be rewritten as dissipative. Traditionally, dissipation is added to Hamiltonians as an arbitrary external factor. However, since the action derived from Matsubara time contains full information about quantum fluctuations, the dissipative nature of the pair condensate emerges naturally in Eq. (3.13). After series expanding the double cosine, we rewrite the derived pair effective action term \mathcal{S}'_2 as explicitly dissipative:

$$\mathcal{S}'_2[\phi] = 2g'_2 \sum_{\langle i,j \rangle} \int_0^\beta d\tau d\tau' \frac{1}{(\tau - \tau')^2} \left[\phi_i(\tau) - \phi_j(\tau') \right]^2. \quad (3.15)$$

In the simpler case of the assumed model, with g_2 in Eq. (3.7), the imaginary time factor does not emerge naturally. To study the dissipative effect of the pair term in Eq. (3.4), we take the more travelled road and treat the two condensates as separate, harmonically coupled systems: condensed bosons submerged in a bath of harmonic potential, formed by the pair condensed system. The derivation of the effective action is typical for such many body systems and has been carried out under various circumstances [6, 35]. The

double cosine action term in Eq. (3.4) is transformed into a dissipative term:

$$\mathcal{S}_2[\phi] = 2g_2 \sum_{\langle i,j \rangle} \int_0^\beta d\tau d\tau' \left[\frac{\phi_i(\tau) - \phi_j(\tau')}{\tau - \tau'} \right]^2. \quad (3.16)$$

Ultimately, the two approaches differ only by their pair condensate coefficients:

$$\begin{array}{l} \begin{array}{l} \nearrow \\ G_0 \\ \searrow \end{array} \begin{array}{l} b_0 \text{ coupled condensates} \\ \\ G_0 \text{ full treatment} \end{array} \begin{array}{l} \rightarrow g_1 \text{ single particle} \\ \rightarrow g_2 \text{ pair} \\ \\ \rightarrow g'_1 \rightarrow g_1 \text{ single particle} \\ \rightarrow g'_2 \text{ pair} \end{array} \end{array} \quad (3.17)$$

At a glance, the difference is trivial, but the two models exhibit substantially distinct behaviour. Most importantly, in the derived model, the dissipation of the condensate does not stem from interactions with any external reservoir, but from internal correlations of the model itself. The proper treatment of quantum fluctuations requires an understanding of the properties of the derived actions, as well as the application of relevant approximations.

3.3 Spherical mapping and critical line equation

The Fourier transformed quantum rotor spherical partition function is

$$\mathcal{Z} = \int_{-i\infty}^{+i\infty} \left[\frac{\mathcal{D}\lambda(\tau)}{2\pi i} \right] e^{-N\phi[\lambda]}, \quad (3.18)$$

where the saddlepoint function is

$$\phi[\lambda] = -\beta\lambda - \frac{1}{2N} \sum_k \ln \left\{ \frac{1}{\beta\pi} [\lambda - g_1 \xi_k + \mathcal{G}^{-1}(\omega_m)] \right\}, \quad (3.19)$$

with Lagrange multiplier λ , lattice constant $\xi_k = 2 \sum_d \cos k_d$ and phase-phase correlator

$$\mathcal{G}(\tau, \tau') = \exp \left\{ \frac{1}{\beta} \sum_m \frac{1 - \cos[\omega_m(\tau - \tau')]}{\frac{1}{2U}\omega_m^2 + 4g_2|\omega_m|} \right\}. \quad (3.20)$$

The critical line equation is derived, as usual, by minimising free energy, this time with respect to the spherical constraint λ :

$$\frac{\partial \mathcal{F}}{\partial \lambda} = 0. \quad (3.21)$$

After rewriting lattice dependence in terms of the density of states function, defined as

$$\rho(E) = \frac{1}{N} \sum_k \delta(E - \xi_k), \quad (3.22)$$

the critical line equation is

$$1 = \frac{1}{2\beta} \int dE \sum_m \frac{\rho(E)}{\lambda - g_1 E + \mathcal{G}^{-1}(\omega_m)}. \quad (3.23)$$

However, this form is too complex to easily incorporate into the critical line equation. In low temperatures and densities, we approximate the inverse of the correlator \mathcal{G} in Eq. (3.20) by

$$\mathcal{G}^{-1}(\tau, \tau') \approx \frac{1}{2U}\omega_m^2 + 4g_2|\omega_m|. \quad (3.24)$$

At the critical point, the Lagrange multiplier λ can be substituted by its saddlepoint value, $\lambda_0 = g_1 \xi_{max}$. The critical line equation, Eq. (3.23), after performing Matsubara summation in the low temperature limit, $\beta \rightarrow \infty$, becomes

$$1 = \frac{1}{2\pi} \int d\xi \frac{\rho(\xi)}{g(\xi)} \left\{ \psi^{(0)} \left[\frac{\beta U}{\pi} (4g_2 + g(\xi)) \right] + \right. \\ \left. - \psi^{(0)} \left[\frac{\beta U}{\pi} (4g_2 - g(\xi)) \right] \right\}, \quad (3.25)$$

where $\psi^{(0)}$ are digamma functions and

$$g(\xi) = \sqrt{(4g_2)^2 - 2\frac{g_1}{U}(\xi_{max} - \xi)}. \quad (3.26)$$

The critical equation, Eq. (3.25), is the second pivotal point in this analysis. It contains all information about the system, including explicitly the geometry of the bipartite lattices, here chosen as two-dimensional square. In the low temperature limit, digamma functions can be approximated as logarithms, leading to the final form of the critical line equation:

$$1 = \frac{1}{2\pi} \int d\xi \frac{\rho(\xi)}{g(\xi)} \ln \left[\frac{4g_2 + g(\xi)}{4g_2 - g(\xi)} \right]. \quad (3.27)$$

Both models, derived and assumed, are analysed and compared in the next section based on this critical line.

3.4 Results

First of all, we look at the full form of the correlator in Eq. (3.20), to determine the range of parameters in which the approximation of Eq. (3.24) is valid.

3.4.1 Analytical limits for parameter range

After Mastubara summation and consequent Fourier transform, the phase-phase correlator, Eq. (3.20), can be rewritten as

$$\mathcal{G}(\omega_m) = \frac{\exp c}{\sqrt{2\pi}} b^{-\frac{a}{2} - \frac{1}{2}} \Gamma\left(\frac{a+1}{2}\right) {}_1F_1\left(\frac{a+1}{2}; \frac{1}{2}; -\frac{\omega_m^2}{4b}\right), \quad (3.28)$$

where

$$a = \frac{2}{8\pi g_2}, \quad (3.29)$$

$$b = \frac{\pi^2}{24\pi\beta^2 g_2}, \quad (3.30)$$

$$c = \frac{2H_{\frac{4g_2\beta}{\pi}} + 2\ln\frac{2\pi}{\beta} - \frac{\pi}{(4\beta g_2 + \pi)}}{8\pi g_2}, \quad (3.31)$$

Γ is the Euler gamma function, ${}_1F_1$ is the Kummer confluent hypergeometric function, and H_n is the n^{th} harmonic number.

The correlator is convergent as long as $g_2 < (8\pi)^{-1}$, which corresponds to an upper limit on the chemical potential for both versions of g_2 , Eq. (3.7) and Eq. (3.14). Within the relevant range of tunnelling parameters t and J_{DIT} , the upper limit is $\mu/U = (1 + \sqrt{3})/2 \simeq 1.366$. We focus on low-density systems in order to remain beneath this value. Other properties can also be calculated from the convergence condition, providing analytical results to compare with the numerical data obtained from the critical line equation.

This work focuses on low temperatures, $T \rightarrow 0$, and low density systems, $\mu/U < (1 + \sqrt{3})/2$, as the essential phenomena take place within this parameter space.

3.4.2 Analytical properties of the full correlator

Within the right range of parameters, especially where the quantum fluctuations are very strong, the analytical predictions obtained from the full correlator, Eq. (3.28), shown in Fig. 3.1, fit very well with numerical experiments. The position and value of the minimum of the normalised hopping can be derived analytically and yields

$$\left(\frac{t}{U}\right)_{min}^{value} = \frac{1}{8\sqrt{3\pi}\sqrt{-2\mu^2 + 2\mu + 1}} \left|\frac{4\mu + 1}{2\mu + 1}\right|, \quad (3.32)$$

$$\left(\frac{J_{DIT}}{U}\right)_{min}^{position} = \sqrt{\frac{2}{3}} \frac{\sqrt{-2\mu^2 + 2\mu + 1}}{2\mu + 1}. \quad (3.33)$$

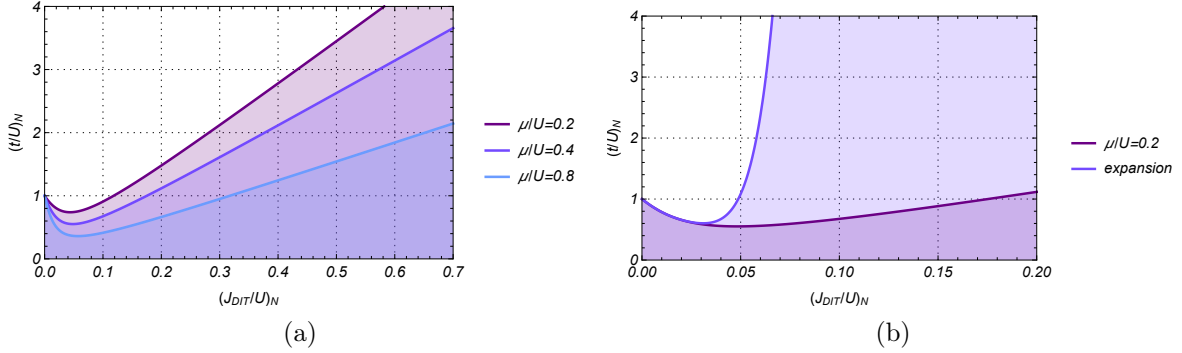


Figure 3.1: Analytical critical line relations. (a): Comparison of the analytical dependence of normalised single hopping t/U on the normalised DIT coefficient J_{DIT}/U at different chemical potentials μ/U , resulting from the critical properties of the phase-phase correlation function Eq. 3.28. (b): Model versus expansion, Eq. 3.34, at $\mu/U = 0.2$.

The boundaries of the model parameters can be deduced from this minimum. The chemical potential dependence of the minimum values is shown in Fig. 3.2.

3.4.3 Numerical comparison between the derived and assumed models

Exemplary critical lines determined by Eq. (3.27), which separate the Mott insulator (MI) and superfluid (SF) phases of the single particle condensate, are shown in Fig. 3.3. The proper energy scale of the system must be determined. For comparison purposes, both nearest-neighbour tunnelling t/U and density-induced tunnelling J_{DIT}/U have been normalised by the critical value $(t/U)_{\text{crit}}$, which separates the MI and SF phases in the absence of the extended interaction. The rapid decrease of the normalised hopping $(t/U)_N$ is associated with two mechanisms. The first stems from the low temperature properties of the phase-phase correlation function in Eq. (3.28). Expanding hopping

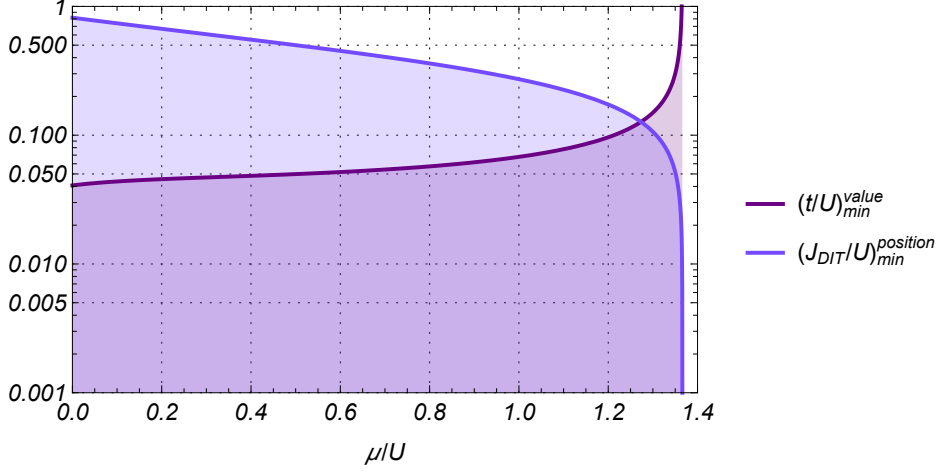


Figure 3.2: Chemical potential dependence of the position $(J_{DIT}/U)_{\min}$ and value $(t/U)_{\min}$ of the minimum seen in Fig 3.1, $\mu/U = 0.2$.

around the critical point, we obtain

$$\begin{aligned}
 (t/U)_N &\simeq 1 - 4\sqrt{2\pi}(4\mu/U + 1)(J_{DIT}/U)_N + \\
 &+ 48\pi(2\mu/U + 1)^2(J_{DIT}/U)_N^2 + \\
 &- \frac{1}{2}(48\pi)^2(2\mu/U + 1)^4(J_{DIT}/U)_N^4 + \\
 &+ \frac{1}{2}(48\pi)^3(2\mu/U + 1)^6(J_{DIT}/U)_N^6 + \dots
 \end{aligned} \tag{3.34}$$

The density-induced interaction J_{DIT} both linearly suppresses the hopping amplitude and supports particle mobility for $(t/U)_N$ with larger powers of $(J_{DIT}/U)_N$. As these two effects interchange with increasing powers of the expansion, this behaviour is easy to miss without looking at higher order terms before rejecting them. The second decreasing mechanism stems from the U(1) approach providing complete suppression of particle mobility; this effect cannot be analytically derived from the critical properties of the Eq. (3.27). A sudden revival of the coherent phase is also observed. As the density-induced tunnelling term increases, the quantum fluctuations reestablish long range order within the system, up until rapid cutoff. At first glance, the results from both models in Fig. 3.3 seem almost identical; the differences clarify themselves in the details.

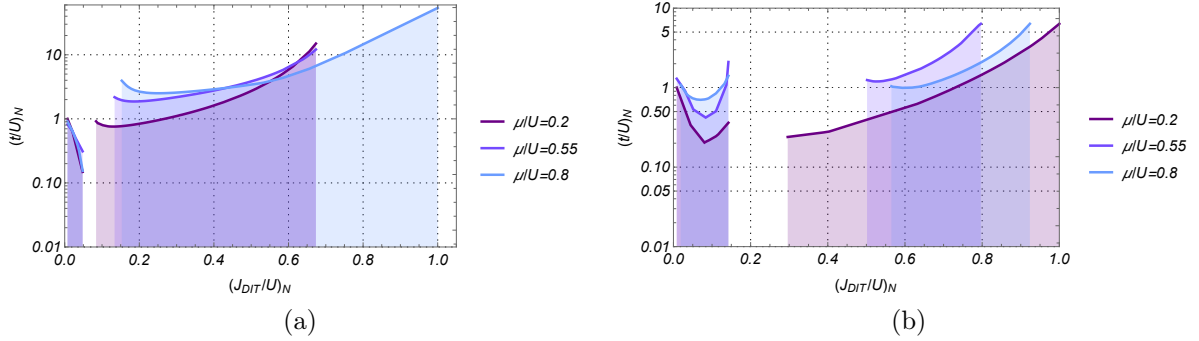


Figure 3.3: Comparison of the dependence of normalised single hopping t/U on the normalised DIT coefficient J_{DIT}/U at different chemical potentials μ/U . The critical lines separate the superfluid (below) and the Mott insulator (above) phases. (a): assumed model, using g_2 , Eq. (5.5). (b): derived model, using g'_2 , Eq. (3.14).

The details of the revival, presented and compared to analytical results in Fig. 3.5, showcase the most important difference between the assumed and derived models. Although the assumption made in the simplified model about the harmonic coupling between two condensates is reasonable and provides a qualitatively good description of the behaviour of the system, it fails to reproduce the disappearance of coherence. It is worth noting that the quadratic potential so often used to describe coupling between condensates cannot explain the critical properties of the system, even though the correlation function, Eq. 3.20, has the same form in both approaches. Particle density is the dominant factor in systems with density-induced tunnelling. The cut-off minimum occurs at the same value of μ/U as the tip of the superfluid–Mott insulator lobe dominated by the density that locally conserves its integer value. The density-induced interaction could be expected to depend strongly on the chemical potential. However, surprisingly, the coherence restored by the density-induced tunnelling behaves non-monotonically and in opposition to the critical values of the single particle superfluid of the standard Bose-Hubbard model. The subtlety of the phenomenon should also be noted: the strongest coherence is not generated by large densities, but rather small fluctuations thereof. The harmonic coupling model does not provide a valid description for small densities, being almost constant throughout the relevant range of the chemical

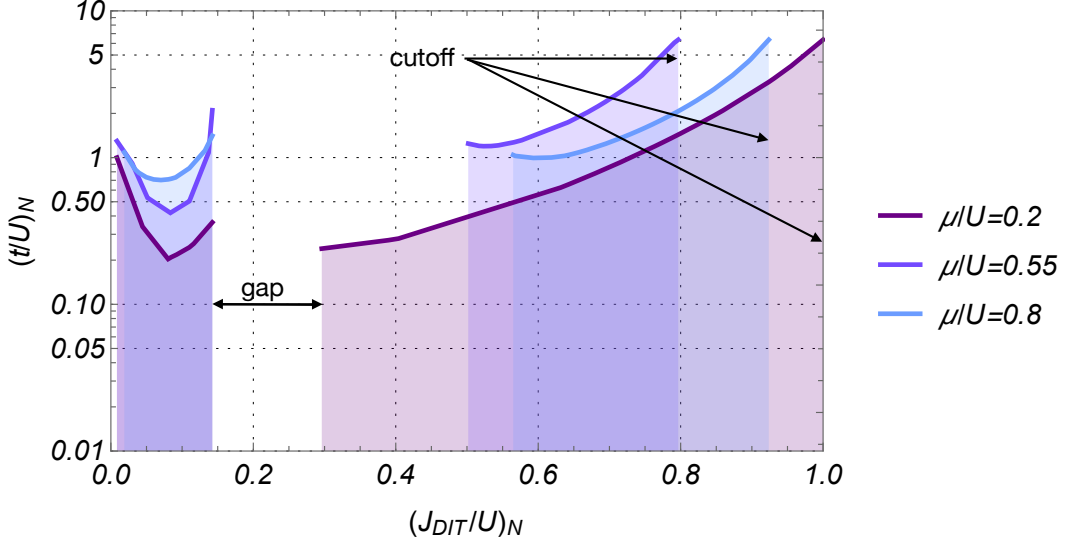
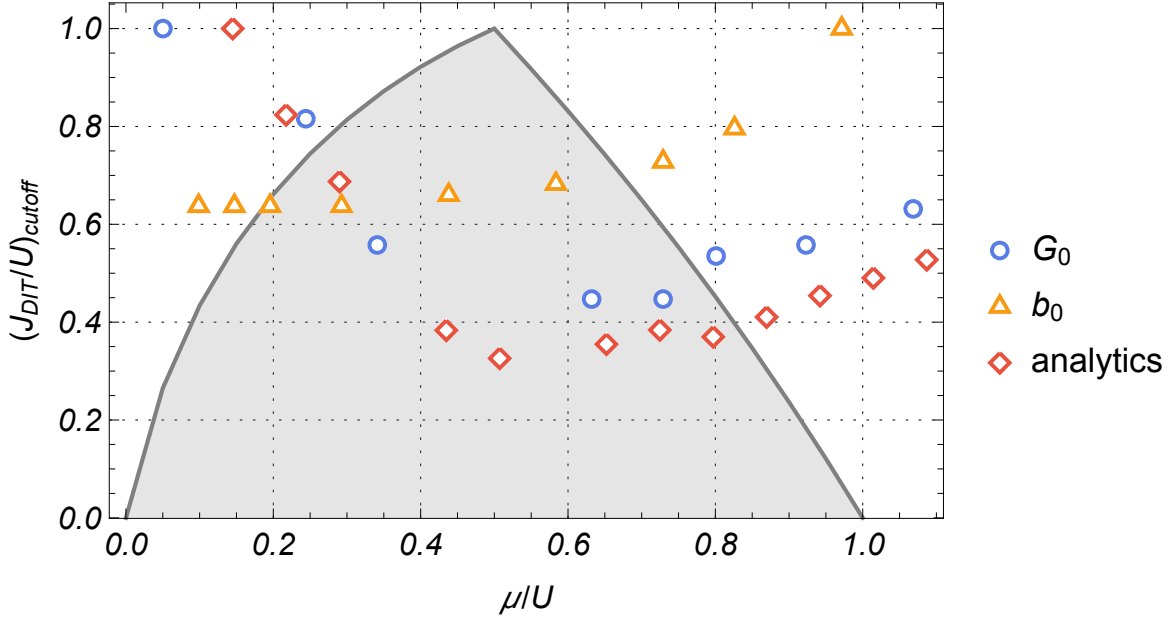


Figure 3.4: Visualisation of the two parameters analysed in Fig. 3.5.

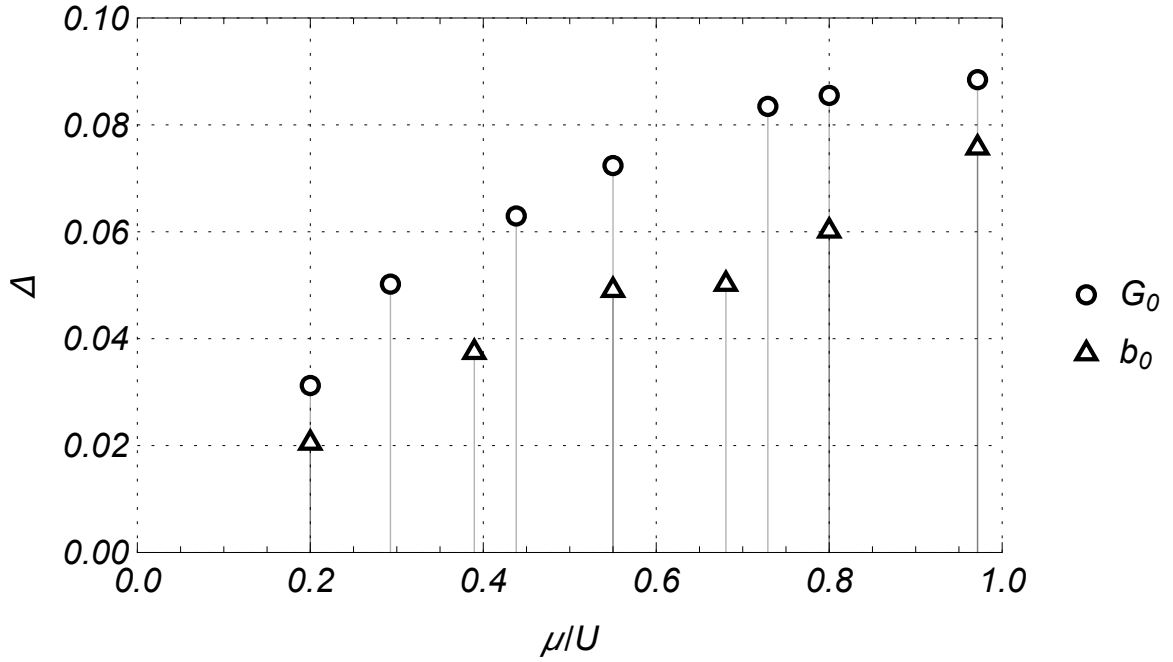
potential.

The decoherence of the system and the revival of superfluidity are separated by the gap Δ , shown in Fig. 3.5b which in both models increases monotonically with particle density. There are no qualitative changes in the gap between both approaches; we conclude that it does not depend on the character of the coupling, but rather on the quantum rotor properties of the critical lines themselves.

The importance of chemical potential when density-induced tunnelling is present led us to analyse the properties of the tunnelling amplitudes relative to density. The interesting diagram in Fig. 3.6 was derived analytically from the phase-phase correlation function in Eq. 3.28. Increasing particle density has different effects on the nearest-neighbour tunnelling t/U and density-induced tunnelling J_{DIT}/U . The single amplitude t/U counterintuitively decreases monotonically, with a rather steep decent, and finally goes to zero. In contrast, the DIT stays almost constant, before diverging rapidly to infinity at high densities. The high-density critical behaviour of both amplitudes occurs at the same point of $\mu/U = (1 + \sqrt{3})/2$. These results suggest that in systems with extended interactions, the chemical potential governs almost all the properties of the system, both diminishing the coherent state and at the same time supporting



(a)



(b)

Figure 3.5: Details of the differences between the derived model (circles, labelled G_0) and the assumed model (triangles, labelled b_0). (a): Cutoff values of $(J_{DIT}/U)_N$, compared to analytics and the first lobe of the zero-temperature square lattice superfluid (above) – Mott insulator (below) phase diagram (shaded area). (b): Width of gap Δ before the revival of superfluidity as a function of chemical potential.

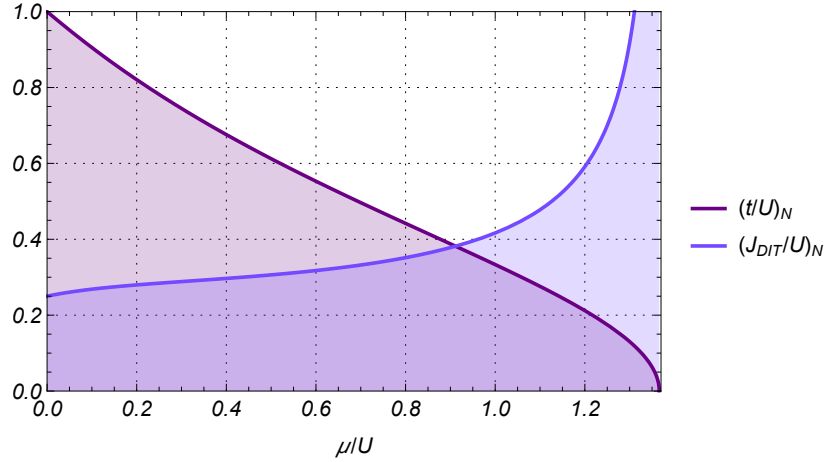


Figure 3.6: *Critical limit of the nearest-neighbour tunnelling and density-induced amplitudes, calculated from the critical properties of the phase-phase correlator, Eq. 3.28.*

correlated hopping between bosons. The magnitude of both tunnelling amplitudes is equal at $\mu/U = (1 + \sqrt{7})/4 \simeq 0.91$, where $(t/U)_N = (J_{DIT}/U)_N = \sqrt{\sqrt{7} - 5}/2 \simeq 0.38$. That provides the boundary of prepotency of the density-induced interaction.

3.5 Conclusions

The properties of the two kinds of pairing-based dissipation are similar enough to conclude that the strange concept of implicit dissipative behaviour might just be grounded in reality. Not only that: numerical data obtained from the derived model is closer to generalised analytical results than that of the safer, assumed coupling; this is especially clear in Fig. 3.5a. There seems to be a wealth of interesting details still waiting to be discovered and described about the bosonic pair condensate phase.

Our main interest, however, is where the mechanisms of pairing itself might emerge from in bosonic systems. Therefore, for now, we abandon the deep waters of interaction-based pairing and resurface to the microscopic level to wonder: since many body correlations clearly play such an important role in the pair condensate, could they themselves be its source?

Chapter 4

Correlation-based pairing

The analysis of extended Bose-Hubbard interactions in Chapter 2 confirms that bosonic pairs condense alongside the single particle Bose-Einstein condensate in the presence of many body correlations. Knowing that pair condensation is represented in the effective phase model, Eq. (2.28), by a double cosine or exponential term containing the double phase difference $2(\phi_i - \phi_j)$, we ask what other sources could generate such terms. Chapter 3 shows that delving deeper into the explicit forms of correlators, while requiring finesse in choosing the proper approximations, can uncover interactions that occur in strongly-correlated systems as new, explicit terms in the effective action.

Therefore, in this chapter, we focus on the standard Bose-Hubbard model (BHM) itself. We know that the Quantum Phase Model, Eq. (1.17), can be derived from the BHM, Eq. (1.1), as an effective phase model [46, 33]. The trace of the bosonic correlator is approximated to first order in a series expansion, resulting in linear phase-phase exponentials. This time, we extend the series expansion of the correlator to second order, expecting to find double exponentials or double cosines representing pair condensation, like the interaction-based pairing term in Eq. (2.28) in Chapter 2.

Once again, detailed calculations for this chapter can be found in Appendix C.

4.1 Model

We start with the standard Bose-Hubbard model, Eq. (1.1):

$$\hat{H} = \frac{U}{2} \sum_i \hat{n}_i (\hat{n}_i - 1) - t \sum_{\langle i,j \rangle} \hat{a}_i^\dagger \hat{a}_j - \mu \sum_i \hat{n}_i, \quad (4.1)$$

where $U > 0$ is the on-site repulsion, μ is the chemical potential, and t is the nearest neighbour exchange integral.

We follow the standard quantum rotor analysis of the BHM [46, 33], up to and including the integration of bosonic fields. The path integral partition function of the quantum rotor phase model is much the same as in the density-induced tunnelling model, Eq. (2.24):

$$\mathcal{Z} = \int \{\mathcal{D}\phi\} e^{-\sum_i \left\{ \int_0^\beta d\tau \left[\frac{1}{2U} (\dot{\phi}_i(\tau))^2 + \frac{\mu}{iU} \phi_i(\tau) \right] + \text{Tr} \ln G^{-1} \right\}}, \quad (4.2)$$

but in this case, the shifted chemical potential is

$$\bar{\mu} = \mu + \frac{U}{2} \quad (4.3)$$

and the Green's function, G , is a scalar:

$$G^{-1} = G_0^{-1} - T_{ij} = G_0^{-1} (1 - T_{ij} G_0), \quad (4.4)$$

with phase-phase correlator

$$G_0^{-1} = \left(\frac{\partial}{\partial \tau} + \bar{\mu} \right) \delta_{ij} \quad (4.5)$$

and the single-particle nearest neighbour exchange term

$$T_{ij} = t_{ij} e^{-i(\phi_i(\tau) - \phi_j(\tau))}. \quad (4.6)$$

In order to preserve the pair condensation term, the trace $\text{Tr} \ln G^{-1}$ in Eq. (4.2) is

approximated to second order:

$$\text{Tr} \ln G^{-1} = -\text{Tr} \ln G_0 - \text{Tr} (T_{ij} G_0) - \frac{1}{2} \text{Tr} (T_{ij} G_0)^2. \quad (4.7)$$

We assume G_0 to be a sum of two components. The first component is the bosonic amplitude b_0^2 . In the quantum rotor approach, b_0 is constant on every site, as all dynamics are contained within the phase. We obtain b_0^2 by minimising the BHM Hamiltonian, Eq. (4.1), in terms of the bosonic amplitude b_0 ,

$$\frac{\partial}{\partial b_0} \hat{H}(b_0) = 0, \quad (4.8)$$

which leads to

$$b_0^2 = \frac{2(zt + \bar{\mu})}{U}. \quad (4.9)$$

The second component of G_0 is the imaginary time-dependent form in Eq. (4.5) itself, which can be Matsubara transformed into

$$G_0 = \frac{1}{\beta} \sum_n \frac{-i\omega_n + \bar{\mu}}{\omega_n^2 + \bar{\mu}^2}. \quad (4.10)$$

By adding the two values in Eqs. (4.9,4.10) together, we obtain an effective phase model approximated from above.

4.2 Effective phase model

The transformations lead to the same effective phase action with pairing obtained from the density-induced tunnelling BHM in Chapter 2, Eq. (2.28):

$$\mathcal{S}[\phi] = \int_0^\beta d\tau \frac{1}{U} \sum_i \left(\frac{\partial \phi_i}{\partial \tau} \right)^2 + \int_0^\beta d\tau \left(-J \sum_{\langle i,j \rangle} \cos \phi_{ij} - J' \sum_{\langle i,j \rangle} \cos 2\phi_{ij} \right). \quad (4.11)$$

The coefficients are much different, however. The single particle condensation coefficient is much the same as in the standard Bose-Hubbard model case [46],

$$\frac{J}{t} = \frac{2(zt + \frac{U}{2} + \mu)}{U}, \quad (4.12)$$

and the pair condensation coefficient, after summing G_n in Eq. (4.10) over Matsubara frequencies, is

$$\frac{J'}{t} = \frac{t}{U} \left[\frac{2(zt + \frac{U}{2} + \mu)}{U} \right]^2 + \frac{t}{U} \frac{z}{2 \sinh^2 \left[\frac{\beta(\frac{U}{2} + \mu)}{2} \right]}. \quad (4.13)$$

Much like in the extended interaction case, Eq. (2.31), two different condensates, single-particle and pair, are generated by the two cosine terms in Eq. (4.11). This time, the pairing mechanism does not stem from many body interactions, but from many body correlations implicit within the standard Bose-Hubbard model.

We change the methodology in further calculations, making use of the self-consistent harmonic approximation rather than the $S = 1$ pseudospin mapping used for the interaction-based pairing in Chapter 2. Since this mechanism stems from correlations, the reasoning behind the change of strategy is to better preserve correlations within the condensate phases. Both pair condensates are later compared under uniform approximations and conditions in Chapter 5.

4.2.1 Self-consistent harmonic approximation

We solve the phase model in the self-consistent harmonic approximation (SCHA), shown in Section 1.2.3. The method is based on the harmonic trial action,

$$\mathcal{S}_0[\phi] = \int_0^\beta d\tau \left[\frac{1}{U} \sum_i \left(\frac{\partial \phi_i}{\partial \tau} \right)^2 + \frac{K}{2} \sum_{\langle i,j \rangle} \phi_{ij}^2 \right]. \quad (4.14)$$

The self-consistent equation for the trial stiffness, K , is obtained from the variational principle for free energy, Eq. (1.34), and takes the form of

$$K = J e^{-\frac{1}{2}\langle\phi_{ij}^2\rangle} + 4J' e^{-2\langle\phi_{ij}^2\rangle}, \quad (4.15)$$

where the trial nearest neighbour phase average, Eq. (1.36),

$$\langle\phi_{ij}^2\rangle = \frac{1}{z} \int d\xi \rho(\xi) \sqrt{\frac{(z-\xi)U}{2K}} \coth\left(\frac{\beta}{2} \sqrt{\frac{(z-\xi)KU}{2}}\right), \quad (4.16)$$

is determined with use of the density of states function,

$$\rho(\xi) = \frac{1}{N} \sum_k \delta(\xi - \xi_k). \quad (4.17)$$

The order parameters in the self-consistent harmonic approximation are defined as in Eqs. (1.37-1.39),

$$\Psi_1 = \langle\cos\phi_i\rangle = e^{-\frac{1}{2}\langle\phi_i^2\rangle}, \quad (4.18)$$

$$\Psi_2 = \langle\cos 2\phi_i\rangle = e^{-2\langle\phi_i^2\rangle}, \quad (4.19)$$

where the trial on-site phase average is as in Eq. (1.39),

$$\langle\phi_i^2\rangle = \frac{1}{2} \int d\xi \rho(\xi) \sqrt{\frac{U}{K(z-\xi)}} \coth\left(\frac{\beta}{2} \sqrt{(z-\xi)KU}\right). \quad (4.20)$$

The phase model, Eq. (4.11), is thus replaced with a harmonic oscillator with the effective phase action in Eq. (4.14). The stiffness K is calculated from the self-consistent equation and depends on the condensate coefficients, J in Eq. (4.12) and J' in Eq. (4.13). Thermodynamic functions can be derived from the trial free energy, \mathcal{F}_0 , in Eq. (1.30).

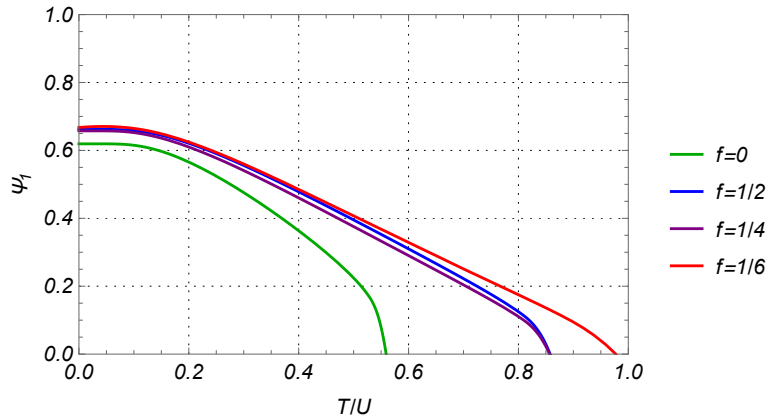
4.3 Thermodynamics of the effective model

Order parameter diagrams are shown in Fig. 4.1 in various magnetic fields, with set parameters of $t/U = 0.085$ and $\mu/U = 1.5$. The two upper diagrams, Figs. 4.1a and 4.1b, show how the single particle order parameter Ψ_1 behaves with and without bosonic pairing. An increase in the critical temperature T_C can be observed in all cases. Of particular interest is how the lines shift with respect to one another as the rotation frustration parameter f is changed. In Fig. 4.1a, without the pairing mechanism, Ψ_1 behaves almost identically at $f = 1/2$ and $f = 1/4$, with the same T_C . When pairing is added in Fig. 4.1b, however, the critical temperatures separate; the $f = 1/4$ line moves closer to $f = 1/6$. This suggests competition between the density of states (DOS) bandwidth and the van Hove singularities within the functions, which shifts as the pairing term is added. The DOS caps at $\xi_{max} = 2\sqrt{2}$ for both $f = 1/2$ and $f = 1/4$, but the latter is far less continuous.

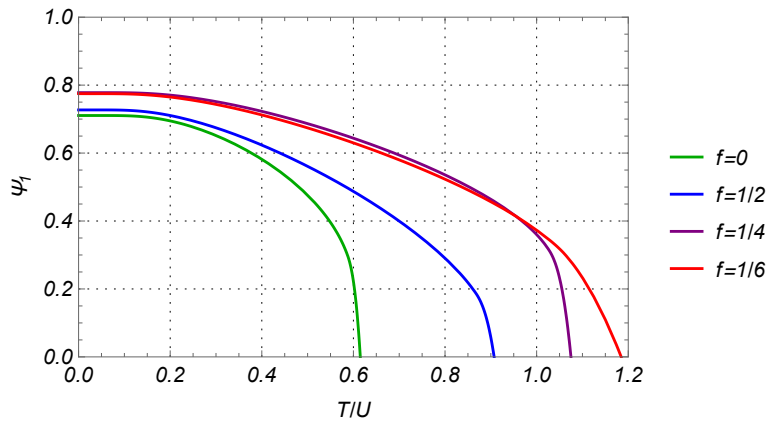
The pair order parameters Ψ_2 in Fig. 4.1c are peculiar: they very gradually decrease to zero, rather than the usual sudden, right angle drop. Furthermore, T_C is always lower for Ψ_2 than for Ψ_1 . Due to those factors, T_C will from now on refer to the single particle critical temperature specifically.

Fig. 4.2 shows entropy diagrams with and without pair condensation, ordered by magnetic field. The pair condensate strengthens the single condensate phase, meaning the superfluid survives in higher temperatures [34]. The strengthening effect on T_C varies depending on f , with the increase being smallest at $f = 1/2$, as seen in Fig. 4.2b. Once again, this has to do with the shift of the balance between the DOS bandwidths and continuity. The red lines of the non-pairing effective model are very similar at $f = 1/2$ and $f = 1/4$. When pairing is included, however, there is more similarity between the blue lines at $f = 1/4$ and $f = 1/6$.

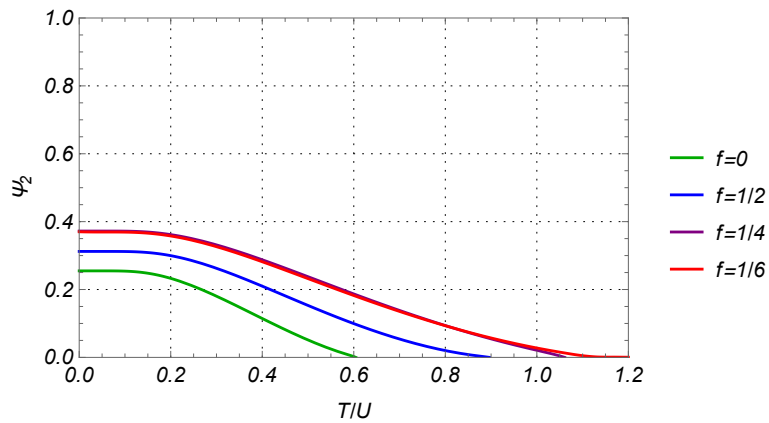
The lack of peaks in the blue lines before cutoff mirrors the slow descent of Ψ_2 . The effect of bosonic pairing is much more pronounced within the condensate phase itself, as seen in the blue shaded areas between the lines. Entropy provides information about order. The decrease in entropy as pair condensation is added, which occurs in every single case, emphasises the ordering effect the pairing mechanism has on the system.



(a)



(b)



(c)

Figure 4.1: Temperature dependence of single particle Ψ_1 and pair Ψ_2 order parameters in magnetic fields ($t/U = 0.085$). (a): Ψ_1 without pair condensation; (b): Ψ_1 with pair condensation; (c): Ψ_2 with pair condensation.

Every line in Fig. 4.2 cuts off abruptly at the respective Ψ_1 critical temperature. These cutoffs signify where the condensate–normal phase transitions occur. The cutoff is a consequence of the self-consistent harmonic approximation, which cannot reproduce the structure of the critical region. The SCHA preserves specific correlations within the condensate phase and therefore can be reliably used to study the thermodynamics thereof, in the regions where $\Psi_1, \Psi_2 \neq 0$. However, the ordering of the system is different in the normal phase and cannot be recreated using the same parameters. While this method cannot reproduce what happens near or beyond the critical point, the critical temperature T_C is determined by the cutoff point.

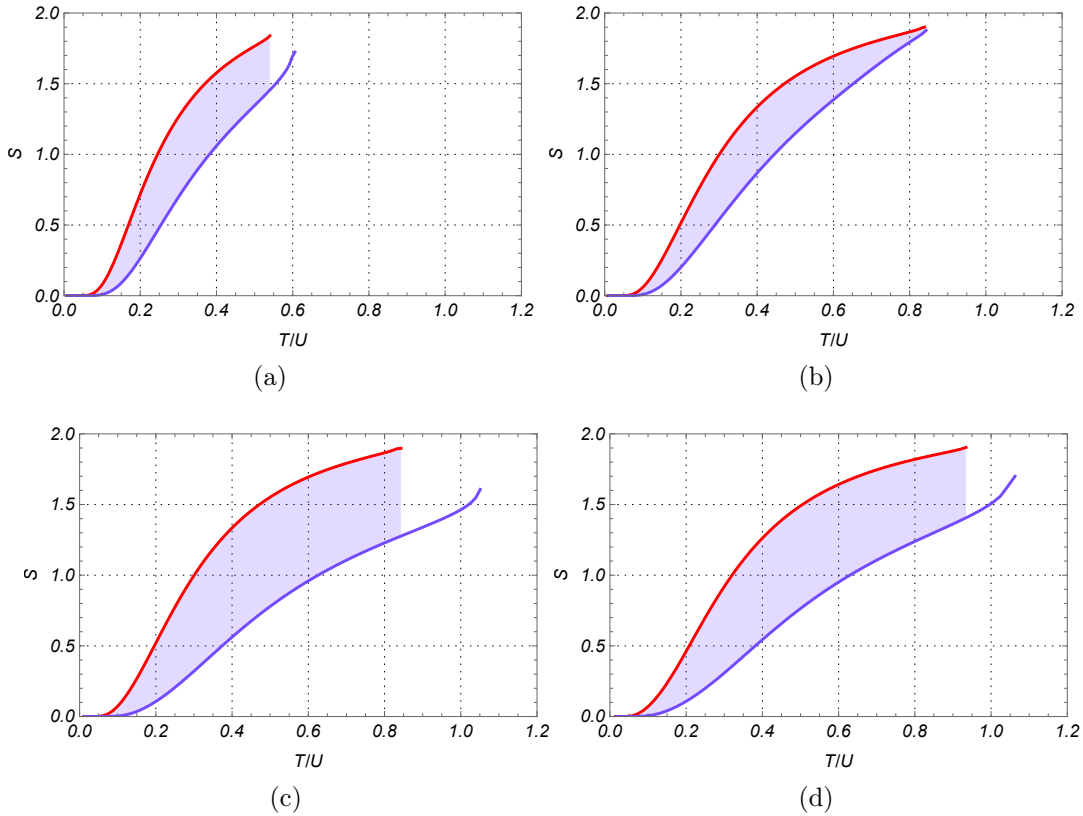


Figure 4.2: Comparison of entropy as a function of temperature with and without bosonic pair condensation in various magnetic fields ($t/U = 0.085$). Red lines depict single particle condensation only; blue lines represent the model with pair condensation. (a): $f = 0$; (b): $f = 1/2$; (c): $f = 1/4$; (d): $f = 1/6$.

4.4 Conclusions

We have confirmed in this chapter that strongly correlated bosons form pairs of their own accord even without the presence of extended interactions, such as density-induced tunnelling. Correlators in the path integral formulation contain a wealth of information, which is usually approximated to first order to focus on the largest contributions. As it turns out, bosonic pairing is one of the processes that occur just beyond this standard boundary; all that was needed for a pair condensate to emerge was considering the single largest term which is usually ignored. This emphasises the importance of many body correlations, including in systems forced into simple interactions [12, 11].

As density-induced tunnelling is a first-order approximation to the Bose-Hubbard model, the interaction-based pairing mechanism derived in Chapter 2 might be easier to detect experimentally. It probably also affects the single particle condensate in a more significant way, especially as the density-induced amplitude is increased. The next logical step is to compare both the derived pair condensates, interaction-based and correlation-based, using a uniform set of approximations, to see what is similar and what different between the two.

Chapter 5

Comparison of pairing mechanisms

In previous chapters, we have derived and analysed two bosonic pairing mechanisms, for which the effective phase models are the same but their coefficients are not. We conclude this work by mapping the similarities and differences in how the two pair condensates with very different sources affect the single particle condensate.

In path integral studies, the model must be narrowed down to fit chosen areas of interest, within specific parameter ranges and limits. Different methods allow access to various information, with differing reliability. Two separate approaches to a single model might even lead to disagreeing results. In order to compare the two derived pairing mechanisms, the methods and approximations used for thermodynamic analysis must be synchronised. Our interest lies in what happens within the condensate phase itself, rather than thermodynamics beyond the critical region. Therefore, in this chapter, we make use of the self-consistent harmonic approximation, preserving the correlations responsible for bosonic condensation.

5.1 Effective phase models

The effective phase model remains the same as in previous chapters, Eqs. (2.31,3.1,4.11):

$$\mathcal{S}[\phi] = \int_0^\beta d\tau \frac{1}{U} \sum_i \left(\frac{\partial \phi_i}{\partial \tau} \right)^2 + \int_0^\beta d\tau \left(-J \sum_{\langle i,j \rangle} \cos \phi_{ij} - J' \sum_{\langle i,j \rangle} \cos 2\phi_{ij} \right). \quad (5.1)$$

This time, we consider both of the pairing mechanisms derived in Chapters 2 and 4, which differ only by their single and pair coefficients. To easily distinguish between the two models, we rename them for this chapter as J_C, J'_C in the correlation-based model and J_I, J'_I in the interaction-based model.

5.1.1 Correlation-based coefficients

The first version of the model is based on the standard Bose-Hubbard model (BHM), as derived in Chapter 4. The correlation-based single and pair condensation coefficients are as in Eqs. (4.12,4.13):

$$\frac{J_C}{t} = \frac{2 \left(zt + \frac{U}{2} + \mu \right)}{U}, \quad (5.2)$$

$$\frac{J'_C}{t} = \frac{t}{U} \left[\frac{2 \left(zt + \frac{U}{2} + \mu \right)}{U} \right]^2 + \frac{t}{U} \frac{z}{2 \sinh^2 \left[\frac{\beta \left(\frac{U}{2} + \mu \right)}{2} \right]}, \quad (5.3)$$

where μ is the chemical potential, $t_{ij} = t$ is the nearest neighbour exchange integral, U is the on-site interaction between two particles and β is the inverse of the temperature.

5.1.2 Interaction-based coefficients

In the interaction-based model, derived in Chapter 2, the pairing mechanism stems from the density-induced interaction with amplitude J_{DIT} . Here, the single condensation

coefficient, Eq. (2.29), is the one dependent on temperature:

$$\begin{aligned} \frac{J_I}{t} = & \frac{z(t - 4J_{DIT}) + \left(\frac{U}{2} + \mu\right)}{U - 8zJ_{DIT}} \left[2(t - 2J_{DIT}) + \frac{8\bar{\mu}}{U} J_{DIT} \right] + \\ & + \left[\frac{z(t - 4J_{DIT}) + \left(\frac{U}{2} + \mu\right)}{U - 8zJ_{DIT}} \right]^2 \left[\frac{64\bar{\mu}}{U^2} J_{DIT}^3 + \frac{16}{U} (t - 2J_{DIT}) J_{DIT}^2 \right] \\ & \times \left\{ 2 \left[\coth \left(-\frac{\beta\mu}{2} \right) + \coth \left(\frac{\beta(\mu + U)}{2} \right) \right] + 1 \right\}, \end{aligned} \quad (5.4)$$

and the pair coefficient, Eq. (2.30), is

$$\begin{aligned} \frac{J'_I}{t} = & \left[\frac{z(t - 4J_{DIT}) + \left(\frac{U}{2} + \mu\right)}{U - 8zJ_{DIT}} \right]^2 \\ & \times \left[(t - 2J_{DIT})^2 + \left(\frac{4\bar{\mu}}{U} J_{DIT} \right)^2 + 2(t - 2J_{DIT}) \frac{8\bar{\mu}}{U} J_{DIT} \right], \end{aligned} \quad (5.5)$$

where the shifted chemical potential, Eq. (2.5), also depends on the density-induced amplitude J_{DIT} ,

$$\bar{\mu} = \frac{U}{2} + \mu - 2J_{DIT}. \quad (5.6)$$

The self-consistent harmonic approximation (SCHA) does not rely on the coefficients J and J' , therefore the calculations are carried out exactly the same as in Section 4.2.1. The self-consistent equation for the critical line, as derived in Section 4.2.1, Eq. (4.15), is

$$K = J e^{-\frac{1}{2}\langle\phi_{ij}^2\rangle} + 4J' e^{-2\langle\phi_{ij}^2\rangle}, \quad (5.7)$$

where the trial phase average, Eq. (4.16), is

$$\langle\phi_{ij}^2\rangle = \frac{1}{z} \int d\xi \rho(\xi) \sqrt{\frac{(z - \xi)U}{2K}} \coth \left(\frac{\beta}{2} \sqrt{\frac{(z - \xi)KU}{2}} \right). \quad (5.8)$$

Both models, with correlation-based and interaction-based pairing mechanisms, are compared in the next section within the same BHM parameters: chemical potential μ/U and hopping t/U , at differing values of the density-induced amplitude J_{DIT} . Orbital magnetic effects are also introduced into the trial phase average, $\langle \varphi_{ij}^2 \rangle$, via density of states, keeping in mind that the phase shift, Eq. (1.55), is effectively different in the pair condensate case by a factor of 2, as mentioned in Section 1.3.1.

5.2 Results

Firstly, chosen properties of the single and pair coefficients are shown in Fig. 5.1. Fig. 5.1a shows the dependence of both interaction-based coefficients, the single J_I in Eq. (5.4) and the pair J_I' in Eq. (5.5), on the density-induced tunnelling amplitude J_{DIT}/U . Areas where a coefficient is positive determine the parameter ranges in which their respective phase can be detected. As expected, both phases occur at low values of the density-induced amplitude, as up to $J_{DIT}/U \approx 0.0314$, both J_I and J_I' are positive. As J_{DIT}/U increases, we observe areas where one coefficient is positive and the other negative, meaning either single particle or pair condensation can occur, but not both simultaneously. We focus on the most interesting range of $J_{DIT}/U < 0.03$, in which both condensates are able to coexist.

In both models, only one of the two condensate coefficients depends on temperature. In the correlation-based model, it is the pair amplitude: $J_C' = f(\beta)$. The interaction-based model is the opposite: $J_I = f(\beta)$. The temperature dependence of the relevant coefficients is shown in Fig. 5.1c. It is clear that the interaction-based single condensate almost doesn't react to changes in temperature. The pair coefficient in the correlation-based model is much more sensitive. That being said, the scale in which substantial changes occur is much larger than the critical temperatures obtained in this section.

Exemplary diagrams of the dependence on temperature of the single particle and pair order parameters, Ψ_1 and Ψ_2 respectively, are shown in Fig. 5.2 in the absence of magnetic fields, where the rotation frustration parameter $f = 0$. Additionally, Fig. 5.3 shows the difference between single particle and pair critical temperatures, $\Delta_{crit} = T_{C_1} - T_{C_2}$, in different magnetic fields and at two different values of the single hopping

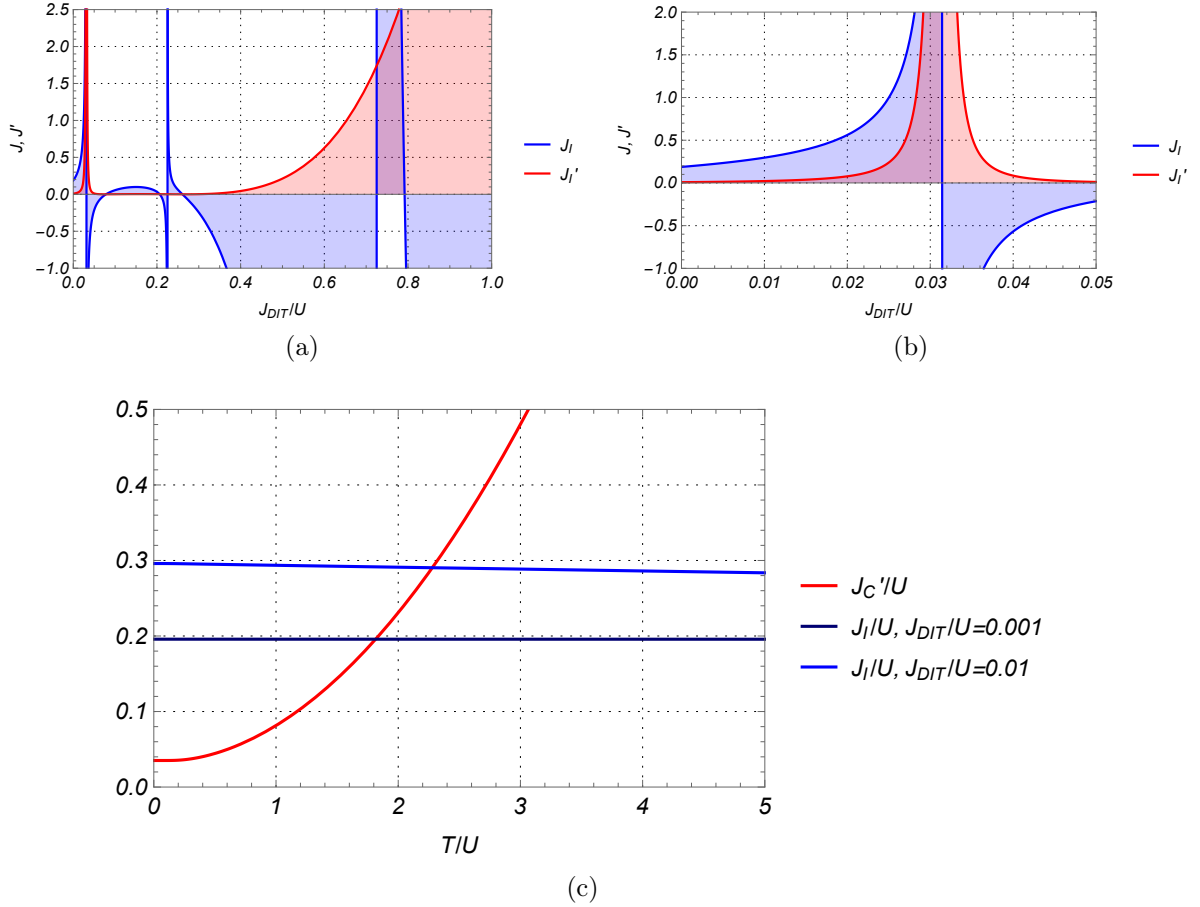


Figure 5.1: Properties of single and pair coefficients. (a): Interaction-based condensate coefficients as functions of the density-induced tunnelling amplitude J_{DIT}/U . (b): As above, magnified for low values of J_{DIT}/U , showing the asymptote in J which determines the parameter range of this work. (c): Temperature dependence of the two temperature-driven condensate coefficients: the correlation-based pair J' and the interaction-based single particle J at two different density-induced interaction J_{DIT}/U values.

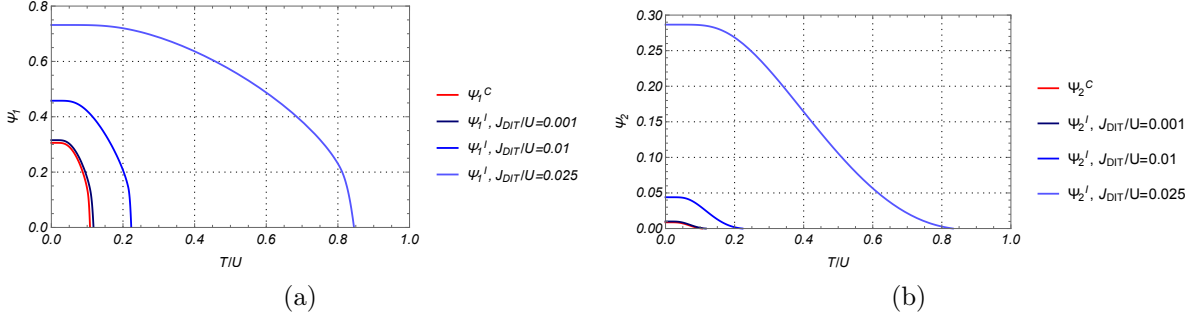


Figure 5.2: Comparison of temperature dependence of single particle and pair order parameters ($\mu/U = 0.45$). (a): single particle order parameter, Ψ_1 ; (b): pair order parameter, Ψ_2 . Superscript $()^C$ denotes correlation-based pairing; superscript $()^I$ denotes interaction-based pairing, driven by density-induced tunnelling J_{DIT} . ($t/U = 0.045$, $\mu/U = 0.45$)

t/U . Interpolations of Δ_{crit} are also included, to further clarify how the difference changes with the rotation frustration parameter f . As opposed to the pseudospin mapping analysis for interaction-based pairing, here the pair condensate fades out slowly and the pair critical temperature is consistently lower than for the single condensate, $T_{C_2} < T_{C_1}$.

Specific heat diagrams for both models under varying synthetic magnetic fields are shown in Fig. 5.4. In the interaction-based model, the critical lambda-shaped peaks clearly degenerate as the density-induced coefficient J_{DIT} increases towards the critical value. In both cases, specific heat flattens out in the presence of magnetic fields, but at the same time the critical temperature increases. The self-consistent harmonic approximation becomes unreliable in the vicinity of the critical point; this is especially pronounced in the red lines of the correlation-based model, where the specific heat c_C seems to increase ever faster, without reaching saturation. The diagrams are sorted by rotation frustration parameter f , to compare the two models in specific external conditions. As temperature increases, it becomes steadily easier to distinguish between specific heat generated by correlation-based pairing (red lines) and interaction-based pairing (blue lines). The two models also differ in the temperature at which the specific heat starts to increase substantially. In the correlation-based model, there is very little

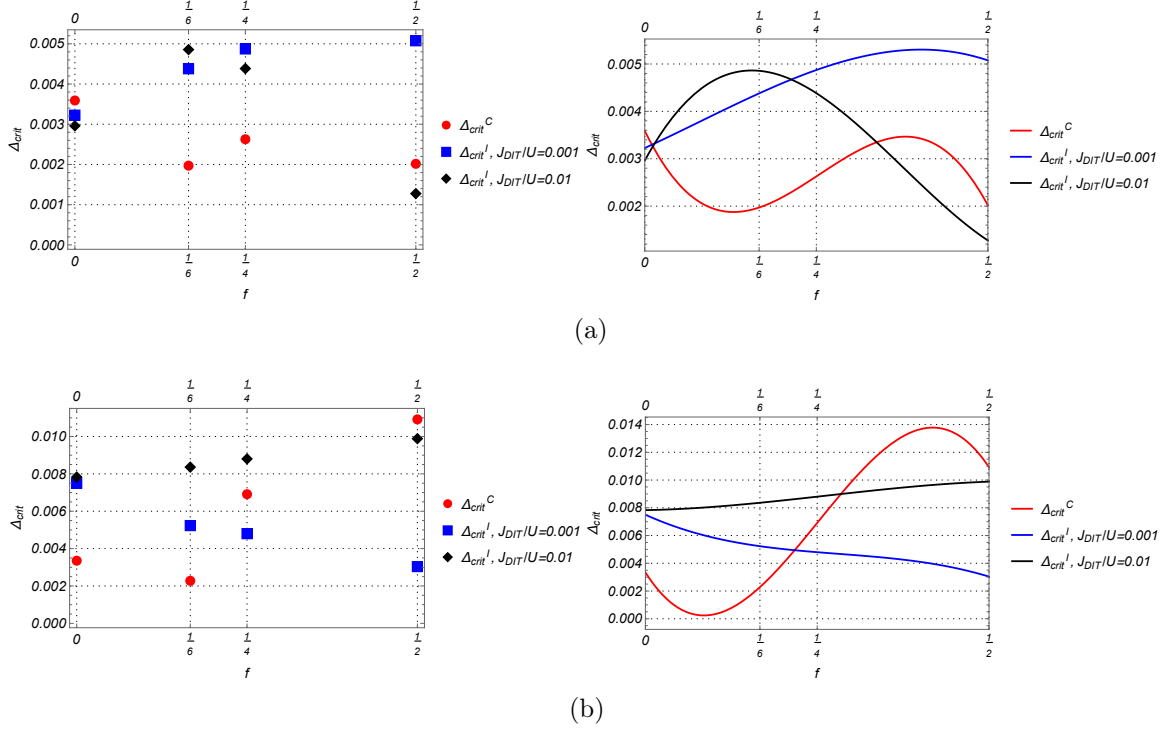


Figure 5.3: $\Delta_{crit} = T_{c1} - T_{c2}$ as a function of rotation frustration parameter f . Superscript $()^C$ denotes correlation-based pairing; superscript $()^I$ denotes interaction-based pairing, driven by density-induced tunnelling J_{DIT} . Right side diagrams are interpolations of the data on the left. (a): $t/U = 0.045$; (b): $t/U = 0.075$.

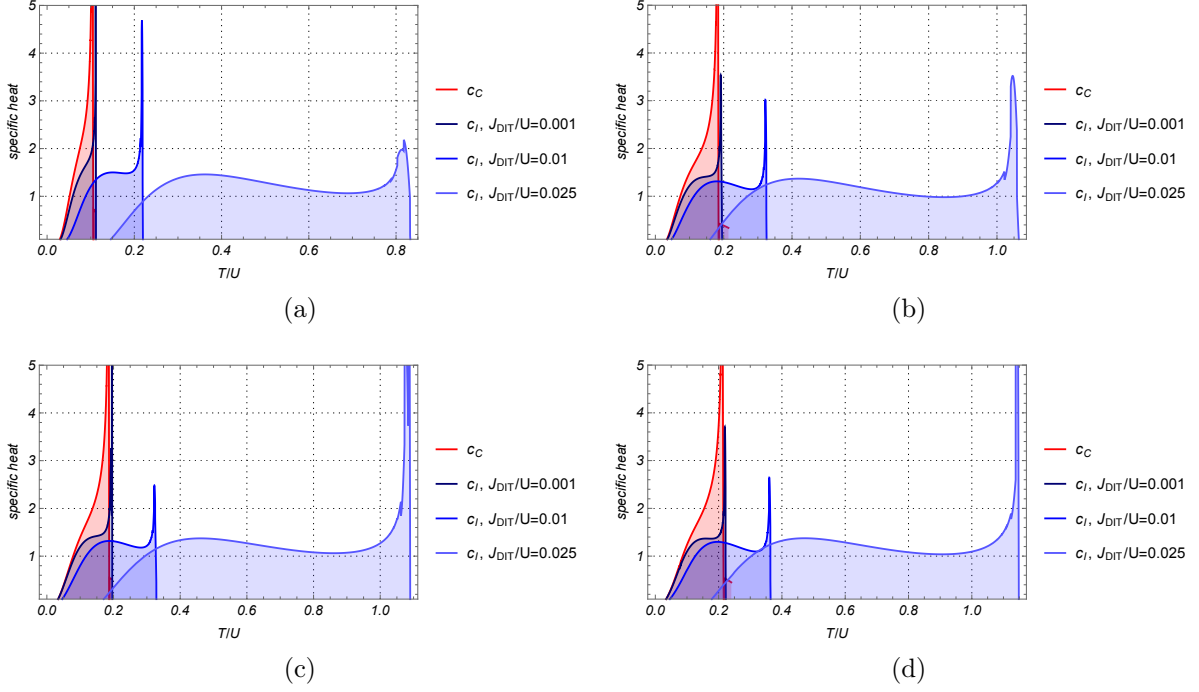


Figure 5.4: *Specific heat as a function of temperature in various magnetic fields ($t/U = 0.045$, $\mu/U = 0.45$). (a): $f = 0$; (b): $f = 1/2$; (c): $f = 1/4$; (d): $f = 1/6$.*

variety, but the interaction-based point of emergence shifts towards higher temperatures as J_{DIT} is increased. The difference between models is also pronounced in how they react to orbital magnetic effects. This distinction is explored in more detail in Fig. 5.5, in the difference $\Delta_c = c_C - c_I$ between the correlation-based (c_C) and interaction-based (c_I) specific heat at discrete values of temperature and in various magnetic fields.

A basic comparison of specific heat diagrams is shown in Fig. 5.6 at $t/U = 0.045$. The two models are presented along with the Standard Phase Model without pairing, the effective action of which is

$$\mathcal{S}[\phi] = \int_0^\beta d\tau \left[\frac{1}{U} \sum_i \left(\frac{\partial \phi_i}{\partial \tau} \right)^2 - J_{SPM} \sum_{\langle i,j \rangle} \cos \phi_{ij} \right], \quad (5.9)$$

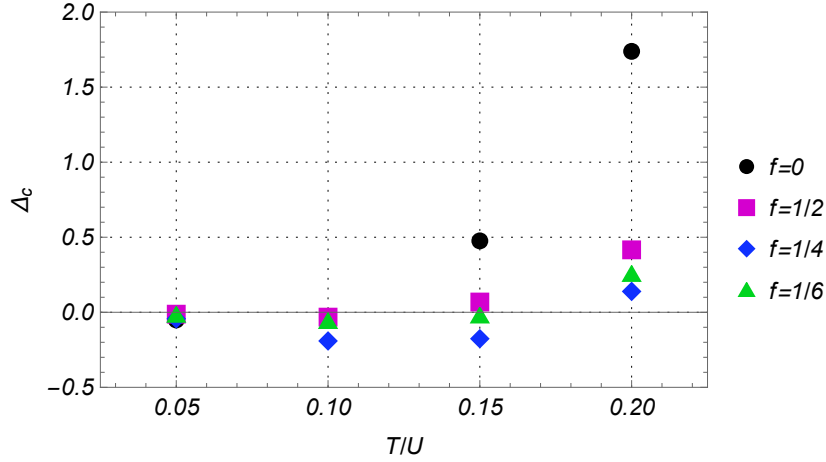


Figure 5.5: Difference $\Delta_c = c_C - c_I$ between the correlation-based (c_C) and interaction-based (c_I) specific heat in chosen temperatures at low density-induced amplitude, $J_{DIT}/U = 0.001$.

where

$$\frac{J_{SPM}}{t} = \frac{2(zt + \frac{U}{2} + \mu)}{U} = \frac{J_C}{t}. \quad (5.10)$$

Compared to the gray line of the Standard Phase Model, the correlation-based specific heat is marginally steeper, but very similar in terms of area, with a slight increase in critical temperature. Interestingly enough, the comparison is very different for the blue lines, representing the interaction-based specific heat. The interaction-based critical temperature increases substantially, but the line now also forms a hump, which is more reminiscent of standard specific heat behaviour.

5.3 Conclusions

Since the behaviour of bosons does not depend as strongly on spin as in the case of fermions, it is easier in the path integral formulation to find terms containing four bosonic field operators and connect those terms to the phenomenon of pairing. This work presents two different mechanisms that lead to the emergence of a new phase, sep-

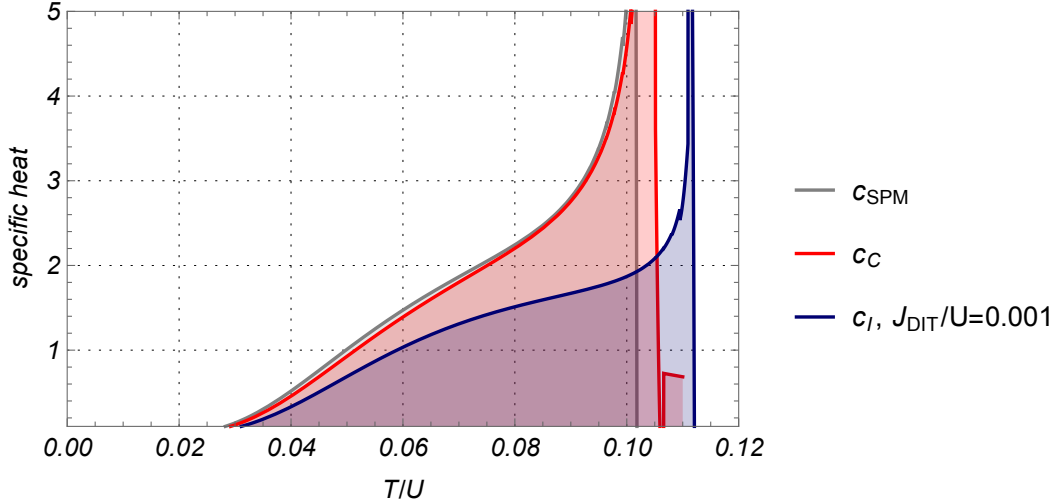


Figure 5.6: *Specific heat as a function of temperature with correlation-based and interaction-based pairing, compared with the standard phase model without a pairing term at $t/U = 0.045$ and $\mu/U = 0.45$.*

arate from but interacting with the well known single particle Bose-Einstein condensate (BEC). The effective phase model in both cases corresponds to an extended Quantum Phase Model (QPM) with two cosine condensation terms, Eq. (5.1), which is usually assumed with arbitrary constant coefficients. In our case, however, both coefficients are explicitly derived and depend on the parameters of the original, microscopic model. The two condensate phases therefore must interact and influence each other. Regardless of its source or the methods used, the presence of bosonic pairing consistently strengthens the BEC in the considered range of parameters.

5.3.1 Self-consistent harmonic approximation vs. $S = 1$ pseudospin

We have seen the similarities and differences between the two derived pairing mechanisms, correlation-based and interaction-based, under the self-consistent harmonic approximation (SCHA). We have seen also the strengths and the limits of the SCHA, and understand the impossibility of finding a single method within the path integral

formulation that would accurately depict the entirety of a system under any chosen conditions. This is especially clear in the interaction-based pair fraction, which under the $S = 1$ pseudospin mean field (MF) survives at higher temperatures than the single particle condensate T_{C_1} and produces a clear λ -shaped peak in the specific heat, but under the SCHA decays slowly and always before T_{C_1} is reached. It is therefore worth checking what information can be retrieved using the $S = 1$ pseudospin mapping from the correlation-based model.

To that end, additional order parameter diagrams of the model with correlation-based pairing under the $S = 1$ pseudospin approximation are shown in Fig. 5.7. The approximation was carried out exactly as in Section 2.2, with only the coefficients exchanged from the interaction-based Eqs. (5.4,5.5) to the correlation-based Eqs. (5.2,5.3). The normalisation parameter here is the single particle hopping t rather than the on-site interaction U , therefore the parameter values are much higher. Regardless, no separation has been found between the single and pair condensate phases.

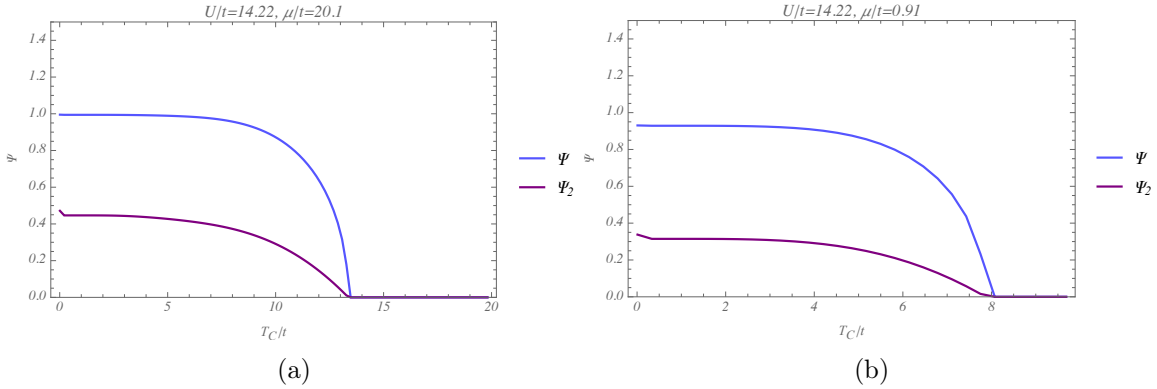


Figure 5.7: *Temperature dependence of single particle Ψ and pair Ψ_2 order parameters at different values of μ/t and constant on-site interaction U .*

The pseudospin mapping is based on a mean field approximation. All this suggests that the SCHA, which does not rely on MF methods, might be better suited to reproducing critical temperature T_C behaviour. On the other hand, the pseudospin mapping preserves energy fluctuations sufficiently to both obtain the λ -shaped peaks in the specific heat c that signify quantum phase transitions and reproduce the behaviour

of c beyond the superfluid phase, whereas the condensate-localised SCHA struggles especially with the latter. Another important factor is the dependence of the single or pair condensate coefficients on temperature, or imaginary time, which is different in the interaction-based and correlation-based pairing models and might also contribute to the T_C differences.

It is always worth remembering that information obtainable from approximations is only relevant in a narrow range of conditions and does not provide a full picture of the properties of the model one starts with. As such, different methods and approximations can reproduce different correlations. Results acquired from two separate approaches might correspond or complement one another, but might also turn out contradicting. Obviously, in such cases, experiments are a reliable means of verification.

Appendices

Appendix A

Interaction-based pairing: calculations

The Hamiltonian of the Bose-Hubbard model with density-induced tunnelling, Eq. (2.1), is:

$$\begin{aligned} \hat{H} = & \frac{U}{2} \sum_i \hat{n}_i (\hat{n}_i - 1) - \frac{1}{2} \sum_{\langle i,j \rangle} t_{ij} (\hat{a}_i^\dagger \hat{a}_j + \hat{a}_j^\dagger \hat{a}_i) - \mu \sum_i \hat{n}_i + \\ & - J_{DIT} \sum_{\langle i,j \rangle} \left[\hat{a}_i^\dagger (\hat{n}_i + \hat{n}_j) \hat{a}_j + \hat{a}_j^\dagger (\hat{n}_i + \hat{n}_j) \hat{a}_i \right], \end{aligned} \quad (\text{A.1})$$

where $\langle i, j \rangle$ identifies a summation over nearest neighbouring sites and:

- $\hat{a}_i^\dagger, \hat{a}_i$ are the bosonic coherent creation and annihilation operators, respectively; they obey the canonical commutation relation, $[\hat{a}_i, \hat{a}_j^\dagger] = \delta_{ij}$;
- $\hat{n}_i = \hat{a}_i^\dagger \hat{a}_i$ is the boson number operator on site i ;
- $U > 0$ is the on-site repulsion;
- μ is the chemical potential;
- J_{DIT} is the density-induced tunnelling amplitude ,

- t_{ij} is the hopping integral, the dispersion of which on a bipartite lattice in d dimensions is

$$t(\mathbf{k}) = 2t \sum_{l=1}^d \cos k_l. \quad (\text{A.2})$$

We assume that hopping is isotropic, $t_{ij} = t$, throughout the entire lattice.

First of all, we rewrite the Hamiltonian to resemble the standard Bose-Hubbard model, Eq. (1.1). This can be done by appending the density-induced term to either the exchange integral, as in [39], or the chemical potential [34].

Commutation relations needed for the density term:

$$[\hat{n}_i, \hat{a}_j^\dagger] = [\hat{a}_i^\dagger \hat{a}_i, \hat{a}_j^\dagger] = \hat{a}_i^\dagger \hat{a}_i \hat{a}_j^\dagger - \hat{a}_j^\dagger \hat{a}_i^\dagger \hat{a}_i = \hat{a}_i^\dagger (\hat{a}_j^\dagger \hat{a}_i + \delta_{ij}) - \hat{a}_j^\dagger \hat{a}_i^\dagger \hat{a}_i = \hat{a}_i^\dagger \delta_{ij}, \quad (\text{A.3})$$

$$[\hat{n}_i, \hat{a}_j] = [\hat{a}_i^\dagger \hat{a}_i, \hat{a}_j] = \hat{a}_i^\dagger \hat{a}_i \hat{a}_j - \hat{a}_j \hat{a}_i^\dagger \hat{a}_i = \hat{a}_i^\dagger \hat{a}_i \hat{a}_j - (\hat{a}_i^\dagger \hat{a}_j + \delta_{ij}) \hat{a}_i = -\hat{a}_i \delta_{ij}. \quad (\text{A.4})$$

Transforming the operators in the density-induced term in Eq. (A.1):

$$\hat{a}_i^\dagger (\hat{n}_i + \hat{n}_j) \hat{a}_j + c.c. = \hat{a}_i^\dagger \hat{n}_i \hat{a}_j + \hat{a}_i^\dagger \hat{n}_j \hat{a}_j + \hat{a}_j^\dagger \hat{n}_i \hat{a}_i + \hat{a}_j^\dagger \hat{n}_j \hat{a}_i \quad (\text{A.5})$$

$$= \hat{a}_i^\dagger (\hat{a}_j \hat{n}_i - \hat{a}_i \delta_{ij}) + \hat{a}_i^\dagger (\hat{a}_j \hat{n}_j - \hat{a}_j) + \hat{a}_j^\dagger (\hat{a}_i \hat{n}_i - \hat{a}_i) + \hat{a}_j^\dagger (\hat{a}_i \hat{n}_j - \hat{a}_j \delta_{ij}) \quad (\text{A.6})$$

$$= \hat{a}_i^\dagger \hat{a}_j \hat{n}_i - \hat{a}_i^\dagger \hat{a}_i \delta_{ij} + \hat{a}_i^\dagger \hat{a}_j \hat{n}_j - \hat{a}_i^\dagger \hat{a}_j + \hat{a}_j^\dagger \hat{a}_i \hat{n}_i - \hat{a}_j^\dagger \hat{a}_i + \hat{a}_j^\dagger \hat{a}_i \hat{n}_j - \hat{a}_j^\dagger \hat{a}_j \delta_{ij} \quad (\text{A.7})$$

$$= \hat{a}_i^\dagger \hat{a}_j \hat{n}_i + \hat{a}_i^\dagger \hat{a}_j \hat{n}_j + \hat{a}_j^\dagger \hat{a}_i \hat{n}_i + \hat{a}_j^\dagger \hat{a}_i \hat{n}_j + \left(\hat{a}_i^\dagger \hat{a}_j + \hat{a}_j^\dagger \hat{a}_i \right) - \left(\hat{a}_i^\dagger \hat{a}_i + \hat{a}_j^\dagger \hat{a}_j \right) \delta_{ij} \quad (\text{A.8})$$

$$= \left(\hat{a}_i^\dagger \hat{a}_j + \hat{a}_j^\dagger \hat{a}_i \right) (\hat{n}_i + \hat{n}_j - 1) - \left(\hat{a}_i^\dagger \hat{a}_i \delta_{ij} + \hat{a}_j^\dagger \hat{a}_j \delta_{ij} \right). \quad (\text{A.9})$$

The Hamiltonian in Eq. (A.1) then takes the form

$$\begin{aligned} \hat{H} = & \sum_i \left[\frac{U}{2} \hat{n}_i^2 - \left(\frac{U}{2} + \mu \right) \hat{n}_i \right] - \frac{1}{2} t \sum_{\langle i,j \rangle} \left(\hat{a}_i^\dagger \hat{a}_j + \hat{a}_j^\dagger \hat{a}_i \right) + \\ & - J_{DIT} \sum_{\langle i,j \rangle} \left[\left(\hat{a}_i^\dagger \hat{a}_j + \hat{a}_j^\dagger \hat{a}_i \right) (\hat{n}_i + \hat{n}_j - 1) - \left(\hat{a}_i^\dagger \hat{a}_i \delta_{ij} + \hat{a}_j^\dagger \hat{a}_j \delta_{ij} \right) \right] \end{aligned} \quad (\text{A.10})$$

$$\begin{aligned} = & \sum_i \left[\frac{U}{2} \hat{n}_i^2 - \left(\frac{U}{2} + \mu - 2T \right) \hat{n}_i \right] + \\ & - \sum_{\langle i,j \rangle} \left[\hat{a}_i^\dagger \hat{a}_j \left(\frac{1}{2} t + T (\hat{n}_i + \hat{n}_j - 1) \right) + \hat{a}_j^\dagger \hat{a}_i \left(\frac{1}{2} t + T (\hat{n}_i + \hat{n}_j - 1) \right) \right]. \end{aligned} \quad (\text{A.11})$$

Rewriting further and including , the DIT term can be appended either to the hopping:

$$\hat{H}_J = \sum_i \frac{U}{2} \hat{n}_i^2 - \sum_i \left(\frac{U}{2} + \mu - 2J_{DIT} \right) \hat{n}_i - \sum_{\langle i,j \rangle} \hat{a}_i^\dagger \hat{a}_j (t + 4J_{DIT} \hat{n}_i - 2J_{DIT}), \quad (\text{A.12})$$

or to the chemical potential:

$$\begin{aligned} \hat{H} = & \sum_i \frac{U}{2} \hat{n}_i^2 - \sum_{\langle i,j \rangle} (t - 2J_{DIT}) \hat{a}_i^\dagger \hat{a}_j + \\ & - \sum_{\langle i,j \rangle} \left[4J_{DIT} \hat{a}_i^\dagger \hat{a}_j + \left(\frac{U}{2} + \mu - 2J_{DIT} \right) \delta_{ij} \right] \hat{n}_i. \end{aligned} \quad (\text{A.13})$$

We choose the chemical potential version, Eq. (A.13). By denoting

$$J = t - 2J_{DIT}, \quad (\text{A.14})$$

$$\bar{\mu} = \frac{U}{2} + \mu - 2J_{DIT}, \quad (\text{A.15})$$

and

$$\hat{\mu}_{ij} = \frac{U}{2} + \mu - 2J_{DIT} + 4J_{DIT} \hat{a}_i^\dagger \hat{a}_j = \bar{\mu} + 4J_{DIT} \hat{a}_i^\dagger \hat{a}_j, \quad (\text{A.16})$$

we can simplify the Hamiltonian to a standard Bose-Hubbard form, Eq. (2.2):

$$\hat{H} = \frac{U}{2} \sum_i \hat{n}_i^2 - J \sum_{\langle i,j \rangle} \hat{a}_i^\dagger \hat{a}_j - \sum_{\langle i,j \rangle} \hat{\mu}_{ij} \hat{n}_i. \quad (\text{A.17})$$

We are now ready to move on to path integrals.

A.1 Quantum rotor derivation

The effective action formulation is scale invariant, so constant multipliers in the partition function have no bearing on the effective model. As the bosonic operators $\hat{a}_i^\dagger, \hat{a}_i$ transform into complex fields \bar{a}_i, a_i in the coherent state basis, the partition function is as in Eq. (1.12):

$$\mathcal{Z} = \int \{\mathcal{D}\bar{a}\mathcal{D}a\} e^{-\mathcal{S}[\bar{a},a]}, \quad (\text{A.18})$$

where the effective action \mathcal{S} , Eq. (1.13), contains the complex field form \mathcal{H} of the Hamiltonian from Eq. (A.17):

$$\mathcal{S}[\bar{a}, a] = \int_0^\beta d\tau \left(\sum_i \bar{a}_i(\tau) \frac{\partial}{\partial \tau} a_i(\tau) + \mathcal{H}(\tau) \right), \quad (\text{A.19})$$

$$\mathcal{H}(\tau) = \frac{U}{2} \sum_i n_i^2 - J \sum_{\langle i,j \rangle} \bar{a}_i a_j - \sum_{\langle i,j \rangle} \tilde{\mu}_{ij} n_i. \quad (\text{A.20})$$

The first step is introducing the effective electrochemical potential V as part of the Hubbard-Stratonovich transformation, Eq. (1.14), which decouples the U -dependent interaction term:

$$e^{-\frac{U}{2} \sum_i \int d\tau n_i^2(\tau)} = \int \frac{dV}{2\pi} e^{-\sum_i \int d\tau \left(\frac{V_i^2(\tau)}{2U} - iV_i(\tau) n_i(\tau) \right)}. \quad (\text{A.21})$$

The effective action terms containing V can be separated within the partition function:

$$\mathcal{Z} = \int \{\mathcal{D}\bar{a}\mathcal{D}a\} e^{-\mathcal{S}_b[\bar{a},a]} \int \frac{dV}{2\pi} e^{-\mathcal{S}_V[n,V]}, \quad (\text{A.22})$$

with bosonic effective action

$$\mathcal{S}_b = \int_0^\beta d\tau \left(\sum_i \bar{a}_i(\tau) \frac{\partial}{\partial \tau} a_i(\tau) - J \sum_{\langle i,j \rangle} \bar{a}_i(\tau) a_j(\tau) \right) \quad (\text{A.23})$$

and electrochemical effective action

$$\mathcal{S}_V = \int_0^\beta d\tau \left[\sum_i \left(\frac{1}{2U} V_i^2(\tau) - iV_i(\tau) n_i(\tau) \right) - \sum_{\langle i,j \rangle} \tilde{\mu}_{ij} n_i(\tau) \right]. \quad (\text{A.24})$$

Shifting the electrochemical potential $V_i(\tau) = V_i^T(\tau) - \frac{\tilde{\mu}_{ij}}{i}$:

$$\mathcal{S}_V = \int_0^\beta d\tau \left\{ \sum_i \left[\frac{1}{2U} (V_i^T(\tau))^2 - \frac{\tilde{\mu}_{ij}}{iU} V_i^T(\tau) - iV_i^T(\tau) n_i(\tau) \right] - \sum_{\langle i,j \rangle} \frac{\tilde{\mu}_{ij}^2}{2U} \right\}. \quad (\text{A.25})$$

At this point, the first phase dependence is introduced: we split the shifted potential V_i^T into static and periodic parts in terms of Matsubara frequency:

$$V_i^T(\tau) = V_i^S(\tau) + V_i^P(\tau), \quad (\text{A.26})$$

$$V_i^S(\tau) = \frac{1}{\beta} V_i^T(\omega_{m=0}), \quad (\text{A.27})$$

$$V_i^P(\tau) = \frac{1}{\beta} \sum_{m=1}^{+\infty} (V_i^T(\omega_m) e^{i\omega_m \tau} + c.c.), \quad (\text{A.28})$$

where the periodic part of the electrochemical potential is Josephson coupled to a $U(1)$ phase field $\phi(\tau)$:

$$V_i^P = \dot{\phi}_i(\tau). \quad (\text{A.29})$$

The periodicity of V^P carries on to the phase field, meaning $\phi_i(\beta) = \phi_i(0)$.

The chemical potential term is expanded using Eq. (A.16):

$$\int_0^\beta d\tau \sum_{\langle i,j \rangle} \frac{\tilde{\mu}_{ij}^2}{2U} = \frac{1}{2U} \int_0^\beta d\tau \sum_{\langle i,j \rangle} [\bar{\mu} + 4J_{DIT}\bar{a}_i(\tau) a_j(\tau)]^2 \quad (\text{A.30})$$

$$\begin{aligned} &= \frac{1}{2U} \int_0^\beta d\tau \sum_{\langle i,j \rangle} \{ \bar{\mu}^2 + 16J_{DIT}^2 [\bar{a}_i(\tau) a_j(\tau)]^2 \} + \\ &+ \frac{1}{2U} \int_0^\beta d\tau \sum_{\langle i,j \rangle} 8\bar{\mu}J_{DIT}\bar{a}_i(\tau) a_j(\tau) \end{aligned} \quad (\text{A.31})$$

$$\begin{aligned} &= \int_0^\beta d\tau \sum_{\langle i,j \rangle} \left\{ \frac{\bar{\mu}^2}{2U} + \frac{8}{U} J_{DIT}^2 [\bar{a}_i(\tau) a_j(\tau)]^2 \right\} + \\ &+ \int_0^\beta d\tau \sum_{\langle i,j \rangle} \frac{4\bar{\mu}}{U} J_{DIT}\bar{a}_i(\tau) a_j(\tau). \end{aligned} \quad (\text{A.32})$$

The partition function in Eq. (A.22) now also contains a phase action term, \mathcal{S}_ϕ :

$$\mathcal{Z} = \int \{ \mathcal{D}\bar{a}\mathcal{D}a \} e^{-\mathcal{S}_b[\bar{a},a]} \int \frac{dV^S}{2\pi} e^{-\mathcal{S}_S[n,V^S]} \int \{ \mathcal{D}\phi \} e^{-\mathcal{S}_\phi[n,\phi]}, \quad (\text{A.33})$$

where

$$\begin{aligned} \mathcal{S}_b &= \int_0^\beta d\tau \left[\sum_i \bar{a}_i(\tau) \frac{\partial}{\partial \tau} a_i(\tau) - \left(J + \frac{4\bar{\mu}}{U} J_{DIT} \right) \sum_{\langle i,j \rangle} \bar{a}_i(\tau) a_j(\tau) \right] + \\ &- \int_0^\beta d\tau \sum_{\langle i,j \rangle} \frac{8}{U} J_{DIT}^2 [\bar{a}_i(\tau) a_j(\tau)]^2, \end{aligned} \quad (\text{A.34})$$

$$\mathcal{S}_V = \sum_i \left[\frac{\beta}{2U} (V_i^S)^2 + \int_0^\beta d\tau \left(-\frac{\bar{\mu}^2}{2U} - \frac{\tilde{\mu}}{iU} V_i^S - iV_i^S n_i(\tau) \right) \right], \quad (\text{A.35})$$

$$\mathcal{S}_\phi = \sum_i \int_0^\beta d\tau \left[\frac{1}{2U} (\dot{\phi}_i(\tau))^2 + \frac{\tilde{\mu}}{iU} \dot{\phi}_i(\tau) - i\dot{\phi}_i(\tau) n_i(\tau) \right]. \quad (\text{A.36})$$

Constant terms do not contribute to the critical line equation due to scale invariance.

Replacing V^S with a constant average at saddlepoint and noting that

$$\int_0^\beta d\tau n_i(\tau) = \langle n_i \rangle, \quad (\text{A.37})$$

most terms in the static potential part of the action, \mathcal{S}_V , are indeed constant. The diagonal chemical potential dependence can be appended to the bosonic action \mathcal{S}_b :

$$\begin{aligned} \mathcal{S}_b = & \int_0^\beta d\tau \left[\sum_i \bar{a}_i(\tau) \left(\frac{\partial}{\partial \tau} + \bar{\mu} \right) a_i(\tau) - \left(J + \frac{4\bar{\mu}}{U} J_{DIT} \right) \sum_{\langle i,j \rangle} \bar{a}_i(\tau) a_j(\tau) \right] + \\ & - \int_0^\beta d\tau \sum_{\langle i,j \rangle} \frac{8}{U} J_{DIT}^2 [\bar{a}_i(\tau) a_j(\tau)]^2, \end{aligned} \quad (\text{A.38})$$

$$\mathcal{S}_\phi = \sum_i \int_0^\beta d\tau \left[\frac{1}{2U} \left(\dot{\phi}_i(\tau) \right)^2 + \frac{\tilde{\mu}}{iU} \dot{\phi}_i(\tau) - i\dot{\phi}_i(\tau) n_i(\tau) \right]. \quad (\text{A.39})$$

At this point, the effective action contains only terms dependent either on phase or on bosonic fields.

A.1.1 Gauge transformation

In order to obtain a phase-only model, we perform a gauge transformation, Eq. (1.15), on the bosonic fields, separating amplitude and phase:

$$a_i(\tau) = e^{i\phi_i(\tau)} b_i(\tau), \quad (\text{A.40})$$

$$\bar{a}_i(\tau) = e^{-i\phi_i(\tau)} \bar{b}_i(\tau). \quad (\text{A.41})$$

The partition function has two effective action terms, one bosonic and one phase-dependent, as shown in Eq. (2.6):

$$\mathcal{Z} = \int \{ \mathcal{D}\bar{b}\mathcal{D}b \} \int \{ \mathcal{D}\phi \} e^{-\mathcal{S}_b[\bar{b},b]} e^{-\mathcal{S}_\phi[n,\phi]}, \quad (\text{A.42})$$

where the bosonic terms are also phase-dependent now, with

$$\begin{aligned} \mathcal{S}_b = & \sum_{\langle i,j \rangle} \int_0^\beta d\tau \bar{b}_i(\tau) \left[\delta_{ij} \left(\frac{\partial}{\partial \tau} + \bar{\mu} \right) - J e^{-i\phi_{ij}(\tau)} - \frac{4\bar{\mu}J_{DIT}}{U} e^{-i\phi_{ij}(\tau)} \right] b_j(\tau) + \\ & - \sum_{\langle i,j \rangle} \int_0^\beta d\tau \frac{8}{U} J_{DIT}^2 e^{-i2\phi_{ij}(\tau)} [\bar{b}_i(\tau) b_j(\tau)]^2, \end{aligned} \quad (\text{A.43})$$

$$\mathcal{S}_\phi = \sum_i \int_0^\beta d\tau \left[\frac{1}{2U} (\dot{\phi}_i(\tau))^2 + \frac{\tilde{\mu}}{iU} \dot{\phi}_i(\tau) \right]. \quad (\text{A.44})$$

The next step is integrating out the bosonic fields to obtain a phase-only model. To that end, the quadruple term can be split into multiple bilinear terms with use of Wick's theorem. In the Fermi-Hubbard model, the interaction term is split as follows:

$$\begin{aligned} U \sum_i f_{i\uparrow}^\dagger f_{i\downarrow}^\dagger f_{i\downarrow} f_{i\uparrow} \simeq & \sum_i \Delta_i f_{i\uparrow}^\dagger f_{i\downarrow}^\dagger + \sum_i \Delta_i^* f_{i\uparrow} f_{i\downarrow} + \sum_i W_{i\downarrow} f_{i\uparrow}^\dagger f_{i\uparrow} + \\ & + \sum_i W_{i\uparrow} f_{i\downarrow}^\dagger f_{i\downarrow} - \sum_i V_i f_{i\uparrow}^\dagger f_{i\downarrow} - \sum_i V_i^* f_{i\downarrow}^\dagger f_{i\uparrow}, \end{aligned} \quad (\text{A.45})$$

where

$$\Delta_i = U \langle f_{i\downarrow} f_{i\uparrow} \rangle, \quad (\text{A.46})$$

$$W_{i\sigma} = U \langle f_{i\sigma}^\dagger f_{i\sigma} \rangle, \quad (\text{A.47})$$

$$V_i = U \langle f_{i\downarrow}^\dagger f_{i\uparrow} \rangle. \quad (\text{A.48})$$

The bosonic case is simpler; neglecting spin, we have Eq. (2.12),

$$\sum_{\langle i,j \rangle} b_i^\dagger b_i^\dagger b_j b_j \simeq \sum_{\langle i,j \rangle} \left[\langle b_j b_j \rangle b_i^\dagger b_i^\dagger + \langle b_i^\dagger b_i^\dagger \rangle b_j b_j + \left(4 \langle b_i^\dagger b_j \rangle + \delta_{ij} \right) b_i^\dagger b_j \right]. \quad (\text{A.49})$$

At this point, the bosonic field terms in the partition function can be brought together as the Gaussian integral in Eq. (2.14),

$$I = \int \{\mathcal{D}\bar{b}_i \mathcal{D}b_i\} \exp \left\{ - \int_0^\beta d\tau \sum_{\langle i,j \rangle} [\bar{b}_i(\tau) S_{ij} b_j(\tau) - \Delta_j \bar{b}_i \bar{b}_i - \bar{\Delta}_i b_j b_j] \right\} \quad (\text{A.50})$$

$$= \int \{\mathcal{D}\bar{b}_i \mathcal{D}b_i\} \exp \{-\mathcal{S}_{eff}\}, \quad (\text{A.51})$$

where

$$S_{ij} = \delta_{ij} \left(\frac{\partial}{\partial \tau} + \bar{\mu} \right) - J e^{-i\phi_{ij}(\tau)} - \frac{4\bar{\mu}}{U} J_{DIT} e^{-i\phi_{ij}(\tau)} + \frac{8}{U} J_{DIT}^2 e^{-i2\phi_{ij}(\tau)} \cdot (4 \langle \bar{b}_i b_j \rangle + \delta_{ij}), \quad (\text{A.52})$$

$$\Delta_i = - \frac{8}{U} J_{DIT}^2 e^{-i2\phi_{ij}(\tau)} \langle b_i b_i \rangle, \quad (\text{A.53})$$

$$\bar{\Delta}_i = - \frac{8}{U} J_{DIT}^2 e^{-i2\phi_{ij}(\tau)} \langle \bar{b}_i \bar{b}_i \rangle. \quad (\text{A.54})$$

At this point, the bosonic terms are quadratic and therefore prepared for Gaussian integration.

A.1.2 Nambu-like matrix form

In order to carry out the integration, we rewrite \mathcal{S}_{eff} in matrix form, creating a Nambu-like space. The elements of this bosonic effective action matrix have to be determined:

$$S_{eff} = \begin{pmatrix} \bar{b}_i & b_i & \bar{b}_j & b_j \end{pmatrix} \begin{pmatrix} A_1 & A_2 & A_3 & A_4 \\ B_1 & B_2 & B_3 & B_4 \\ C_1 & C_2 & C_3 & C_4 \\ D_1 & D_2 & D_3 & D_4 \end{pmatrix} \begin{pmatrix} b_i \\ \bar{b}_i \\ b_j \\ \bar{b}_j \end{pmatrix} \quad (\text{A.55})$$

$$= \begin{pmatrix} \bar{b}_i & b_i & \bar{b}_j & b_j \end{pmatrix} \begin{pmatrix} A_1 b_i + A_2 \bar{b}_i + A_3 b_j + A_4 \bar{b}_j \\ B_1 b_i + B_2 \bar{b}_i + B_3 b_j + B_4 \bar{b}_j \\ C_1 b_i + C_2 \bar{b}_i + C_3 b_j + C_4 \bar{b}_j \\ D_1 b_i + D_2 \bar{b}_i + D_3 b_j + D_4 \bar{b}_j \end{pmatrix} \quad (\text{A.56})$$

$$\begin{aligned} &= A_1 \bar{b}_i b_i + A_2 \bar{b}_i \bar{b}_i + A_3 \bar{b}_i b_j + A_4 \bar{b}_i \bar{b}_j + B_1 b_i b_i + B_2 \bar{b}_i b_i + \\ &\quad + B_3 b_j b_i + B_4 \bar{b}_j b_i + C_1 \bar{b}_j b_i + C_2 \bar{b}_j \bar{b}_i + C_3 \bar{b}_j b_j + C_4 \bar{b}_j \bar{b}_j + \\ &\quad + D_1 b_i b_j + D_2 \bar{b}_i b_j + D_3 b_j b_j + D_4 \bar{b}_j b_j. \end{aligned} \quad (\text{A.57})$$

The coefficients are:

$$A_1 = 0, \quad B_1 = \frac{1}{2} \delta_{ij} \bar{\Delta}_i, \quad C_1 = 0, \quad D_1 = 0, \quad (\text{A.58})$$

$$A_2 = \frac{1}{2} \delta_{ij} \Delta_i, \quad B_2 = 0, \quad C_2 = 0, \quad D_2 = \frac{1}{2} S_{ij}, \quad (\text{A.59})$$

$$A_3 = \frac{1}{2} S_{ij}, \quad B_3 = 0, \quad C_3 = 0, \quad D_3 = \frac{1}{2} \delta_{ij} \bar{\Delta}_i, \quad (\text{A.60})$$

$$A_4 = 0; \quad B_4 = 0; \quad C_4 = \frac{1}{2} \delta_{ij} \bar{\Delta}_i; \quad D_4 = 0. \quad (\text{A.61})$$

The effective action can then be written as the matrix product in Eq. (2.20):

$$S_{eff} = \bar{B} \Gamma B, \quad (\text{A.62})$$

where the bosonic Nambu-like vectors are defined as

$$B = \begin{pmatrix} b_i \\ \bar{b}_i \\ b_j \\ \bar{b}_j \end{pmatrix}, \quad (\text{A.63})$$

$$\bar{B} = \begin{pmatrix} \bar{b}_i & b_i & \bar{b}_j & b_j \end{pmatrix}, \quad (\text{A.64})$$

and the correlation matrix is

$$\Gamma = \begin{pmatrix} 0 & \frac{1}{2}\delta_{ij}\Delta_i & \frac{1}{2}S_{ij} & 0 \\ \frac{1}{2}\delta_{ij}\bar{\Delta}_i & 0 & 0 & 0 \\ 0 & 0 & 0 & \frac{1}{2}\delta_{ij}\Delta_i \\ 0 & \frac{1}{2}S_{ij} & \frac{1}{2}\delta_{ij}\bar{\Delta}_i & 0 \end{pmatrix}. \quad (\text{A.65})$$

The next step is diagonalising Γ , the eigenvalues of which are:

$$\Gamma_{11} = -\frac{1}{2}\sqrt{\bar{\Delta}_i\Delta_i - S_{ij}\sqrt{\bar{\Delta}_i\Delta_i}}, \quad (\text{A.66})$$

$$\Gamma_{22} = \frac{1}{2}\sqrt{\bar{\Delta}_i\Delta_i - S_{ij}\sqrt{\bar{\Delta}_i\Delta_i}}, \quad (\text{A.67})$$

$$\Gamma_{33} = -\frac{1}{2}\sqrt{\bar{\Delta}_i\Delta_i + S_{ij}\sqrt{\bar{\Delta}_i\Delta_i}}, \quad (\text{A.68})$$

$$\Gamma_{44} = \frac{1}{2}\sqrt{\bar{\Delta}_i\Delta_i + S_{ij}\sqrt{\bar{\Delta}_i\Delta_i}}. \quad (\text{A.69})$$

The integral in Eq. (A.51) equals the trace of the inverse of the diagonalised bosonic correlator Γ :

$$I = \int \{\mathcal{D}\bar{b}'_i \mathcal{D}b'_i \mathcal{D}\bar{b}'_j \mathcal{D}b'_j\} e^{-\int_0^\beta d\tau \bar{B}\Gamma B} = \int_0^\beta d\tau \det \Gamma = e^{\int_0^\beta d\tau \text{Tr} \ln \Gamma^{-1}}. \quad (\text{A.70})$$

The partition function itself now takes the much simpler form of Eq. (2.24):

$$\mathcal{Z} = \int \{\mathcal{D}\phi\} e^{-\sum_i \int_0^\beta d\tau \left[\frac{1}{2U} (\dot{\phi}_i(\tau))^2 + \frac{\mu}{iU} \dot{\phi}_i(\tau) \right]} e^{\int_0^\beta d\tau \text{Tr} \ln \Gamma^{-1}}. \quad (\text{A.71})$$

Now that all the elements are in place, we can move out of matrix form by calculating the trace of the correlator Γ .

A.1.3 Trace calculations

Remembering that constants can be ignored in the path integral framework due to scale invariance, we rewrite the trace of the correlator in Eq. (A.71) as

$$\begin{aligned} \text{Tr} \ln \Gamma^{-1} = & - \left[\ln \left(-\frac{1}{2} \sqrt{\bar{\Delta}_i \Delta_i - S_{ij} \sqrt{\bar{\Delta}_i \Delta_i}} \right) + \ln \left(\frac{1}{2} \sqrt{\bar{\Delta}_i \Delta_i - S_{ij} \sqrt{\bar{\Delta}_i \Delta_i}} \right) + \right. \\ & \left. + \ln \left(-\frac{1}{2} \sqrt{\bar{\Delta}_i \Delta_i + S_{ij} \sqrt{\bar{\Delta}_i \Delta_i}} \right) + \ln \left(\frac{1}{2} \sqrt{\bar{\Delta}_i \Delta_i + S_{ij} \sqrt{\bar{\Delta}_i \Delta_i}} \right) \right] \end{aligned} \quad (\text{A.72})$$

$$\begin{aligned} = & - \ln \left[\left(-\frac{1}{2} \sqrt{\bar{\Delta}_i \Delta_i - S_{ij} \sqrt{\bar{\Delta}_i \Delta_i}} \right) \left(\frac{1}{2} \sqrt{\bar{\Delta}_i \Delta_i - S_{ij} \sqrt{\bar{\Delta}_i \Delta_i}} \right) \right. \\ & \left. \times \left(-\frac{1}{2} \sqrt{\bar{\Delta}_i \Delta_i + S_{ij} \sqrt{\bar{\Delta}_i \Delta_i}} \right) \left(\frac{1}{2} \sqrt{\bar{\Delta}_i \Delta_i + S_{ij} \sqrt{\bar{\Delta}_i \Delta_i}} \right) \right] \end{aligned} \quad (\text{A.73})$$

$$= - \ln \left[\frac{1}{16} \sqrt{\bar{\Delta}_i \Delta_i - S_{ij} \sqrt{\bar{\Delta}_i \Delta_i}}^2 \sqrt{\bar{\Delta}_i \Delta_i + S_{ij} \sqrt{\bar{\Delta}_i \Delta_i}}^2 \right] \quad (\text{A.74})$$

$$= - \ln \frac{1}{16} \ln \left[\left(\bar{\Delta}_i \Delta_i - S_{ij} \sqrt{\bar{\Delta}_i \Delta_i} \right) \left(\bar{\Delta}_i \Delta_i + S_{ij} \sqrt{\bar{\Delta}_i \Delta_i} \right) \right] \quad (\text{A.75})$$

$$= \ln 16 \ln \left[\left(\bar{\Delta}_i \Delta_i - S_{ij} \sqrt{\bar{\Delta}_i \Delta_i} \right) \left(\bar{\Delta}_i \Delta_i + S_{ij} \sqrt{\bar{\Delta}_i \Delta_i} \right) \right]. \quad (\text{A.76})$$

Further,

$$Tr \ln \Gamma^{-1} = \ln \left[(\bar{\Delta}_i \Delta_i)^2 - \left(S_{ij} \sqrt{\bar{\Delta}_i \Delta_i} \right)^2 \right] \quad (\text{A.77})$$

$$= \ln \left[(\bar{\Delta}_i \Delta_i)^2 - S_{ij}^2 \bar{\Delta}_i \Delta_i \right] \quad (\text{A.78})$$

$$= \ln \bar{\Delta}_i \Delta_i (\bar{\Delta}_i \Delta_i - S_{ij}^2) \quad (\text{A.79})$$

$$= \ln \bar{\Delta}_i \Delta_i + \ln (\bar{\Delta}_i \Delta_i - S_{ij}^2) \quad (\text{A.80})$$

$$= \ln (\bar{\Delta}_i \Delta_i - S_{ij}^2) \left[1 + \frac{\ln \bar{\Delta}_i \Delta_i}{\ln (\bar{\Delta}_i \Delta_i - S_{ij}^2)} \right] \quad (\text{A.81})$$

$$\approx \ln (\bar{\Delta}_i \Delta_i - S_{ij}^2). \quad (\text{A.82})$$

At this point, we separate the phase-phase correlator from the hopping terms in S_{ij} :

$$S_{ij} = G_0^{-1} + S'_{ij}, \quad (\text{A.83})$$

$$G_0^{-1} = \delta_{ij} \left(\frac{\partial}{\partial \tau} + \bar{\mu} \right), \quad (\text{A.84})$$

$$S'_{ij} = -J e^{-i\phi_{ij}(\tau)} - \frac{4\bar{\mu}}{U} J_{DIT} e^{-i\phi_{ij}(\tau)} - \frac{8}{U} J_{DIT}^2 e^{-i2\phi_{ij}(\tau)} \cdot (4 \langle \bar{b}_i b_j \rangle + \delta_{ij}). \quad (\text{A.85})$$

Rewriting the entire logarithm in Eq. (A.82),

$$\ln (\bar{\Delta}_i \Delta_i - S_{ij}^2) = \ln \left[\bar{\Delta}_i \Delta_i - \left(S'_{ij} + G_0^{-1} \right)^2 \right] \quad (\text{A.86})$$

$$= \ln \left\{ \bar{\Delta}_i \Delta_i - \left[\left(S'_{ij} \right)^2 + 2S'_{ij} G_0^{-1} + \left(G_0^{-1} \right)^2 \right] \right\} \quad (\text{A.87})$$

$$= \ln \left(G_0^{-1} \right)^2 \left[G_0^2 \bar{\Delta}_i \Delta_i - G_0^2 \left(S'_{ij} \right)^2 + 2S'_{ij} G_0 + 1 \right] \quad (\text{A.88})$$

$$= \ln \left(G_0^{-1} \right)^2 \ln \left[G_0^2 \bar{\Delta}_i \Delta_i - G_0^2 \left(S'_{ij} \right)^2 + 2S'_{ij} G_0 + 1 \right] \quad (\text{A.89})$$

$$= \ln \left\{ G_0^2 \left[\bar{\Delta}_i \Delta_i - \left(S'_{ij} \right)^2 \right] + 2S'_{ij} G_0 + 1 \right\}. \quad (\text{A.90})$$

Approximating $\ln(x+1) \approx x$ (for small x), we get

$$\ln \left\{ G_0^2 \left[\bar{\Delta}_i \Delta_i - \left(S'_{ij} \right)^2 \right] + 2S'_{ij} G_0 + 1 \right\} \approx G_0^2 \left[\bar{\Delta}_i \Delta_i - \left(S'_{ij} \right)^2 \right] + 2S'_{ij} G_0. \quad (\text{A.91})$$

All in all, the trace is replaced by the form in Eq. (2.27):

$$\text{Tr} \ln \Gamma^{-1} = G_0^2 \left[\bar{\Delta}_i \Delta_i - \left(S'_{ij} \right)^2 \right] + 2S'_{ij} G_0. \quad (\text{A.92})$$

The next step is to determine all the terms within this approximation, keeping in mind that both S'_{ij} , Eq. (A.85), and $\bar{\Delta}_i, \Delta_i$, Eqs. (A.53-A.54), contain bosonic averages.

A.1.3.1 Approximating the phase-phase correlator

The phase-phase correlator G_0 , Eq. (A.84), is approximated by the bosonic amplitude $G_0 = b_0^2$, which can be calculated by minimising the Hamiltonian at $b = b_0$:

$$\begin{aligned} \mathcal{H}(b_0) &= \frac{U}{2} \sum_i b_0^2 b_0^2 - J_{ij} \sum_{\langle i,j \rangle} b_0 b_0 + \\ &\quad - \sum_{\langle i,j \rangle} \left[\left(\frac{U}{2} + \mu \right) \delta_{ij} - 2(J_{DIT})_{ij} + 4(J_{DIT})_{ij} b_0^2 \right] b_0^2 \end{aligned} \quad (\text{A.93})$$

$$\begin{aligned} &= \frac{U}{2} \sum_i b_0^2 b_0^2 - J_{ij} \sum_{\langle i,j \rangle} b_0 b_0 + \\ &\quad - \sum_{\langle i,j \rangle} \left[4(J_{DIT})_{ij} b_0^2 - 2(J_{DIT})_{ij} \right] b_0^2 - \sum_i \left(\frac{U}{2} + \mu \right) b_0^2 \end{aligned} \quad (\text{A.94})$$

$$= N \left(\frac{U}{2} - 4z J_{DIT} \right) b_0^4 + N \left[2z J_{DIT} - (t - 2J_{DIT}) z - \left(\frac{U}{2} + \mu \right) \right] b_0^2 \quad (\text{A.95})$$

$$= N \left\{ \left(\frac{U}{2} - 4z J_{DIT} \right) b_0^4 - \left[z(t - 4J_{DIT}) + \left(\frac{U}{2} + \mu \right) \right] b_0^2 \right\}. \quad (\text{A.96})$$

The minimisation condition is

$$0 = \frac{\partial \mathcal{H}(b_0)}{\partial b_0} = \frac{\partial}{\partial b_0} N \left\{ \left(\frac{U}{2} - 4zJ_{DIT} \right) b_0^4 - \left[z(t - 4J_{DIT}) + \left(\frac{U}{2} + \mu \right) \right] b_0^2 \right\} \quad (\text{A.97})$$

$$= N \left\{ \left(\frac{U}{2} - 4zJ_{DIT} \right) 4b_0^3 - \left[z(t - 4J_{DIT}) + \left(\frac{U}{2} + \mu \right) \right] 2b_0 \right\} \quad (\text{A.98})$$

$$= \left\{ 4 \left(\frac{U}{2} - 4zJ_{DIT} \right) b_0^2 - 2 \left[z(t - 4J_{DIT}) + \left(\frac{U}{2} + \mu \right) \right] \right\}, \quad (\text{A.99})$$

giving the amplitude in Eq. (2.26),

$$b_0^2 = \frac{z(t - 4J_{DIT}) + \left(\frac{U}{2} + \mu \right)}{U - 8zJ_{DIT}}. \quad (\text{A.100})$$

The current form of the trace of the correlation function, Eq. (A.92), is therefore

$$\text{Tr} \ln \Gamma^{-1} = b_0^4 \left[\bar{\Delta}_i \Delta_i - \left(S'_{ij} \right)^2 \right] + 2S'_{ij} b_0^2 \quad (\text{A.101})$$

$$= \left[\frac{z(t - 4J_{DIT}) + \left(\frac{U}{2} + \mu \right)}{U - 8zJ_{DIT}} \right]^2 \left[\bar{\Delta}_i \Delta_i - \left(S'_{ij} \right)^2 \right] + 2S'_{ij} \frac{z(t - 4J_{DIT}) + \left(\frac{U}{2} + \mu \right)}{U - 8zJ_{DIT}}. \quad (\text{A.102})$$

The last step in calculating the trace is inserting diagonal and anomalous bosonic averages into S'_{ij} , Eq. (A.85), and $\bar{\Delta}_i, \Delta_i$, Eqs. (A.53-A.54).

A.1.3.2 Bosonic averages

The diagonal average in Eq. (A.85),

$$\langle \bar{b}_i b_j \rangle = \frac{\int \{ \mathcal{D}\phi_i \} e^{-i[\phi_i(\tau) - \phi_j(\tau')]} \exp \left\{ \int_0^\beta d\tau \sum_i \left[\frac{1}{2U} \left(\dot{\phi}_i(\tau) \right)^2 + \frac{\bar{\mu}}{iU} \dot{\phi}_i(\tau) \right] \right\}}{\int \{ \mathcal{D}\phi_i \} \exp \left\{ \int_0^\beta d\tau \sum_i \left[\frac{1}{2U} \left(\dot{\phi}_i(\tau) \right)^2 + \frac{\bar{\mu}}{iU} \dot{\phi}_i(\tau) \right] \right\}}, \quad (\text{A.103})$$

is treated the same as in the standard Bose-Hubbard model [46]. Winding numbers n_i are separated from the phase and the phase integrated, after which the average can be summed over n_i . After Matsubara transform,

$$\langle \bar{b}_i b_j \rangle = \delta_{ij} e^{\frac{U}{2} |\tau - \tau'|} \frac{\sum_{n_i} \exp \left[-\frac{U\beta}{2} \left(n_i + \frac{\bar{\mu}}{U} \right)^2 \right] \exp \left[-U \left(n_i + \frac{\bar{\mu}}{U} \right) (\tau - \tau') \right]}{\sum_{n_i} \exp \left[-\frac{U\beta}{2} \left(n_i + \frac{\bar{\mu}}{U} \right)^2 \right]} = \quad (\text{A.104})$$

$$= \delta_{ij} \frac{1}{\frac{U}{4} - \frac{1}{U} (\bar{\mu} - i\omega_m^2)}, \quad (\text{A.105})$$

where $\omega_m = 2\pi\beta m$ are the Matsubara frequencies. This can be further summed over ω_m , giving

$$\langle \bar{b}_i b_j \rangle = \delta_{ij} \frac{\coth \left[\frac{\beta}{2} \left(\frac{U}{2} - \bar{\mu} \right) \right] + \coth \left[\frac{\beta}{2} \left(\frac{U}{2} + \bar{\mu} \right) \right]}{2}. \quad (\text{A.106})$$

With that, the diagonal term is

$$S'_{ij} = -J e^{-i\phi_{ij}(\tau)} - \frac{4\bar{\mu}}{U} J_{DIT} e^{-i\phi_{ij}(\tau)} - \frac{8}{U} J_{DIT}^2 \cdot \alpha, \quad (\text{A.107})$$

where we have designated

$$\alpha = 2 \left\{ \coth \left[\frac{\beta}{2} \left(\frac{U}{2} - \bar{\mu} \right) \right] + \coth \left[\frac{\beta}{2} \left(\frac{U}{2} + \bar{\mu} \right) \right] \right\}. \quad (\text{A.108})$$

Since in the quantum rotor method the amplitude of field operators is constant, the anomalous averages in Eqs. (A.53-A.54) can be rewritten as

$$\langle b_i b_i \rangle = b_0^2 \langle e^{i2\phi_i} \rangle = b_0^2 \Psi_2, \quad (\text{A.109})$$

$$\langle \bar{b}_i \bar{b}_i \rangle = b_0^2 \langle e^{-i2\phi_i} \rangle = b_0^2 \Psi_2, \quad (\text{A.110})$$

where Ψ_2 is the pair condensation order parameter. The chirality of the phase is neglected; the anomalous averages are assumed to be the same in both directions.

Thus, the anomalous term in Eq. (A.102) is

$$\bar{\Delta}_i \Delta_i = \left(-\frac{8}{U} J_{DIT}^2 e^{-i2\phi_{ij}(\tau)} \right)^2 \cdot b_0^2 \Psi_2 b_0^2 \Psi_2 = \left(\frac{8J_{DIT}^2 b_0^2}{U} \right)^2 e^{-i4\phi_{ij}(\tau)} \Psi_2^2 \quad (\text{A.111})$$

$$= \left[\frac{z(t - 4J_{DIT}) + \left(\frac{U}{2} + \mu\right) \frac{8J_{DIT}^2}{U}}{U - 8zJ_{DIT}} \right]^2 e^{-i4\phi_{ij}(\tau)} \Psi_2^2. \quad (\text{A.112})$$

We limit further calculations to $2\phi_{ij}$, which means the anomalous $\bar{\Delta}_i \Delta_i$ term does not contribute to the effective action at all.

Returning to the trace in Eq. (A.102),

$$\begin{aligned} Tr \ln \Gamma^{-1} &= \left[\frac{z(t - 4J_{DIT}) + \left(\frac{U}{2} + \mu\right)}{U - 8zJ_{DIT}} \right]^2 \left[\bar{\Delta}_i \Delta_i - \left(S'_{ij}\right)^2 \right] + \\ &\quad + 2S'_{ij} \frac{z(t - 4J_{DIT}) + \left(\frac{U}{2} + \mu\right)}{U - 8zJ_{DIT}} \end{aligned} \quad (\text{A.113})$$

$$= \frac{z(t - 4J_{DIT}) + \left(\frac{U}{2} + \mu\right)}{U - 8zJ_{DIT}} \cdot g_{ij}, \quad (\text{A.114})$$

where

$$g_{ij} = \frac{z(t - 4J_{DIT}) + \left(\frac{U}{2} + \mu\right)}{U - 8zJ_{DIT}} \left[\bar{\Delta}_i \Delta_i - \left(S'_{ij}\right)^2 \right] + 2S'_{ij}. \quad (\text{A.115})$$

We approximate g_{ij} up to $\exp(2\phi_{ij})$:

$$\begin{aligned}
g_{ij} = & -\frac{z(t - 4J_{DIT}) + \left(\frac{U}{2} + \mu\right)}{U - 8zJ_{DIT}} \\
& \times \left(-Je^{-i\phi_{ij}(\tau)} - \frac{4\bar{\mu}}{U}J_{DIT}e^{-i\phi_{ij}(\tau)} - \frac{8}{U}J_{DIT}^2 \cdot \alpha \right)^2 + \\
& + 2 \left(-Je^{-i\phi_{ij}(\tau)} - \frac{4\bar{\mu}}{U}J_{DIT}e^{-i\phi_{ij}(\tau)} - \frac{8}{U}J_{DIT}^2 \cdot \alpha \right) \quad (A.116)
\end{aligned}$$

$$\begin{aligned}
= & -2Je^{-i\phi_{ij}(\tau)} - \frac{8\bar{\mu}}{U}J_{DIT}e^{-i\phi_{ij}(\tau)} - \frac{16}{U}J_{DIT}^2 \cdot \alpha + \\
& -\frac{z(t - 4J_{DIT}) + \left(\frac{U}{2} + \mu\right)}{U - 8zJ_{DIT}} \cdot g_{ij}^{(2)}. \quad (A.117)
\end{aligned}$$

Further transformations on the second order term $g_{ij}^{(2)}$:

$$g_{ij}^{(2)} = \left[-Je^{-i\phi_{ij}(\tau)} - \frac{4\bar{\mu}}{U} J_{DIT} e^{-i\phi_{ij}(\tau)} - \frac{8}{U} J_{DIT}^2 \cdot \alpha \right]^2 \quad (\text{A.118})$$

$$\begin{aligned} &= (Je^{-i\phi_{ij}(\tau)})^2 + \left(\frac{4\bar{\mu}}{U} J_{DIT} e^{-i\phi_{ij}(\tau)} \right)^2 + \left(\frac{8}{U} J_{DIT}^2 \cdot \alpha \right)^2 + \\ &\quad + 2(-Je^{-i\phi_{ij}(\tau)}) \left(-\frac{4\bar{\mu}}{U} J_{DIT} e^{-i\phi_{ij}(\tau)} \right) + \\ &\quad + 2(-Je^{-i\phi_{ij}(\tau)}) \left(-\frac{8}{U} J_{DIT}^2 \cdot \alpha \right) + \\ &\quad + 2 \left(-\frac{4\bar{\mu}}{U} J_{DIT} e^{-i\phi_{ij}(\tau)} \right) \left(-\frac{8}{U} J_{DIT}^2 \cdot \alpha \right) \end{aligned} \quad (\text{A.119})$$

$$\begin{aligned} &= (Je^{-i\phi_{ij}(\tau)})^2 + \left(\frac{4\bar{\mu}}{U} J_{DIT} e^{-i\phi_{ij}(\tau)} \right)^2 + C + \\ &\quad + 2Je^{-i\phi_{ij}(\tau)} \frac{4\bar{\mu}}{U} J_{DIT} e^{-i\phi_{ij}(\tau)} + \\ &\quad + 2Je^{-i\phi_{ij}(\tau)} \frac{8}{U} J_{DIT}^2 \cdot \alpha + 2 \frac{4\bar{\mu}}{U} J_{DIT} e^{-i\phi_{ij}(\tau)} \frac{8}{U} J_{DIT}^2 \cdot \alpha \end{aligned} \quad (\text{A.120})$$

$$\begin{aligned} &= J^2 e^{-2i\phi_{ij}(\tau)} + \left(\frac{4\bar{\mu}}{U} J_{DIT} \right)^2 e^{-2i\phi_{ij}(\tau)} + \frac{8\bar{\mu}}{U} J J_{DIT} e^{-2i\phi_{ij}(\tau)} + \\ &\quad + \frac{16}{U} J J_{DIT}^2 \cdot \alpha e^{-i\phi_{ij}(\tau)} + \left(\frac{64\bar{\mu}}{U^2} J_{DIT}^3 \cdot \alpha \right) e^{-i\phi_{ij}(\tau)} \end{aligned} \quad (\text{A.121})$$

$$\begin{aligned} &= \left(\frac{64\bar{\mu}}{U^2} J_{DIT}^3 + \frac{16}{U} J J_{DIT}^2 \right) \cdot \alpha e^{-i\phi_{ij}(\tau)} + \\ &\quad + \left[J^2 + \left(\frac{4\bar{\mu}}{U} J_{DIT} \right)^2 + \frac{8\bar{\mu}}{U} J J_{DIT} \right] e^{-2i\phi_{ij}(\tau)}. \end{aligned} \quad (\text{A.122})$$

This concludes the trace calculations. We return a final time to the full trace of the

Nambu-like propagator matrix, Eq. (A.114),

$$\begin{aligned}
Tr \ln \Gamma^{-1} = & - \left[J^2 + \left(\frac{4\bar{\mu}}{U} J_{DIT} \right)^2 + \frac{8\bar{\mu}}{U} J J_{DIT} \right] \left[\frac{z(t - 4J_{DIT}) + \left(\frac{U}{2} + \mu \right)}{U - 8zJ_{DIT}} \right]^2 e^{-i2\phi_{ij}(\tau)} + \\
& - \left(\frac{64\bar{\mu}}{U^2} J_{DIT}^3 + \frac{16}{U} J J_{DIT}^2 \right) \cdot \left[\frac{z(t - 4J_{DIT}) + \left(\frac{U}{2} + \mu \right)}{U - 8zJ_{DIT}} \right]^2 \alpha e^{-i\phi_{ij}(\tau)} + \\
& - \left(2J + \frac{8\bar{\mu}}{U} J_{DIT} \right) \frac{z(t - 4J_{DIT}) + \left(\frac{U}{2} + \mu \right)}{U - 8zJ_{DIT}} e^{-i\phi_{ij}(\tau)}, \tag{A.123}
\end{aligned}$$

which can enter the partition function to form the effective phase-only model.

A.1.4 Effective phase model

Assuming $U \rightarrow \infty$, which is a reasonable condition for this model, we can ignore the troublesome complex phase term in \mathcal{S}_ϕ in Eq. (A.44); the final form of the partition function, Eq. (2.28), is

$$\mathcal{Z} = \int \{ \mathcal{D}\phi \} e^{-\sum_i \int_0^\beta d\tau \frac{1}{2U} (\dot{\phi}_i(\tau))^2 + \sum_{\langle i,j \rangle} \int_0^\beta d\tau (g_1 e^{-i\phi_{ij}(\tau)} + g_2 e^{-i2\phi_{ij}(\tau)})}, \tag{A.124}$$

where

$$\begin{aligned}
g_1 = & \left[\left(\frac{64\bar{\mu}}{U^2} - \frac{32}{U} \right) J_{DIT}^3 + \frac{16}{U} t J_{DIT}^2 \right] \left[\frac{z(t - 4J_{DIT}) + \left(\frac{U}{2} + \mu \right)}{U - 8zJ_{DIT}} \right]^2 \cdot \alpha + \\
& - \left(2t + \frac{8\bar{\mu}}{U} J_{DIT} - 4J_{DIT} \right) \frac{z(t - 4J_{DIT}) + \left(\frac{U}{2} + \mu \right)}{U - 8zJ_{DIT}}, \tag{A.125}
\end{aligned}$$

$$\begin{aligned}
g_2 = & \left[\frac{z(t - 4J_{DIT}) + \left(\frac{U}{2} + \mu \right)}{U - 8zJ_{DIT}} \right]^2 \left[(t - 2J_{DIT})^2 + \left(\frac{4\bar{\mu}}{U} J_{DIT} \right)^2 \right] + \\
& + \left[\frac{z(t - 4J_{DIT}) + \left(\frac{U}{2} + \mu \right)}{U - 8zJ_{DIT}} \right]^2 \left[2(t - 2J_{DIT}) \frac{8\bar{\mu}}{U} J_{DIT} \right] \tag{A.126}
\end{aligned}$$

and inserting the chemical potential in Eq. (A.15) into the parameter α , Eq. (A.108), we get

$$\alpha = 2 \left\{ \coth \left[\frac{\beta}{2} \left(\frac{U}{2} - \frac{U}{2} + \mu - 2J_{DIT} \right) \right] + \coth \left[\frac{\beta}{2} \left(\frac{U}{2} + \frac{U}{2} + \mu - 2J_{DIT} \right) \right] \right\} \quad (\text{A.127})$$

$$= 2 \left\{ \coth \left[\frac{\beta}{2} (\mu - 2J_{DIT}) \right] + \coth \left[\frac{\beta}{2} (U + \mu - 2J_{DIT}) \right] \right\}, \quad (\text{A.128})$$

thus obtaining the forms in Eqs. (2.29-2.30).

Having derived the effective phase model, we move onto analysing specifics. To that end, we apply an $S = 1$ pseudospin mapping.

A.2 Pseudospin mapping

The phase terms are transformed into spin operators as shown in Section 1.2.2, using the eigenstates of the number operator,

$$\langle k | N(\phi) | m \rangle = \int_0^{2\pi} \frac{d\phi}{2\pi} e^{-ik\phi} \left(\frac{1}{i} \frac{\partial}{\partial \phi} \right) e^{im\phi} = m \delta_{k,m}, \quad (\text{A.129})$$

which extends to trigonometric functions as

$$\langle k | \cos \phi | m \rangle = \int_0^{2\pi} \frac{d\phi}{2\pi} e^{-i(k-m)\phi} \cos \phi = \frac{1}{2} (\delta_{k-m-1,0} + \delta_{k-m+1,0}), \quad (\text{A.130})$$

$$\langle k | \sin \phi | m \rangle = \frac{i}{2} (\delta_{k-m-1,0} - \delta_{k-m+1,0}). \quad (\text{A.131})$$

To obtain $S = 1$, k, m are limited to the lowest-energy states: $-1, 0, 1$ at $k_B T/U < 1$, as in Eqs. (2.32-2.34):

$$N(\phi) = S_z, \quad (\text{A.132})$$

$$\cos \phi_i = \frac{1}{\sqrt{2}} S_i^x, \quad (\text{A.133})$$

$$\sin \phi_i = \frac{1}{\sqrt{2}} S_i^y. \quad (\text{A.134})$$

Introducing quadrupolar superexchange operators as in Eqs. (2.35-2.36),

$$Q_i = (S_i^x)^2 - (S_i^y)^2, \quad (\text{A.135})$$

$$Q_i^{xy} = 2S_i^x S_i^y, \quad (\text{A.136})$$

the $S = 1$ pseudospin Hamiltonian is

$$\mathcal{H} = U \sum_i (S_i^z)^2 - \frac{1}{2} g_1 \sum_{\langle i,j \rangle} (S_i^x S_j^x + S_i^y S_j^y) - \frac{1}{4} g_2 \sum_{\langle i,j \rangle} (Q_i Q_j + Q_i^{xy} Q_j^{xy}). \quad (\text{A.137})$$

The mean field approximation is next, assuming that due to rotational symmetry in the XY plane $\langle S_i^y \rangle = 0$ and $\langle Q_i^{xy} \rangle = 0$,

$$S_i^x S_j^x \approx \langle S_i^x \rangle S_j^x + S_i^x \langle S_j^x \rangle - \langle S_i^x \rangle \langle S_j^x \rangle \quad (\text{A.138})$$

$$Q_i Q_j \approx \langle Q_i \rangle Q_j + Q_i \langle Q_j \rangle - \langle Q_i \rangle \langle Q_j \rangle \quad (\text{A.139})$$

The mean field approximated hamiltonian, Eq. (2.37), is

$$\mathcal{H}_{MF} = U (S_i^z)^2 - \frac{1}{2} z g_1 S_i^x \langle S_i^x \rangle - \frac{1}{4} z g_2 (Q_i \langle Q_i \rangle) \quad (\text{A.140})$$

$$= J \left[\frac{U}{J} (S_i^z)^2 - S_i^x \Psi_\phi - \frac{J_2}{J} Q_i \Psi_{2\phi} \right]. \quad (\text{A.141})$$

The new condensate coefficients are

$$J = \frac{1}{2}z g_1, \quad (\text{A.142})$$

$$J_2 = \frac{1}{4}z g_2. \quad (\text{A.143})$$

The $\frac{1}{2}$ and the $\frac{1}{4}$ stem from the spin transformation itself, and z enters via mean field approximation.

The single Ψ_ϕ and pair $\Psi_{2\phi}$ condensate order parameters are defined as in Eqs. (2.40-2.41),

$$\Psi_\phi = \langle S_i^x \rangle, \quad (\text{A.144})$$

$$\Psi_{2\phi} = \langle Q_i \rangle, \quad (\text{A.145})$$

and minimise the on-site free energy, Eq. (2.42),

$$f = \frac{1}{2} (J\Psi_\phi^2 + J_2\Psi_{2\phi}^2) - \frac{1}{\beta} \ln Z, \quad (\text{A.146})$$

where the partition function,

$$Z = \text{Tr} \{ e^{-\beta H} \} = \sum_{n=1}^3 e^{-\beta E_n} \quad (\text{A.147})$$

$$= e^{-\beta(U+J_2\Psi_{2\phi})} + 2e^{\beta J_2\Psi_{2\phi}/2 - \beta U/2} \cosh \left(\frac{\beta}{2} \sqrt{(U - J\Psi_\phi)^2 + 4J^2\Psi_\phi^2} \right), \quad (\text{A.148})$$

is calculated from the system's eigenvalues, E_n :

$$E_1 = (J_2\Psi_{2\phi} + U), \quad (\text{A.149})$$

$$E_2 = \frac{1}{2} \left[U - J_2\Psi_{2\phi} - \frac{1}{2} \sqrt{16J^2\Psi_\phi^2 + (2J_2\Psi_{2\phi} - 2U)^2} \right], \quad (\text{A.150})$$

$$E_3 = \frac{1}{2} \left[U - J_2\Psi_{2\phi} + \frac{1}{2} \sqrt{16J^2\Psi_\phi^2 + (2J_2\Psi_{2\phi} - 2U)^2} \right]. \quad (\text{A.151})$$

The critical line equations are as in Eq. (2.43),

$$\frac{\partial f}{\partial \Psi_\phi} = 0, \quad \frac{\partial f}{\partial \Psi_{2\phi}} = 0, \quad (\text{A.152})$$

and expanded become the self-consistent equations in Eqs. (2.44-2.45),

$$1 = \frac{4J \tanh\left(\frac{\beta}{2} \sqrt{(U - J_2 \Psi_{2\phi})^2 + 4J^2 \Psi_\phi^2}\right)}{\sqrt{(U - J_2 \Psi_{2\phi})^2 + 4J^2 \Psi_\phi^2} [X + 2]}, \quad (\text{A.153})$$

$$\Psi_{2\phi} = \frac{U}{J_2 - 4J} + \frac{4J}{4J - J_2} \cdot \frac{1 - X}{2 + X}, \quad (\text{A.154})$$

where

$$X = \frac{e^{-\frac{\beta}{2}(U + 3J_2 \Psi_{2\phi})}}{\cosh\left(\frac{\beta}{2} \sqrt{(U - J_2 \Psi_{2\phi})^2 + 4J^2 \Psi_\phi^2}\right)}. \quad (\text{A.155})$$

These equations are ready for numerical solving for any thermodynamic properties of the two condensates.

Appendix B

Dissipative interaction-based pairing: calculations

We start with the effective phase model with interaction-based pairing. As in Eqs. (3.1-3.4) in Chapter 3, the effective action of the model,

$$\mathcal{S}[\phi] = \mathcal{S}_U[\phi] + \mathcal{S}_1[\phi] + \mathcal{S}_2[\phi], \quad (\text{B.1})$$

can be divided into three terms: interaction,

$$\mathcal{S}_U[\phi] = \frac{1}{2U} \sum_{\langle i,j \rangle} \int_0^\beta d\tau \left(\frac{\partial \phi_i}{\partial \tau} \right)^2 + \frac{\bar{\mu}}{iU} \dot{\phi}_i(\tau), \quad (\text{B.2})$$

single condensation,

$$\mathcal{S}_1[\phi] = g_1 \sum_{\langle i,j \rangle} \int_0^\beta d\tau \cos[\phi_i(\tau) - \phi_j(\tau)], \quad (\text{B.3})$$

and pair condensation,

$$\mathcal{S}_2[\phi] = g_2 \sum_{\langle i,j \rangle} \int_0^\beta d\tau \cos 2[\phi_i(\tau) - \phi_j(\tau)]. \quad (\text{B.4})$$

B.1 Coefficients

The standard approach bases on the effective phase model in Eq. (2.28), where the phase-phase correlator G_0 , Eq. (2.16), is replaced with the constant amplitude b_0 in Eq. (2.26), as shown in more detail in Section A.1.3.1. In that case, the single and pair coefficients g_1 , Eq. (3.6), and g_2 , Eq. (3.7), are as in Eqs. (A.125) and (A.126), respectively:

$$g_1 = \left[\left(\frac{64\bar{\mu}}{U^2} - \frac{32}{U} \right) J_{DIT}^3 + \frac{16}{U} t J_{DIT}^2 \right] \left[\frac{z(t - 4J_{DIT}) + \left(\frac{U}{2} + \mu\right)}{U - 8zJ_{DIT}} \right]^2 \cdot \alpha + \\ - \left(2t + \frac{8\bar{\mu}}{U} J_{DIT} - 4J_{DIT} \right) \frac{z(t - 4J_{DIT}) + \left(\frac{U}{2} + \mu\right)}{U - 8zJ_{DIT}}, \quad (\text{B.5})$$

$$g_2 = \left[\frac{z(t - 4J_{DIT}) + \left(\frac{U}{2} + \mu\right)}{U - 8zJ_{DIT}} \right]^2 \left[(t - 2J_{DIT})^2 + \left(\frac{4\bar{\mu}}{U} J_{DIT} \right)^2 \right] + \\ + \left[\frac{z(t - 4J_{DIT}) + \left(\frac{U}{2} + \mu\right)}{U - 8zJ_{DIT}} \right]^2 \left[2(t - 2J_{DIT}) \frac{8\bar{\mu}}{U} J_{DIT} \right], \quad (\text{B.6})$$

where

$$\alpha = 2 \left\{ \coth \left[\frac{\beta}{2} \left(\frac{U}{2} - \frac{U}{2} + \mu - 2J_{DIT} \right) \right] + \coth \left[\frac{\beta}{2} \left(\frac{U}{2} + \frac{U}{2} + \mu - 2J_{DIT} \right) \right] \right\} \quad (\text{B.7})$$

$$= 2 \left\{ \coth \left[\frac{\beta}{2} (\mu - 2J_{DIT}) \right] + \coth \left[\frac{\beta}{2} (U + \mu - 2J_{DIT}) \right] \right\}. \quad (\text{B.8})$$

A second, more robust approach is also considered, based on conserving the original correlator G_0 , Eq. (2.16). We are interested in what sort of imaginary time dependence is generated, keeping in mind how dissipative terms are represented in the effective action [6].

B.1.1 Derivation of imaginary time coefficients

We return to the trace of the density-induced tunnelling BHM correlator, Eq. (A.92) in Appendix A:

$$\text{Tr} \ln \Gamma^{-1} = G_0^2 \left[\bar{\Delta}_i \Delta_i - \left(S'_{ij} \right)^2 \right] + 2S'_{ij} G_0, \quad (\text{B.9})$$

with phase-phase correlator as in Eq. (2.16),

$$G_0^{-1} = \left(\frac{\partial}{\partial \tau} + \bar{\mu} \right), \quad (\text{B.10})$$

the tunnelling S'_{ij} , Eq. (A.85), and the non-diagonal terms $\bar{\Delta}_i, \Delta_i$, Eqs. (A.53-A.54),

$$S'_{ij} = -J e^{-i\phi_{ij}(\tau)} - \frac{4\bar{\mu}}{U} T e^{-i\phi_{ij}(\tau)} - \frac{8}{U} T^2 e^{-i2\phi_{ij}(\tau)} \cdot (4 \langle \bar{b}_i b_j \rangle + \delta_{ij}), \quad (\text{B.11})$$

$$\Delta_i = -\frac{8}{U} T^2 e^{-i2\phi_{ij}(\tau)} \langle b_i b_i \rangle, \quad (\text{B.12})$$

$$\bar{\Delta}_i = -\frac{8}{U} T^2 e^{-i2\phi_{ij}(\tau)} \langle \bar{b}_i \bar{b}_i \rangle. \quad (\text{B.13})$$

In this model, we preserve the original form of G_0 , Eq. (B.10), which after Matsubara transform becomes Eq. (3.8):

$$G_0 = \frac{-i\omega_m + \bar{\mu}}{\omega_m^2 + \bar{\mu}^2}. \quad (\text{B.14})$$

The trace in Eq. (B.9) also contains G_0^2 , which is

$$G_0^2 = (-i\omega_m + \bar{\mu})^{-2} = \frac{1}{(-i\omega_m + \bar{\mu})^2}. \quad (\text{B.15})$$

Thus, the single and pair coefficients of this effective phase model, Eqs. (3.11,3.12) depend on imaginary time:

$$g'_1(\omega_m) = -\frac{-i\omega_m + \bar{\mu}}{\omega_m^2 + \bar{\mu}^2} \left[2(t - 2J_{DIT}) + \frac{8\bar{\mu}}{U} J_{DIT} \right] + \quad (\text{B.16})$$

$$+ \frac{1}{(-i\omega_m + \bar{\mu})^2} \left(\frac{64\bar{\mu}}{U^2} J_{DIT}^3 + \frac{16}{U} J J_{DIT}^2 \right) \quad (\text{B.17})$$

$$\times \left\{ 2 \left[\coth \left(-\frac{\beta\mu}{2} \right) + \coth \left(\frac{\beta(\mu + U)}{2} \right) \right] + 1 \right\}, \quad (\text{B.18})$$

$$g'_2(\omega_m) = \frac{1}{(-i\omega_m + \bar{\mu})^2} \times \left[(t - 2J_{DIT})^2 + \left(\frac{4\bar{\mu}}{U} J_{DIT} \right)^2 + 2(t - 2J_{DIT}) \frac{8\bar{\mu}}{U} J_{DIT} \right]. \quad (\text{B.19})$$

Imaginary time-dependent terms are present in both condensation parts of the effective phase model, \mathcal{S}_1 in Eq. (B.3) and \mathcal{S}_2 in Eq. (B.4). The single coefficient g'_1 generates two contributions, one of which has an additional dissipation-like impact, Eq. (B.16). However, this term depends on higher orders of J_{DIT}/U than g'_2 in Eq. (B.19), so at $J_{DIT}/U \ll 1$ the pair dissipation is much stronger. The second g'_1 contribution, Eq. (B.17), is negligible in low temperatures after Matsubara summation. As our focus is on the pair condensate, we forgo the marginally relevant contributions introduced by the single condensation coefficient g'_1 and replace it with the approximated g_1 of Eq. (B.5), focusing on the properties of the pairing mechanism in low temperatures.

The effective action remains the same, Eq. (B.1). We rewrite the pair term, \mathcal{S}'_2 , to separate the imaginary time dependency from the pair coefficient g'_2 , as in Eq. (3.13):

$$\mathcal{S}'_2[\phi] = g'_2 \sum_{\langle i,j \rangle} \int_0^\beta d\tau d\tau' \frac{1}{(\tau - \tau')^2} \cos 2 \left[\phi_i(\tau) - \phi_j(\tau') \right], \quad (\text{B.20})$$

where

$$g'_2 = (t - 2J_{DIT})^2 + \left(\frac{4\bar{\mu}}{U} J_{DIT} \right)^2 + 2(t - 2J_{DIT}) \frac{8\bar{\mu}}{U} J_{DIT} \quad (\text{B.21})$$

is the derived pair condensate coefficient.

B.2 Dissipative models

Traditionally, dissipative terms are added to many body Hamiltonians as arbitrary external factors. In this model, however, the microscopic Hamiltonian already contains the relevant term. We implement a series expansion of the double cosine to second order as

$$\cos(2x) = 1 - 2x^2 + \mathcal{O}(x^3), \quad (\text{B.22})$$

after which, following Caldeira and Leggett, 1981 [6], the pair condensation part of the effective action \mathcal{S}'_2 in Eq. (B.20) can be rewritten as explicitly dissipative, as in Eq. (3.15):

$$\mathcal{S}'_2[\phi] = 2g'_2 \sum_{\langle i,j \rangle} \int_0^\beta d\tau d\tau' \frac{1}{(\tau - \tau')^2} \left[\phi_i(\tau) - \phi_j(\tau') \right]^2. \quad (\text{B.23})$$

In the b_0 -approximated version of the model, with g_2 in Eq. (B.6), the imaginary time factor does not emerge naturally. To study the dissipative effect of the pair term in Eq. (B.4), we treat it as a bath of harmonic potential, artificially coupled to the single particle condensate defined by Eqs. (B.2-B.3). The pairing term \mathcal{S}_2 of the assumed model, Eq. (B.4), is series expanded to second order and assumed to be dissipative as well, as in Eq. (3.16):

$$\mathcal{S}_2[\phi] = 2g_2 \sum_{\langle i,j \rangle} \int_0^\beta d\tau d\tau' \left[\frac{\phi_i(\tau) - \phi_j(\tau')}{\tau - \tau'} \right]^2. \quad (\text{B.24})$$

Ultimately, since \mathcal{S}_2 has the same form in Eqs. (B.23) and (B.24), the two approaches differ only by their pair condensate coefficients:

$$\begin{array}{rcl}
 & & b_0 \text{ coupled condensates} \quad \rightarrow g_1 \text{ single particle} \\
 & & \quad \quad \quad \quad \quad \quad \quad \rightarrow g_2 \text{ pair} \\
 G_0 \begin{array}{l} \nearrow \\ \searrow \end{array} & & \\
 & & G_0 \text{ full treatment} \quad \rightarrow g'_1 \quad \rightarrow g_1 \text{ single particle} \\
 & & \quad \quad \quad \quad \quad \quad \quad \rightarrow g'_2 \text{ pair}
 \end{array} \quad (\text{B.25})$$

While the idea of coupling a single particle condensate with an external dissipative term

is widely accepted and utilised, the derived version of \mathcal{S}_2 exhibits intrinsic dissipative properties.

B.2.1 Preparing dissipative effective action

We move on with a single model, as defined by Eq. (B.1), and analyse it in terms of both the assumed g_2 , Eq. (B.6), and the derived g'_2 , Eq. (B.21). In order to map the model onto pseudospin and introduce the quantum spherical model,

We rewrite the quadratic term in \mathcal{S}_2 , Eq. (B.24) as:

$$[\phi_i(\tau) - \phi_j(\tau)]^2 = \phi_i^2(\tau) - 2\phi_i(\tau)\phi_j(\tau) + \phi_j^2(\tau) \quad (\text{B.26})$$

and rearrange the index:

$$\sum_{i,j} \phi_i^2(\tau) = N \sum_{i,j} \phi_i(\tau)\phi_j(\tau)\delta_{ji} = N \sum_{i,j} \int_0^\beta d\tau \phi_i(\tau)\phi_j(\tau)\delta_{ji}, \quad (\text{B.27})$$

$$-2\phi_i(\tau)\phi_j(\tau) = -2 \int_0^\beta d\tau \phi_i(\tau)\phi_j(\tau), \quad (\text{B.28})$$

$$\sum_{i,j} \phi_j^2(\tau) = N \sum_{i,j} \phi_i(\tau)\phi_j(\tau)\delta_{ji} = N \sum_{i,j} \int_0^\beta d\tau \phi_i(\tau)\phi_j(\tau)\delta_{ji}. \quad (\text{B.29})$$

At this point,

$$\sum_{i,j} [\phi_i(\tau) - \phi_j(\tau')]^2 = 2 \sum_{i,j} \int_0^\beta d\tau (N\delta_{ji} - 1) \phi_i(\tau)\phi_j(\tau') I_{ij}, \quad (\text{B.30})$$

where additionally

$$N \sum_{i,j} I_{ij} \delta_{ij} \phi_i(\tau)\phi_j(\tau') = 0, \quad (\text{B.31})$$

meaning the dissipative action itself, Eq. (B.24), takes the form

$$\mathcal{S}_2 = \sum_{i,j} \int_0^\beta d\tau \frac{4g_2}{\tau^2} \phi_i(\tau)\phi_j(\tau) I_{ij}. \quad (\text{B.32})$$

To obtain a Gaussian form in terms of phase exponential terms, we carry out the following transformation:

$$e^{i\phi(\tau)} = \psi, \quad (\text{B.33})$$

$$e^{-i\phi(\tau)} = \psi^*, \quad (\text{B.34})$$

for which the derivatives will be

$$\frac{\partial}{\partial \tau} \psi = \frac{\partial}{\partial \tau} e^{i\phi(\tau)} = i \frac{\partial \phi}{\partial \tau} e^{i\phi(\tau)} = i \frac{\partial \phi}{\partial \tau} \psi, \quad (\text{B.35})$$

$$\frac{\partial}{\partial \tau} \psi^* = \frac{\partial}{\partial \tau} e^{-i\phi(\tau)} = -i \frac{\partial \phi}{\partial \tau} e^{-i\phi(\tau)} = -i \frac{\partial \phi}{\partial \tau} \psi^*, \quad (\text{B.36})$$

$$\frac{\partial \psi}{\partial \tau} \frac{\partial \psi^*}{\partial \tau} = i \frac{\partial \phi}{\partial \tau} \psi (-i) \frac{\partial \phi}{\partial \tau} \psi^* = \left(\frac{\partial \phi}{\partial \tau} \right)^2 |\psi|^2 = \left(\frac{\partial \phi}{\partial \tau} \right)^2. \quad (\text{B.37})$$

After Fourier and Matsubara transforms, the effective action terms in Eq. (B.1) are as follows: interaction

$$\mathcal{S}_U[\psi] = \frac{1}{2U\beta N} \sum_{ij} \sum_m \sum_k \omega_m^2 \psi_{k,m} \psi_{-k,m}; \quad (\text{B.38})$$

single particle condensation

$$\mathcal{S}_1[\phi] = g_1 \sum_{i,j} \int_0^\beta d\tau \psi_i(\tau) \psi_j^*(\tau) I_{ij}, \quad (\text{B.39})$$

where I_{ij} singles out nearest neighbours:

$$I_{ij} = \begin{cases} 1 & |i-j| \leq a, \\ 0 & |i-j| > a; \end{cases} \quad (\text{B.40})$$

and dissipation, which from this point onwards we rename from \mathcal{S}_2 to \mathcal{S}_D ,

$$\mathcal{S}_D = \frac{4g_2}{N\beta} \sum_k \sum_a \sum_m \cos kd_a |\omega_m| \phi_{k,-m} \phi_{-k,m}. \quad (\text{B.41})$$

This form of the effective action can be mapped onto the quantum spherical model, shown in Section 1.2.4.

B.3 Quantum spherical mapping

To rewrite the effective action, both the pseudospin mapping and the spherical constraint are introduced as Dirac delta functions,

$$1 \equiv \int \{\mathcal{D}\psi\mathcal{D}\psi^*\} \delta\left(\sum_i |\psi(\tau)|^2 - N\right) \times \prod_i \delta[\Re\psi_i(\tau) - S_i^x(\phi(\tau))] \delta[\Im\psi_i(\tau) - S_i^y(\phi(\tau))], \quad (\text{B.42})$$

and inserted into the partition function:

$$\mathcal{Z} = \int \{\mathcal{D}\psi\mathcal{D}\psi^*\} \delta\left(\sum_i |\psi(\tau)|^2 - N\right) e^{-\mathcal{S}_1[\psi]} \times \int \{\mathcal{D}\phi\} e^{-\mathcal{S}_{\text{U+D}}[\phi]} \prod_i \delta[\Re\psi_i(\tau) - S_i^x(\phi(\tau))] \delta[\Im\psi_i(\tau) - S_i^y(\phi(\tau))], \quad (\text{B.43})$$

where the spin equivalents,

$$\mathbf{S}_i(\phi) = [S_i^x(\phi), S_i^y(\phi)] = [\cos(\phi_i), \sin(\phi_i)], \quad (\text{B.44})$$

according to the spherical model sum up to 1,

$$\frac{1}{N} \sum_i |\mathbf{S}_i(\phi)|^2 = 1. \quad (\text{B.45})$$

The Dirac delta is expanded into an integral:

$$\delta[\psi_i(\tau)] = \int_{-i\infty}^{+i\infty} \left[\prod_i \frac{\mathcal{D}\mu_i(\tau)}{2\pi i} \right] \exp\left[\int_0^\beta d\tau \mu_i(\tau) \psi_i(\tau)\right], \quad (\text{B.46})$$

which transforms the partition function as follows:

$$\begin{aligned} \mathcal{Z} &= \int \{\mathcal{D}\psi\mathcal{D}\psi^*\} \delta\left(\sum_i |\psi(\tau)|^2 - N\right) e^{-\mathcal{S}_1[\psi]} \\ &\quad \times \int \{\mathcal{D}\phi\} e^{-\mathcal{S}_{\text{U+D}}[\phi]} \int \left[\prod_i \frac{D\mu_i(\tau)}{2\pi i}\right] e^{\sum_i \int_0^\beta d\tau \mu_i(\tau) [\mathbf{S}_i - \boldsymbol{\Psi}_i]} \end{aligned} \quad (\text{B.47})$$

$$\begin{aligned} &= \int \{\mathcal{D}\psi\mathcal{D}\psi^*\} \delta\left(\sum_i |\psi(\tau)|^2 - N\right) e^{-\mathcal{S}_1[\psi]} \\ &\quad \times \int \{\mathcal{D}\phi\} \int \left[\prod_i \frac{D\mu_i(\tau)}{2\pi i}\right] e^{-(\mathcal{S}_{\text{U+D}}[\phi] + \sum_i \int_0^\beta d\tau \mu_i(\tau) [\mathbf{S}_i - \boldsymbol{\Psi}_i])} \end{aligned} \quad (\text{B.48})$$

$$= \int \{\mathcal{D}\psi\mathcal{D}\psi^*\} \delta\left(\sum_i |\psi(\tau)|^2 - N\right) e^{-(\mathcal{S}_1[\psi] + \Phi_{\text{U+D}}[\psi])} \quad (\text{B.49})$$

$$= \int \{\mathcal{D}\psi\mathcal{D}\psi^*\} \delta\left(\sum_i |\psi(\tau)|^2 - N\right) e^{-\mathcal{S}_{\text{eff}}[\psi]}, \quad (\text{B.50})$$

where the interaction integral is

$$\Phi_{\text{U+D}}[\psi] = \ln \int \{\mathcal{D}\phi\} \int \left[\prod_i \frac{D\mu_i(\tau)}{2\pi i}\right] e^{-(\mathcal{S}_{\text{U+D}}[\phi] + \sum_i \int_0^\beta d\tau \mu_i(\tau) [\boldsymbol{\Psi}_i - \mathbf{S}_i])} \quad (\text{B.51})$$

$$= \ln \int \{\mathcal{D}\phi\} \int \left[\prod_i \frac{D\mu_i(\tau)}{2\pi i}\right] e^{-\sum_i \int_0^\beta d\tau \mu_i(\tau) \boldsymbol{\Psi}_i} e^{\sum_i \int_0^\beta d\tau \mu_i(\tau) \mathbf{S}_i - \mathcal{S}_{\text{U+D}}[\phi]} \quad (\text{B.52})$$

$$= \ln \int \left[\prod_i \frac{D\mu_i(\tau)}{2\pi i}\right] e^{-\sum_i \int_0^\beta d\tau \mu_i(\tau) \boldsymbol{\Psi}_i + \ln \int \{\mathcal{D}\phi\} \exp[\sum_i \int_0^\beta d\tau \mu_i(\tau) \mathbf{S}_i - \mathcal{S}_{\text{U+D}}[\phi]]} \quad (\text{B.53})$$

$$= \ln \int \left[\prod_i \frac{D\mu_i(\tau)}{2\pi i}\right] e^{-(\sum_i \int_0^\beta d\tau \mu_i(\tau) \boldsymbol{\Psi}_i - \mathcal{G}[\mu])}. \quad (\text{B.54})$$

We expand the correlator \mathcal{G} ,

$$\mathcal{G}[\mu] = \ln \int \{\mathcal{D}\phi\} \exp \left[\sum_i \int_0^\beta d\tau \mu_i(\tau) \mathbf{S}_i - \mathcal{S}_{\text{U+D}}[\phi] \right], \quad (\text{B.55})$$

using the loop expansion:

$$\mathcal{G}[\mu] = \sum_{m=1}^{\infty} \frac{1}{m!} \int dx_1 \dots dx_m \mathcal{G}_{0m}(x_1, \dots, x_m), \quad (\text{B.56})$$

where variables have been shifted to

$$x_m \equiv (i_m, \tau_m, a_m), \quad \int dx \dots \equiv \int_0^\beta d\tau \sum_{i_m} \sum_{a_m} \dots \quad (\text{B.57})$$

We obtain

$$\mathcal{G}_{0m}(x_1, \dots, x_m) = \langle S_{i_1}^{a_1}[\phi(\tau)] \dots S_{i_m}^{a_m}[\phi(\tau)] \rangle_0^{\text{cum}}, \quad (\text{B.58})$$

where the average is defined on the two interaction action terms,

$$\langle \dots \rangle_0 = \frac{\int [\prod_i \mathcal{D}\phi_i] \dots e^{-\mathcal{S}_{\text{U+T}}[\phi]}}{\int [\prod_i \mathcal{D}\phi_i] e^{-\mathcal{S}_{\text{U+T}}[\phi]}}. \quad (\text{B.59})$$

The expansion is limited to second order,

$$\mathcal{G}[\mu] = \int dx_1 \mathcal{G}_{01}(x_1) \mu(x_1) + \frac{1}{2} \int dx_1 dx_2 \mathcal{G}_{02}(x_1, x_2) \mu(x_1) \mu(x_2) + \mathcal{O}(\mu^3), \quad (\text{B.60})$$

where the first order term integrates out to

$$\int dx_1 \mathcal{G}_{01}(x_1) \mu(x_1) = 0. \quad (\text{B.61})$$

Therefore, the correlator \mathcal{G} can be replaced by

$$\mathcal{G}[\mu] = \frac{1}{2} \int \sum_{i,j} d\tau d\tau' \mathcal{G}_{02}(i\tau, j\tau') \mu_i(\tau) \mu_j(\tau'), \quad (\text{B.62})$$

where

$$\mathcal{G}_{02}(i\tau, j\tau') = \langle S_i[\phi(\tau)] S_j[\phi(\tau')] \rangle_0^{\text{cum}} \quad (\text{B.63})$$

$$= \frac{1}{\mathcal{Z}_0} \sum_{\{n_i\}} \prod_i \int_0^{2\pi} d\theta(0) \int_{\theta(0)}^{\theta(0)+2\pi n_i} \mathcal{D}\phi e^{i[\theta_i(\tau)-\theta_j(\tau')]} e^{-\mathcal{S}_{\text{U+D}}[\phi]}, \quad (\text{B.64})$$

and the partial partition function is

$$\mathcal{Z}_0 = \sum_{\{n_i\}} \prod_i \int_0^{2\pi} d\theta(0) \int_{\theta(0)}^{\theta(0)+2\pi n_i} \mathcal{D}\phi e^{-\mathcal{S}_{\text{U+D}}[\phi]}. \quad (\text{B.65})$$

Returning with the approximated correlator \mathcal{G}_{02} , Eq. (B.64), to the interaction integral, Eq. (B.54)

$$\Phi_{\text{U+D}}[\psi] = \ln \int \left[\prod_i \frac{D\mu_i(\tau)}{2\pi i} \right] e^{-(\sum_i \int_0^\beta d\tau \mu_i(\tau) \Psi_i - \mathcal{G}[\mu])} \quad (\text{B.66})$$

$$= \ln \int \left[\prod_i \frac{D\mu_i(\tau)}{2\pi i} \right] e^{-[\sum_i \int_0^\beta d\tau \mu_i(\tau) \Psi_i - \frac{1}{2} \int \sum_{i,j} d\tau d\tau' \mathcal{G}_{02}(i\tau, j\tau') \mu_i(\tau) \mu_j(\tau')]} \quad (\text{B.67})$$

$$= \ln \sqrt{\frac{2\pi^N}{\det \mathcal{G}_{02}(i\tau, j\tau')}} e^{\int \sum_{i,j} d\tau d\tau' \psi_i \mathcal{G}_{02}(i\tau, j\tau') \psi_j^*} \quad (\text{B.68})$$

$$= \int \sum_{i,j} d\tau d\tau' \psi_i \mathcal{G}_{02}^{-1}(i\tau, j\tau') \psi_j^*. \quad (\text{B.69})$$

The full partition function, Eq. (B.50), is now

$$\mathcal{Z} = \int \{\mathcal{D}\psi \mathcal{D}\psi^*\} \delta \left(\sum_i |\psi(\tau)|^2 - N \right) e^{-S_{\text{eff}}[\psi]} \quad (\text{B.70})$$

$$= \int \{\mathcal{D}\psi \mathcal{D}\psi^*\} \delta \left(\sum_i |\psi(\tau)|^2 - N \right) e^{-(S_1[\psi] + \Phi_{\text{U+D}}[\psi])} \quad (\text{B.71})$$

$$= \int \{\mathcal{D}\psi \mathcal{D}\psi^*\} \delta \left(\sum_i |\psi(\tau)|^2 - N \right) \times \exp \left[- \left(\sum_{\langle i,j \rangle} \int_0^\beta d\tau g_1 I_{ij} \psi_i(\tau) \psi_j^*(\tau) + \int \sum_{i,j} d\tau d\tau' \psi_i \mathcal{G}_{02}^{-1}(i\tau, j\tau') \psi_j^* \right) \right]. \quad (\text{B.72})$$

We expand the spherical condition as an integral, introducing the spherical constraint λ :

$$\delta \left(\sum_i |\psi(\tau)|^2 - N \right) = \int_{-i\infty}^{+i\infty} \left[\prod_i \frac{D\lambda(\tau)}{2\pi i} \right] e^{\int_0^\beta d\tau \lambda(\tau) (\sum_i |\psi(\tau)|^2 - N)} \quad (\text{B.73})$$

into the partition function

$$\mathcal{Z} = \int \{\mathcal{D}\psi \mathcal{D}\psi^*\} \int_{-i\infty}^{+i\infty} \left[\prod_i \frac{D\lambda(\tau)}{2\pi i} \right] e^{-S_{\text{QSA}}[\psi, \lambda]}, \quad (\text{B.74})$$

where

$$S_{\text{QSA}}[\psi, \lambda] = \sum_{\langle i,j \rangle} \int_0^\beta d\tau g_1 I_{ij} \psi_i(\tau) \psi_j^*(\tau) + \int \sum_{i,j} d\tau d\tau' \psi_i \mathcal{G}_{02}^{-1}(i\tau, j\tau') \psi_j^* +$$

$$- \int_0^\beta d\tau \lambda(\tau) \left(\sum_i |\psi(\tau)|^2 - N \right) \quad (\text{B.75})$$

$$= \sum_{\langle i,j \rangle} \int_0^\beta d\tau d\tau' [g_1 I_{ij} \psi_i(\tau) \psi_j^*(\tau) \delta(\tau - \tau') + \psi_i \mathcal{G}_{02}^{-1}(i\tau, j\tau') \psi_j^*] +$$

$$+ \sum_{\langle i,j \rangle} \int_0^\beta d\tau d\tau' [-(\psi_i \psi_j^* \delta_{ij} - N) \lambda(\tau) \delta(\tau - \tau')] \quad (\text{B.76})$$

$$= \sum_{\langle i,j \rangle} \int_0^\beta d\tau d\tau' [g_1 I_{ij} \psi_i(\tau) \psi_j^*(\tau) \delta(\tau - \tau') + \psi_i \mathcal{G}_{02}^{-1}(i\tau, j\tau') \psi_j^*] +$$

$$+ \sum_{\langle i,j \rangle} \int_0^\beta d\tau d\tau' [-\psi_i \psi_j^* \lambda(\tau) \delta_{ij} \delta(\tau - \tau') + N \lambda(\tau) \delta(\tau - \tau')]. \quad (\text{B.77})$$

At this point, the partition function satisfies the saddlepoint condition, taking the form in Eq. (3.18),

$$\mathcal{Z} = \int_{-i\infty}^{+i\infty} \left[\prod_i \frac{D\lambda(\tau)}{2\pi i} \right] e^{-N\phi[\lambda]}, \quad (\text{B.78})$$

where

$$\phi[\lambda] = - \int_0^\beta d\tau d\tau' \lambda(\tau) \delta(\tau - \tau') - \frac{1}{N} \ln \int \{\mathcal{D}\psi \mathcal{D}\psi^*\}$$

$$\times e^{\sum_{i,j} \int_0^\beta d\tau d\tau' [\lambda(\tau) \delta_{ij} \delta(\tau - \tau') - g_1 I_{ij} \delta(\tau - \tau') + \mathcal{G}_{02}^{-1}(i\tau, j\tau')] \psi_i(\tau) \psi_j^*(\tau)}. \quad (\text{B.79})$$

After Matsubara transform, the single hopping term takes the form

$$\int_0^\beta d\tau d\tau' g_1 I_{ij} \delta(\tau - \tau') \psi_i(\tau) \psi_j^*(\tau') = \int_0^\beta d\tau d\tau' g_1 \delta(\tau - \tau') \psi_{im} \psi_{jn}^* e^{-i\omega_m \tau} e^{-i\omega_n \tau'} \quad (\text{B.80})$$

$$= \int_0^\beta d\tau g_1 \psi_{im} \psi_{jn}^* e^{-i(\omega_m - \omega_n)\tau} \quad (\text{B.81})$$

$$= g_1 I_{ij} \psi_{im} \psi_{jm}^*, \quad (\text{B.82})$$

sp the saddlepoint function can be rewritten as

$$\begin{aligned} \phi[\lambda] &= -\beta\lambda - \frac{1}{N} \ln \int \{\mathcal{D}\psi \mathcal{D}\psi^*\} \\ &\times \exp \left\{ - \sum_{i,j} [\lambda(\tau) \delta_{ij} - g_1 I_{ij} + \mathcal{G}_{02}^{-1}(i\omega_m, j\omega_m)] \psi_{im} \psi_{jm}^* \right\}. \end{aligned} \quad (\text{B.83})$$

After Fourier transform, we get the form in Eq. (3.19),

$$\phi[\lambda] = -\beta\lambda - \frac{1}{2N} \sum_k \ln \left\{ \frac{1}{\beta\pi} [\lambda - g_1 \xi_k + \mathcal{G}_{02}^{-1}(k, \omega_m)] \right\}, \quad (\text{B.84})$$

where $\xi_k = 2 \sum_d \cos k_d$.

The next step in the saddlepoint approximation is minimising the free energy,

$$\mathcal{F} = -\lambda - \frac{1}{2\beta N} \sum_k \ln \left\{ \frac{1}{\beta\pi} [\lambda - g_1 \xi_k + \mathcal{G}_{02}^{-1}(k, \omega_m)] \right\}, \quad (\text{B.85})$$

in terms of the spherical constraint

$$\frac{\partial \mathcal{F}}{\partial \lambda} = 0, \quad (\text{B.86})$$

to obtain the critical line equation in Eq. (3.23):

$$1 = \frac{1}{2\beta N} \sum_k \sum_m \frac{1}{\lambda - g_1 \xi_k + \mathcal{G}_{02}^{-1}(k, \omega_m)}. \quad (\text{B.87})$$

Inserting density of states,

$$\rho(E) = \frac{1}{N} \sum_k \delta(E - \xi_k), \quad (\text{B.88})$$

we obtain the form in Eq. (3.23):

$$1 = \frac{1}{2\beta N} \sum_k \sum_m \frac{1}{\lambda - g_1 \xi_k + \mathcal{G}_{02}^{-1}(k, \omega_m)} \quad (\text{B.89})$$

$$= \frac{1}{2\beta} \left[\int dE \frac{1}{N} \sum_k \delta(E - \xi_k) \right] \sum_m \frac{1}{\lambda - g_1 E + \mathcal{G}_{02}^{-1}(k, \omega_m)} \quad (\text{B.90})$$

$$= \frac{1}{2\beta} \int dE \sum_m \frac{\rho(E)}{\lambda - g_1 E + \mathcal{G}_{02}^{-1}(E, \omega_m)}. \quad (\text{B.91})$$

The final remaining step is evaluating the correlator, \mathcal{G}_{02} .

B.4 Evaluating the correlator

Returning to the second order correlator, Eq. (B.64),

$$\mathcal{G}_{02}(i\tau, j\tau') = \frac{1}{\mathcal{Z}_0} \int \{\mathcal{D}\phi\} e^{i[\phi_i(\tau) - \phi_j(\tau')]} e^{-\mathcal{S}_{\text{U+D}}[\phi]}, \quad (\text{B.92})$$

where the interaction partition function is

$$\mathcal{Z}_0 = \int \{\mathcal{D}\phi\} e^{-\mathcal{S}_{\text{U+D}}[\phi]} \quad (\text{B.93})$$

and the interaction effective action is

$$\mathcal{S}_{\text{U+D}}[\phi] = \frac{1}{2U} \sum_{ij} \int_0^\beta d\tau \left(\frac{\partial \phi_i}{\partial \tau} \right) \left(\frac{\partial \phi_j}{\partial \tau} \right) + 4g_2 \sum_{i,j} \int_0^\beta d\tau d\tau' \frac{1}{\tau^2} \phi_i(\tau) \phi_j(\tau'). \quad (\text{B.94})$$

Matsubara transformation:

$$\mathcal{S}_{\text{U+D}}[\phi] = -\frac{1}{2U\beta} \sum_{i,j} \sum_m \omega_m^2 \phi_{i,m} \phi_{j,m}^* - 4\frac{g_2}{\beta} \sum_{i,j} \sum_a \sum_m |\omega_m| \phi_{i,m} \phi_{j,m}^* \quad (\text{B.95})$$

$$= \sum_{i,j} \sum_m \left(-\frac{1}{2U\beta} \omega_m^2 + 4\frac{g_2}{\beta} |\omega_m| \right) \phi_{i,m} \phi_{j,m}^*, \quad (\text{B.96})$$

$$i[\phi_i(\tau) - \phi_j(\tau')] = \frac{i}{\beta} \sum_m e^{-i\omega_m \tau} \phi_{i,m} - \frac{i}{\beta} \sum_n e^{-i\omega_n \tau'} \phi_{j,m} \quad (\text{B.97})$$

$$= \frac{i}{\beta} (\phi_{i,0} - \phi_{j,0}) + \frac{i}{\beta} \left(\sum_{m=1} e^{-i\omega_m \tau} \phi_{i,m} - \sum_{n=1} e^{-i\omega_n \tau'} \phi_{j,m} \right) +$$

$$+ \frac{i}{\beta} \left(\sum_{m=1} e^{i\omega_m \tau} \phi_{i,m}^* - \sum_{n=1} e^{i\omega_n \tau'} \phi_{j,m}^* \right) \quad (\text{B.98})$$

$$= \frac{i}{\beta} (\phi_{i,0} - \phi_{j,0}) + \frac{i}{\beta} \sum_{m=1} \phi_{i,m} (e^{-i\omega_m \tau} - e^{-i\omega_n \tau'}) +$$

$$+ \frac{i}{\beta} \sum_{m=1} \phi_{i,m}^* (e^{i\omega_m \tau} - e^{i\omega_n \tau'}). \quad (\text{B.99})$$

Inserting the necessary terms into the Eq. (B.92), we get

$$\mathcal{G}_{02}(i\tau, j\tau') = \frac{1}{\mathcal{Z}_0} \int \{\mathcal{D}\phi\} \delta_{i,j} \exp \left[\sum_{i,j} \sum_m \left(-\frac{\omega_m^2}{2U\beta} + 4\frac{g_2}{\beta} |\omega_m| \right) \phi_{i,m} \phi_{j,m}^* \right]$$

$$\times \exp \left[\frac{i}{\beta} \sum_{m=1} \phi_{i,m} (e^{-i\omega_m \tau} - e^{-i\omega_n \tau'}) + \frac{i}{\beta} \sum_{m=1} \phi_{i,m}^* (e^{i\omega_m \tau} - e^{i\omega_n \tau'}) \right], \quad (\text{B.100})$$

where

$$\mathcal{Z}_0 = \int \{\mathcal{D}\phi\} \exp \left[\sum_{i,j} \sum_m \left(-\frac{1}{2U\beta} \omega_m^2 + 4\frac{g_2}{\beta} |\omega_m| \right) \phi_{i,m} \phi_{j,m}^* \right]. \quad (\text{B.101})$$

After Gaussian integration,

$$\mathcal{G}_{02}(i\tau, j\tau') = \delta_{i,j} \exp \left[\left(\frac{i}{\beta} \right)^2 \sum_{i,j} \sum_m \frac{(e^{-i\omega_m\tau} - e^{-i\omega_m\tau'}) (e^{i\omega_m\tau} - e^{i\omega_m\tau'})}{\frac{-\omega_m^2}{2U\beta} + \frac{4g_2}{\beta} |\omega_m|} \right]. \quad (\text{B.102})$$

Fourier transform brings us to the form in Eq. (3.20),

$$\mathcal{G}_{02}(\tau, \tau') = \exp \left\{ \frac{1}{\beta N} \sum_k \sum_m \frac{1 - \cos[\omega_m(\tau - \tau')]}{\frac{1}{2U}\omega_m^2 + 4g_2|\omega_m|} \right\}. \quad (\text{B.103})$$

This term is still too complex for comfortable usage. From this full form of \mathcal{G}_{02} , we can determine the parameter range in which it is safe to approximate with a more manageable expression.

B.4.1 Full correlator

The interior part of the correlator \mathcal{G}_{02} , Eq. (B.103), designating $(\tau - \tau') = x$, is

$$\begin{aligned} \frac{2}{\beta} \sum_{m=0}^{\infty} \frac{1 - \cos \omega_m x}{\frac{1}{2U}\omega_m^2 + 4g_2\omega_m} &= \frac{1}{8\pi g_2} \left[2H_{\frac{4g_2 U \beta}{\pi}} + e^{\frac{2i\pi x}{\beta}} \Phi \left(e^{\frac{2i\pi x}{\beta}}, 1, \frac{4g_2 U \beta}{\pi} + 1 \right) + \right. \\ &+ e^{-\frac{2i\pi x}{\beta}} \Phi \left(e^{-\frac{2i\pi x}{\beta}}, 1, \frac{4g_2 U \beta}{\pi} + 1 \right) + \\ &\left. + \ln \left(1 - e^{\frac{2i\pi x}{\beta}} \right) + \ln \left(1 - e^{-\frac{2i\pi x}{\beta}} \right) \right], \quad (\text{B.104}) \end{aligned}$$

where H_n is the n^{th} harmonic number and $\Phi(z, s, a)$ is the Hurwitz-Lerch transcendent. Rewriting further,

$$\frac{2}{\beta} \sum_{m=0}^{\infty} \frac{1 - \cos \omega_m x}{\frac{1}{2U} \omega_m^2 + 4g_2 \omega_m} = \frac{2H_{\frac{4g_2 U \beta}{\pi}} - \frac{\pi}{4\beta U g_2 + \pi} + \ln \left[\left(1 - e^{\frac{2i\pi x}{\beta}}\right) \left(1 - e^{-\frac{2i\pi x}{\beta}}\right) \right]}{8\pi g_2} \quad (\text{B.105})$$

$$= \frac{(4\beta g_2 U + \pi) \left\{ 2H_{\frac{4g_2 U \beta}{\pi}} + \ln \left[4 \sin^2 \left(\frac{\pi x}{\beta} \right) \right] \right\} - \pi}{8\pi g_2 (4\beta g_2 U + \pi)} \quad (\text{B.106})$$

$$= \frac{2H_{\frac{4g_2 U \beta}{\pi}} + \ln \left[4 \sin^2 \left(\frac{\pi x}{\beta} \right) \right] - \frac{\pi}{(4\beta g_2 U + \pi)}}{8\pi g_2}. \quad (\text{B.107})$$

The logarithm can be approximated to second order as

$$\ln \left[4 \sin^2 \left(\frac{\pi x}{\beta} \right) \right] = \ln \left[\left(\frac{2\pi x}{\beta} \right)^2 \right] - \frac{\pi^2 x^2}{3\beta^2} + O[x^3] \quad (\text{B.108})$$

$$= 2 \ln \left| \frac{2\pi x}{\beta} \right| - \frac{\pi^2 x^2}{3\beta^2} + O[x^3] \quad (\text{B.109})$$

$$= 2 \ln \left(\frac{2\pi}{\beta} |x| \right) - \frac{\pi^2 x^2}{3\beta^2} + O[x^3] \quad (\text{B.110})$$

$$= 2 \ln |x| + 2 \ln \frac{2\pi}{\beta} - \frac{\pi^2 x^2}{3\beta^2} + O[x^3], \quad (\text{B.111})$$

in which case

$$\begin{aligned} \frac{2}{\beta} \sum_{m=0}^{\infty} \frac{1 - \cos \omega_m x}{\frac{1}{2U} \omega_m^2 + 4g_2 \omega_m} &\approx \frac{2}{8\pi g_2} \ln |x| - \frac{\pi^2}{24\pi \beta^2 g_2} x^2 + \\ &+ \frac{2H_{\frac{4g_2 U \beta}{\pi}} + 2 \ln \frac{2\pi}{\beta} - \frac{\pi}{(4\beta g_2 U + \pi)}}{8\pi g_2}. \end{aligned} \quad (\text{B.112})$$

Returning from x to the imaginary time variable, the full form of the correlator in

Eq. (B.103) is

$$\mathcal{G}_{02}(\tau, \tau') = \exp \left\{ \frac{2}{\beta N} \sum_{m=0}^{\infty} \frac{1 - \cos[\omega_m(\tau - \tau')]}{\frac{1}{2U}\omega_m^2 + 4g_2|\omega_m|} \right\} \quad (\text{B.113})$$

$$\begin{aligned} &= \exp \left[\frac{1}{N} \frac{2}{8\pi g_2} \ln |\tau - \tau'| - \frac{\pi}{24\beta^2 g_2} (\tau - \tau')^2 \right] + \\ &\quad + \exp \frac{2H_{\frac{4g_2 U \beta}{\pi}} + 2 \ln \frac{2\pi}{\beta} - \frac{\pi}{(4\beta g_2 U + \pi)}}{8\pi g_2}. \end{aligned} \quad (\text{B.114})$$

After Matsubara transform, we obtain Eq. (3.28):

$$\mathcal{G}_{02}(\omega_m) = \frac{\exp(c) b^{-\frac{a}{2} - \frac{1}{2}}}{\sqrt{2\pi}} \Gamma\left(\frac{a+1}{2}\right) {}_1F_1\left(\frac{a+1}{2}; \frac{1}{2}; -\frac{\omega_m^2}{4b}\right), \quad (\text{B.115})$$

where Γ is the Euler gamma function, ${}_1F_1$ is the Kummer confluent hypergeometric function, and the parameters are

$$a = \frac{2}{8\pi g_2}, \quad (\text{B.116})$$

$$b = \frac{\pi^2}{24\pi\beta^2 g_2}, \quad (\text{B.117})$$

$$c = \frac{2H_{\frac{4g_2 U \beta}{\pi}} + 2 \ln \frac{2\pi}{\beta} - \frac{\pi}{(4\beta g_2 U + \pi)}}{8\pi g_2}. \quad (\text{B.118})$$

This form is used to analytically determine the range of parameters for further calculations in Section 3.4.1. Within that range, we assume that at low enough temperatures, the imaginary time cosine oscillates quickly around 0 and averages out to 0. In that case, the inverse of the correlator can be approximated by its denominator:

$$\mathcal{G}_{02}^{-1}(k\tau, k\tau') \approx \frac{1}{2U}\omega_m^2 + 4g_2|\omega_m|. \quad (\text{B.119})$$

The last unknown left in the critical equation, Eq. (B.91), is the spherical constraint λ , which can be approximated at saddlepoint by $\lambda = \lambda_0$, where

$$\lambda_0 = g_1 \xi_{max} - \mathcal{G}_{02}^{-1}(\omega_{m=0}) = g_1 \xi_{max} - 0 = g_1 \xi_{max}. \quad (\text{B.120})$$

Having determined the correlator \mathcal{G}_{02} and the spherical constraint λ , we can obtain an explicit form of the critical line equation.

B.5 Critical line equation

Inserting the approximated correlator in Eq. (B.119) and the saddlepoint spherical constraint value λ_0 in Eq. (B.120) into the critical line equation, Eq. (B.91), we obtain

$$1 = \frac{1}{2\beta} \int d\xi \sum_m \frac{\rho(\xi)}{g_1(\xi_{max} - \xi) + \frac{1}{2U}\omega_m^2 + 4g_2|\omega_m|}. \quad (\text{B.121})$$

The final step is the Matsubara sum, which can be separated into three terms, depending on the sign of m ,

$$\sum_m \frac{1}{g_1(\xi_{max} - \xi) + \frac{1}{2U}\omega_m^2 + 4g_2|\omega_m|} = \begin{cases} \sum_{m=-\infty}^{-1} \frac{1}{g_1(\xi_{max} - \xi) + \frac{1}{2U}\omega_m^2 - 4g_2\omega_m}, & m < 0, \\ \frac{1}{g_1(\xi_{max} - \xi)}, & m = 0, \\ \sum_{m=1}^{+\infty} \frac{1}{g_1(\xi_{max} - \xi) + \frac{1}{2U}\omega_m^2 + 4g_2\omega_m}, & m > 0. \end{cases} \quad (\text{B.122})$$

These terms sum up to digamma functions, $\psi^{(0)}$, as in Eq. (3.25):

$$\begin{aligned} \frac{1}{2\beta} \sum_m \frac{1}{g_1(\xi_{max} - \xi) + \frac{1}{2U}\omega_m^2 + 4g_2|\omega_m|} &= \frac{1}{2\pi\gamma} \psi^{(0)} \left[\frac{\beta U}{2\pi} (4g_2 + \gamma) \right] + \\ &\quad - \frac{1}{2\pi\gamma} \psi^{(0)} \left[\frac{\beta U}{2\pi} (4g_2 - \gamma) \right], \end{aligned} \quad (\text{B.123})$$

where

$$\gamma = \sqrt{(4g_2)^2 - 4g_1 (\xi_{max} - \xi) \frac{1}{2U}} \quad (\text{B.124})$$

$$= \sqrt{(4g_2)^2 - 2\frac{g_1}{U} (\xi_{max} - \xi)}. \quad (\text{B.125})$$

At low temperatures, $\beta \rightarrow \infty$, digamma functions can be approximated as logarithms,

$$\psi^{(0)}(\beta X) \approx \ln \beta X. \quad (\text{B.126})$$

The final version of the critical line equation used in numerics is thus Eq. (3.27):

$$1 = \frac{1}{2\pi} \int d\xi \rho(\xi) \sqrt{\frac{\frac{U}{2}}{(4g_2)^2 \frac{U}{2} - g_1 (\xi_{max} - \xi)}} \ln \left[\frac{4g_2 + \gamma}{4g_2 - \gamma} \right] \quad (\text{B.127})$$

$$= \frac{1}{2\pi} \int d\xi \rho(\xi) \sqrt{\frac{1}{(4g_2)^2 - 2\frac{g_1}{U} (\xi_{max} - \xi)}} \ln \left[\frac{4g_2 + \gamma}{4g_2 - \gamma} \right]. \quad (\text{B.128})$$

Both models can be analysed numerically using this equation by entering the proper forms of the single and pair coefficients, g_1 and g_2 .

Appendix C

Correlation-based pairing: calculations

We follow the standard quantum rotor derivation [46, 33] up until the trace of the correlator.

We start with the standard Bose-Hubbard Hamiltonian, Eq. (4.1):

$$\hat{H} = \frac{U}{2} \sum_i \hat{n}_i (\hat{n}_i - 1) - \sum_{\langle i,j \rangle} t_{ij} \hat{a}_i^\dagger \hat{a}_j - \mu \sum_i \hat{n}_i \quad (\text{C.1})$$

$$= \frac{U}{2} \sum_i \hat{n}_i^2 - \sum_{\langle i,j \rangle} t_{ij} \hat{a}_i^\dagger \hat{a}_j - \bar{\mu} \sum_i \hat{n}_i, \quad (\text{C.2})$$

where

$$\bar{\mu} = \mu + \frac{U}{2} \quad (\text{C.3})$$

is the shifted chemical potential.

C.1 Quantum rotor derivation

The path integral partition function is

$$\mathcal{Z} = \int \{\mathcal{D}\bar{a}\mathcal{D}a\} e^{-S[\bar{a},a]}, \quad (\text{C.4})$$

with effective action

$$\mathcal{S} = \mathcal{S}_B[\bar{a}, a] + \int_0^\beta d\tau \mathcal{H}(\tau), \quad (\text{C.5})$$

$$\mathcal{S}_B = \sum_i \int_0^\beta d\tau \bar{a}_i(\tau) \frac{\partial}{\partial \tau} a_i(\tau). \quad (\text{C.6})$$

The U interaction term is decoupled by the Hubbard-Stratonovich transformation, Eq. (1.14). The effective action can then be separated into bosonic \mathcal{S}_b and effective electrochemical potential \mathcal{S}_V parts:

$$\mathcal{Z} = \int \{\mathcal{D}\bar{a}\mathcal{D}a\} e^{-\mathcal{S}_b[\bar{a},a]} \int \frac{dV}{2\pi} e^{-\mathcal{S}_V[n,V]}, \quad (\text{C.7})$$

$$\mathcal{S}_b = \int_0^\beta d\tau \left(\sum_i \bar{a}_i(\tau) \frac{\partial}{\partial \tau} a_i(\tau) - \sum_{\langle i,j \rangle} t_{ij} \bar{a}_i(\tau) a_j(\tau) \right), \quad (\text{C.8})$$

$$\mathcal{S}_V = \sum_i \int_0^\beta d\tau \left(\frac{1}{2U} V_i^2(\tau) - (iV_i(\tau) - \bar{\mu}) n_i(\tau) \right). \quad (\text{C.9})$$

The effective potential is shifted $V_i(\tau) = V_i^T(\tau) + \frac{\bar{\mu}}{i}$,

$$\mathcal{S}_V = \sum_i \int_0^\beta d\tau \left\{ \frac{1}{2U} \left(V_i^T(\tau) + \frac{\bar{\mu}}{i} \right)^2 - \left[i \left(V_i^T(\tau) + \frac{\bar{\mu}}{i} \right) - \bar{\mu} \right] n_i(\tau) \right\} \quad (\text{C.10})$$

$$= \sum_i \int_0^\beta d\tau \left\{ \frac{1}{2U} \left[(V_i^T(\tau))^2 - \bar{\mu}^2 + 2 \frac{V_i^T(\tau) \bar{\mu}}{i} \right] - i V_i^T(\tau) n_i(\tau) \right\} \quad (\text{C.11})$$

$$= \sum_i \int_0^\beta d\tau \left[\frac{1}{2U} (V_i^T(\tau))^2 - \frac{1}{2U} \bar{\mu}^2 + \frac{V_i^T(\tau) \bar{\mu}}{iU} - i V_i^T(\tau) n_i(\tau) \right], \quad (\text{C.12})$$

and split into static and periodic parts,

$$V_i^T(\tau) = V_i^S(\tau) + V_i^P(\tau), \quad (\text{C.13})$$

$$V_i^S(\tau) = \frac{1}{\beta} V_i^T(\omega_{m=0}), \quad (\text{C.14})$$

$$V_i^P(\tau) = \frac{1}{\beta} \sum_{m=1}^{+\infty} (V_i^T(\omega_m) e^{i\omega_m \tau} + c.c.), \quad (\text{C.15})$$

where the periodic part is coupled to a $U(1)$ periodic phase field $\phi(\tau)$:

$$V_i^P = \dot{\phi}_i(\tau). \quad (\text{C.16})$$

A phase-dependent effective action term can now be separated out in the partition function:

$$\mathcal{Z} = \int \{\mathcal{D}\bar{a}\mathcal{D}a\} e^{-\mathcal{S}_b[\bar{a},a]} \int \left[\frac{dV^S}{2\pi} \right] e^{-\mathcal{S}_2[n,V^S]} \int \{\mathcal{D}\phi\} e^{-\mathcal{S}_\phi[n,\phi]}, \quad (\text{C.17})$$

where

$$\mathcal{S}_b = \int_0^\beta d\tau \left(\sum_i \bar{a}_i(\tau) \frac{\partial}{\partial \tau} a_i(\tau) - \sum_{\langle i,j \rangle} t_{ij} \bar{a}_i(\tau) a_j(\tau) \right), \quad (\text{C.18})$$

$$\mathcal{S}_V = \beta \sum_i \left[\frac{1}{2U} (V_i^S(\tau))^2 - \frac{\bar{\mu}^2}{2U} + \frac{\bar{\mu}}{iU} V_i^S(\tau) - \frac{iV_i^S(\tau)}{\beta} \int_0^\beta d\tau n_i(\tau) \right], \quad (\text{C.19})$$

$$\mathcal{S}_\phi = \sum_i \int_0^\beta d\tau \left[\frac{1}{2U} (\dot{\phi}_i(\tau))^2 + \frac{\bar{\mu}}{iU} \dot{\phi}_i(\tau) - i\dot{\phi}_i(\tau) n_i(\tau) \right]. \quad (\text{C.20})$$

The next step is a gauge transformation, which introduces explicit phase terms based on the bosonic action, Eq. (C.18).

C.1.1 Gauge transformation

Phase and amplitude are separated in the bosonic fields as in Eq. (1.15):

$$a_i(\tau) = e^{i\phi_i(\tau)} b_i(\tau), \quad (\text{C.21})$$

$$\bar{a}_i(\tau) = e^{-i\phi_i(\tau)} \bar{b}_i(\tau), \quad (\text{C.22})$$

for the bosonic action:

$$\mathcal{S}_b = \int_0^\beta d\tau \left(\sum_i \bar{a}_i(\tau) \frac{\partial}{\partial \tau} a_i(\tau) - \sum_{\langle i,j \rangle} t_{ij} \bar{a}_i(\tau) a_j(\tau) \right) \quad (\text{C.23})$$

$$\begin{aligned} &= \int_0^\beta d\tau \sum_i e^{-i\phi_i(\tau)} \bar{b}_i(\tau) \frac{\partial}{\partial \tau} (e^{i\phi_i(\tau)} b_i(\tau)) + \\ &\quad - \int_0^\beta d\tau \sum_{\langle i,j \rangle} t_{ij} e^{-i\phi_i(\tau)} \bar{b}_i(\tau) e^{i\phi_j(\tau)} b_j(\tau) \end{aligned} \quad (\text{C.24})$$

$$\begin{aligned} &= \int_0^\beta d\tau \left(\sum_i i\dot{\phi}_i(\tau) \bar{b}_i(\tau) b_i(\tau) + \sum_i \bar{b}_i(\tau) \frac{\partial}{\partial \tau} b_i(\tau) \right) + \\ &\quad - \int_0^\beta d\tau \sum_{\langle i,j \rangle} t_{ij} e^{-i\phi_{ij}(\tau)} \bar{b}_i(\tau) b_j(\tau), \end{aligned} \quad (\text{C.25})$$

and for the phase action, where $\phi_{ij} = \phi_i - \phi_j$:

$$\mathcal{S}_\phi = \sum_i \int_0^\beta d\tau \left[\frac{1}{2U} (\dot{\phi}_i(\tau))^2 + \frac{\bar{\mu}}{iU} \dot{\phi}_i(\tau) - i\dot{\phi}_i(\tau) n_i(\tau) \right] \quad (\text{C.26})$$

$$= \sum_i \int_0^\beta d\tau \left[\frac{1}{2U} (\dot{\phi}_i(\tau))^2 + \frac{\bar{\mu}}{iU} \dot{\phi}_i(\tau) - i\dot{\phi}_i(\tau) e^{-i\phi_i(\tau)} \bar{b}_i(\tau) e^{i\phi_i(\tau)} b_i(\tau) \right] \quad (\text{C.27})$$

$$= \sum_i \int_0^\beta d\tau \left[\frac{1}{2U} (\dot{\phi}_i(\tau))^2 + \frac{\bar{\mu}}{iU} \dot{\phi}_i(\tau) - i\dot{\phi}_i(\tau) \bar{b}_i(\tau) b_i(\tau) \right]. \quad (\text{C.28})$$

Similarly to the density-induced model in Appendix A, the static \mathcal{S}_V is treated with a saddlepoint approximation. Since the chemical potential in this model is constant, the entire expression averages out to a constant, which can be omitted. Thus, the partition

function is

$$\mathcal{Z} = \int \{\mathcal{D}\bar{b}\mathcal{D}b\} \int \mathcal{D}\phi e^{-\mathcal{S}_b[\bar{b},b,\phi]} e^{-\mathcal{S}_\phi[\bar{b},b,\phi]}, \quad (\text{C.29})$$

where

$$\mathcal{S}_b = \int_0^\beta d\tau \left[\sum_i \bar{b}_i(\tau) \left(\frac{\partial}{\partial \tau} + \bar{\mu} \right) b_i(\tau) - \sum_{\langle i,j \rangle} t_{ij} e^{-i\phi_{ij}(\tau)} \bar{b}_i(\tau) b_j(\tau) \right], \quad (\text{C.30})$$

$$\mathcal{S}_\phi = \sum_i \int_0^\beta d\tau \left[\frac{1}{2U} \left(\dot{\phi}_i(\tau) \right)^2 + \frac{\bar{\mu}}{iU} \dot{\phi}_i(\tau) \right]. \quad (\text{C.31})$$

We integrate over the bosonic amplitudes, b_i , which in this model is straightforward:

$$\int \{\mathcal{D}\bar{b}\mathcal{D}b\} e^{-\int_0^\beta d\tau \left\{ \sum_i \bar{b}_i(\tau) \left(\frac{\partial}{\partial \tau} + \bar{\mu} \right) b_i(\tau) - \sum_{\langle i,j \rangle} t_{ij} e^{-i\phi_{ij}(\tau)} \bar{b}_i(\tau) b_j(\tau) \right\}} = \det G \quad (\text{C.32})$$

$$= e^{\text{Tr} \ln G^{-1}}, \quad (\text{C.33})$$

which leaves us with the phase-only partition function, Eq. (4.2),

$$\mathcal{Z} = \int \{\mathcal{D}\phi\} e^{-\sum_i \int_0^\beta d\tau \left(\frac{1}{2U} (\dot{\phi}_i(\tau))^2 + \frac{\bar{\mu}}{iU} \dot{\phi}_i(\tau) \right) + \text{Tr} \ln G^{-1}}, \quad (\text{C.34})$$

where G is the phase-only Green's function, Eq. (4.4),

$$G^{-1} = G_0^{-1} - T_{ij} = G_0^{-1} (1 - T_{ij} G_0), \quad (\text{C.35})$$

with phase-phase correlator

$$G_0^{-1} = \left(\frac{\partial}{\partial \tau} + \bar{\mu} \right) \delta_{ij} \quad (\text{C.36})$$

and the single-particle nearest neighbour exchange term,

$$T_{ij} = t_{ij} e^{-i(\phi_i(\tau) - \phi_j(\tau))}. \quad (\text{C.37})$$

We assume the phase-phase correlator G_0 to be a sum of two components. The first

component is the constant bosonic amplitude b_0^2 , which is the standard approximation for G_0 . We obtain b_0^2 by minimising the BHM Hamiltonian, Eq. (C.2), in terms of the bosonic amplitude b_0 ,

$$\frac{\partial}{\partial b_0} \hat{H}(b_0) = 0, \quad (\text{C.38})$$

which leads to Eq. (4.9),

$$b_0^2 = \frac{2(zt + \bar{\mu})}{U}. \quad (\text{C.39})$$

The second component of G_0 is the imaginary time-dependent form in Eq. (C.36) itself, which after Matsubara transform, as in Eq. (B.14), takes the form

$$G_0 = \frac{1}{\beta} \sum_n \frac{-i\omega_n + \bar{\mu}}{\omega_n^2 + \bar{\mu}^2}. \quad (\text{C.40})$$

The next step is estimating the trace.

C.1.2 Approximating the trace

Usually, the trace in Eq. (C.34) is approximated to first order [46]. To look for bosonic pairing terms, the following series expansion is used, approximated to second order:

$$\ln \left[\frac{1}{x} (1 - xy) \right] = -\ln x - xy - \frac{(xy)^2}{2} + \mathcal{O}(x^3), \quad (\text{C.41})$$

which transforms the trace in Eq. (C.34) into Eq. (4.7),

$$\text{Tr} \ln G^{-1} = \text{Tr} \left[-\ln G_0 - (TG_0) - \frac{(TG_0)^2}{2} \right] \quad (\text{C.42})$$

$$= -\text{Tr} \ln G_0 - \text{Tr} (TG_0) - \frac{1}{2} \text{Tr} (TG_0)^2 \quad (\text{C.43})$$

The first term in Eq. (C.43) is

$$\text{Tr} \ln G_0 = \text{Tr} \ln (G_0 + G(\tau)) = \text{Tr} \ln \left(\frac{2(zt + \bar{\mu})}{U} + \frac{1}{\beta} \sum_n \frac{-i\omega_n + \bar{\mu}}{\omega_n^2 + \bar{\mu}^2} \right). \quad (\text{C.44})$$

The sum in here doesn't converge and the first term is constant, so we ignore this term altogether.

The second term in Eq. (C.43) is

$$\text{Tr} (TG_0) = \text{Tr} (T(G_0 + G(\tau))) = \text{Tr} (TG_0 + TG(\tau)) \quad (\text{C.45})$$

$$= \text{Tr} (TG_0) + \text{Tr} (TG(\tau)). \quad (\text{C.46})$$

Of these, the second term doesn't converge, so we only consider the first one, which is

$$\text{Tr} (TG_0) = \sum_{\langle i,j \rangle} \int_0^\beta d\tau \int_0^\beta d\tau' \frac{2(zt + \bar{\mu})}{U} t_{ij} e^{-i[\phi_i(\tau) - \phi_j(\tau)]} \delta(\tau - \tau') \quad (\text{C.47})$$

$$= \sum_{\langle i,j \rangle} \frac{2t_{ij}(zt + \bar{\mu})}{U} \int_0^\beta d\tau \int_0^\beta d\tau' e^{-i[\phi_i(\tau) - \phi_j(\tau)]} \delta(\tau - \tau') \quad (\text{C.48})$$

$$= \sum_{\langle i,j \rangle} \frac{2t_{ij}(zt + \bar{\mu})}{U} \int_0^\beta d\tau 2 \cos[\phi_i(\tau) - \phi_j(\tau)] \quad (\text{C.49})$$

$$= \sum_{\langle i,j \rangle} J_{ij} \int_0^\beta d\tau \cos(\phi_{ij}(\tau)), \quad (\text{C.50})$$

where

$$J_{ij} = \frac{2t_{ij}(zt + \bar{\mu})}{U}. \quad (\text{C.51})$$

Finally, the second order term in Eq. (C.43) is

$$\frac{1}{2}Tr (TG_0)^2 = \frac{1}{2}Tr [T(G_0 + G(\tau))]^2 = \frac{1}{2}Tr [TG_0 + TG(\tau)]^2 \quad (C.52)$$

$$= \frac{1}{2}Tr [T^2G_0^2 + T^2G(\tau)^2 + 2T^2G_0G(\tau)] \quad (C.53)$$

$$= \frac{1}{2}Tr (T^2G_0^2) + \frac{1}{2}Tr [T^2G(\tau)^2] + \frac{1}{2}Tr [2T^2G_0G(\tau)]. \quad (C.54)$$

The last term of these doesn't converge. The first is

$$\frac{1}{2}Tr (T^2G_0^2) = \sum_{\langle i,j \rangle} \int_0^\beta d\tau \int_0^\beta d\tau' \left[\frac{2(z\tau + \bar{\mu})}{U} \right]^2 t_{ij} \frac{t_{ij}}{U} e^{-2i[\phi_i(\tau) - \phi_j(\tau)]} \delta(\tau - \tau') \quad (C.55)$$

$$= \frac{1}{2} \sum_{\langle i,j \rangle} t_{ij} \frac{t_{ij}}{U} \left[\frac{2(z\tau + \bar{\mu})}{U} \right]^2 \int_0^\beta d\tau \int_0^\beta d\tau' e^{-2i[\phi_i(\tau) - \phi_j(\tau)]} \delta(\tau - \tau') \quad (C.56)$$

$$= \frac{1}{2} \sum_{\langle i,j \rangle} t_{ij} \frac{t_{ij}}{U} \left[\frac{2(z\tau + \bar{\mu})}{U} \right]^2 \int_0^\beta d\tau 2 \cos 2[\phi_i(\tau) - \phi_j(\tau)] \quad (C.57)$$

$$= \sum_{\langle i,j \rangle} t_{ij} \frac{t_{ij}}{U} \left[\frac{2(z\tau + \bar{\mu})}{U} \right]^2 \int_0^\beta d\tau \cos 2[\phi_i(\tau) - \phi_j(\tau)] \quad (C.58)$$

$$= \sum_{\langle i,j \rangle} J'_{ij} \int_0^\beta d\tau \cos [2\phi_{ij}(\tau)], \quad (C.59)$$

where

$$J'_{ij} = t_{ij} \frac{t_{ij}}{U} \left[\frac{2(z\tau + \bar{\mu})}{U} \right]^2, \quad (C.60)$$

and the second term is

$$\frac{1}{2} \text{Tr} (T^2 G(\tau)^2) = \sum_{\langle i,j \rangle} \int_0^\beta d\tau \int_0^\beta d\tau' t_{ij}^2 e^{-2i[\phi_i(\tau) - \phi_j(\tau)]} G(\tau) \delta(\tau - \tau') \quad (\text{C.61})$$

$$= \sum_{\langle i,j \rangle} t_{ij}^2 \int_0^\beta d\tau e^{-2i[\phi_i(\tau) - \phi_j(\tau)]} G(\tau) \quad (\text{C.62})$$

$$= \sum_{\langle i,j \rangle} 2t_{ij}^2 \int_0^\beta d\tau \cos \{2[\phi_i(\tau) - \phi_j(\tau)]\} G(\tau). \quad (\text{C.63})$$

$G(\tau)$ is Matsubara transformed and calculated separately, after which we merge both double cosine terms with a single J' .

Thus we have reached the expected effective phase action with bosonic pairing, Eq. (4.11), assuming $U \rightarrow \infty$,

$$\mathcal{S}[\phi] = \int_0^\beta d\tau \frac{1}{U} \sum_i \left(\frac{\partial \phi_i}{\partial \tau} \right)^2 + \int_0^\beta d\tau \left(-J \sum_{\langle i,j \rangle} \cos \phi_{ij} - J' \sum_{\langle i,j \rangle} \cos 2\phi_{ij} \right). \quad (\text{C.64})$$

The single and pair coefficients are, respectively,

$$J = \frac{2t(zt + \bar{\mu})}{U}, \quad (\text{C.65})$$

$$J' = t \frac{t}{U} \left[\frac{2(zt + \bar{\mu})}{U} \right]^2 + 2t \frac{t}{U} \left(\frac{1}{\beta} \sum_n \frac{-i\omega_n + \bar{\mu}}{\omega_n^2 + \bar{\mu}^2} \right)^2. \quad (\text{C.66})$$

Performing the Matsubara sum in the second term in J' ,

$$\sum_n \left(\frac{1 - i\omega_n + \bar{\mu}}{\beta \omega_n^2 + \bar{\mu}^2} \right)^2 = \frac{1}{4} \sinh^{-2} \left(\frac{\beta \bar{\mu}}{2} \right). \quad (\text{C.67})$$

Finally, we obtain Eqs. (4.12-4.13),

$$J = \frac{2t(zt + \bar{\mu})}{U}, \quad (\text{C.68})$$

$$J' = t \frac{t}{U} \left[\frac{2(zt + \bar{\mu})}{U} \right]^2 + t \frac{t}{U} \frac{z}{2 \sinh^2 \left(\frac{\beta \bar{\mu}}{2} \right)}. \quad (\text{C.69})$$

The effective phase model is now ready for analysis.

C.2 Self-consistent harmonic approximation

The variational principle, Eq. (1.29) states that, for any trial function \mathcal{S}_0 ,

$$\mathcal{F} \leq \tilde{\mathcal{F}} = \mathcal{F}_0 + \frac{1}{\beta} \langle \mathcal{S} - \mathcal{S}_0 \rangle_0, \quad (\text{C.70})$$

where the average

$$\frac{1}{\beta} \langle \mathcal{S} - \mathcal{S}_0 \rangle_0 = \frac{1}{\beta \mathcal{Z}_0} \int \{ \mathcal{D}\phi \} e^{-\mathcal{S}_0[\phi]} (\mathcal{S} - \mathcal{S}_0) \quad (\text{C.71})$$

is calculated within the trial system, with partition function

$$\mathcal{Z}_0 = \int \{ \mathcal{D}\phi \} e^{-\mathcal{S}_0[\phi]}. \quad (\text{C.72})$$

The trial free energy is defined as

$$\mathcal{F}_0 = -\frac{1}{\beta} \ln \mathcal{Z}_0 = -\frac{1}{\beta} \ln \int \{ \mathcal{D}\phi \} e^{-\mathcal{S}_0[\phi]}. \quad (\text{C.73})$$

The trial function we choose here is harmonic, with stiffness K , as in Eq. (1.33):

$$\mathcal{S}_0[\phi] = \int_0^\beta d\tau \left[\frac{1}{U} \sum_i \left(\frac{\partial \phi_i}{\partial \tau} \right)^2 + \frac{K}{2} \sum_{\langle i,j \rangle} \phi_{ij}^2 \right]. \quad (\text{C.74})$$

The trigonometric relations between phase operators can be rewritten as

$$\langle \cos \phi_{ij} \rangle = e^{-\frac{1}{2} \langle \phi_{ij}^2 \rangle_0}, \quad (\text{C.75})$$

$$\langle \cos 2\phi_{ij} \rangle = e^{-2 \langle \phi_{ij}^2 \rangle_0}, \quad (\text{C.76})$$

where the expectation values are also calculated within the trial system.

For simplicity, we designate the trial phase average as

$$D_{ij} = \langle \phi_{ij}^2 \rangle_0. \quad (\text{C.77})$$

The effective action expectation value is

$$\begin{aligned} \langle \mathcal{S} - \mathcal{S}_0 \rangle_0 &= -\frac{1}{\mathcal{Z}_0} \int \{ \mathcal{D}\phi \} e^{-\mathcal{S}_0[\phi]} \\ &\quad \times \int_0^\beta d\tau \left(J \sum_{\langle i,j \rangle} \cos \phi_{ij} + J' \sum_{\langle i,j \rangle} \cos 2\phi_{ij} + \frac{K}{2} \sum_{\langle i,j \rangle} \phi_{ij}^2 \right) \end{aligned} \quad (\text{C.78})$$

$$\begin{aligned} &= -\int_0^\beta d\tau \sum_{\langle i,j \rangle} \left(J \frac{1}{\mathcal{Z}_0} \int \{ \mathcal{D}\phi \} e^{-\mathcal{S}_0[\phi]} \cos \phi_{ij} \right) + \\ &\quad - \int_0^\beta d\tau \sum_{\langle i,j \rangle} \left(J' \frac{1}{\mathcal{Z}_0} \int \{ \mathcal{D}\phi \} e^{-\mathcal{S}_0[\phi]} \cos 2\phi_{ij} \right) + \\ &\quad - \int_0^\beta d\tau \sum_{\langle i,j \rangle} \left(\frac{K}{2} \frac{1}{\mathcal{Z}_0} \int \{ \mathcal{D}\phi \} e^{-\mathcal{S}_0[\phi]} \phi_{ij}^2 \right) \end{aligned} \quad (\text{C.79})$$

$$= -\int_0^\beta d\tau \sum_{\langle i,j \rangle} \left(J \langle \cos \phi_{ij} \rangle + J' \langle \cos 2\phi_{ij} \rangle + \frac{K}{2} \langle \phi_{ij}^2 \rangle \right) \quad (\text{C.80})$$

$$= -\int_0^\beta d\tau \sum_{\langle i,j \rangle} \left(J e^{-\frac{1}{2} \langle \phi_{ij}^2 \rangle} + J' e^{-2 \langle \phi_{ij}^2 \rangle} + \frac{K}{2} \langle \phi_{ij}^2 \rangle \right) \quad (\text{C.81})$$

$$= -\int_0^\beta d\tau \sum_{\langle i,j \rangle} \left(J e^{-\frac{1}{2} D_{ij}} + J' e^{-2 D_{ij}} + \frac{K}{2} D_{ij} \right). \quad (\text{C.82})$$

To find the stiffness K , we minimise the free action according to Eq. (1.34),

$$\delta\tilde{\mathcal{F}} = \delta \left(\mathcal{F}_0 + \frac{1}{\beta} \langle \mathcal{S} - \mathcal{S}_0 \rangle \right) = 0. \quad (\text{C.83})$$

The variation is a sum of two partial derivatives,

$$\left(\frac{\partial\tilde{\mathcal{F}}}{\partial K} \right)_{D_{ij}} + \left(\frac{\partial\tilde{\mathcal{F}}}{\partial D_{ij}} \right)_K \left(\frac{\partial D_{ij}}{\partial K} \right) = 0. \quad (\text{C.84})$$

The stiffness derivative is

$$\left(\frac{\partial\tilde{\mathcal{F}}}{\partial K} \right)_{D_{ij}} = \frac{\partial}{\partial K} \left(\mathcal{F}_0 + \frac{1}{\beta} \langle \mathcal{S} - \mathcal{S}_0 \rangle \right), \quad (\text{C.85})$$

where

$$\frac{\partial}{\partial K} \mathcal{F}_0 = -\frac{1}{\beta} \frac{\partial}{\partial K} \left\{ \ln \int \{ \mathcal{D}\phi \} e^{-\int_0^\beta d\tau \left[\frac{1}{U} \sum_i \left(\frac{\partial\phi_i}{\partial\tau} \right)^2 + \frac{K}{2} \sum_{\langle i,j \rangle} \phi_{ij}^2 \right]} \right\} \quad (\text{C.86})$$

$$= -\frac{1}{\beta} \frac{\int \{ \mathcal{D}\phi \} \sum_{\langle i,j \rangle} \left(-\int_0^\beta d\tau \right) \frac{1}{2} \phi_{ij}^2 e^{-\int_0^\beta d\tau \left[\frac{1}{U} \sum_i \left(\frac{\partial\phi_i}{\partial\tau} \right)^2 + \frac{K}{2} \sum_{\langle i,j \rangle} \phi_{ij}^2 \right]}}{\int [\mathcal{D}\phi] e^{-\int_0^\beta d\tau \left[\frac{1}{U} \sum_i \left(\frac{\partial\phi_i}{\partial\tau} \right)^2 + \frac{K}{2} \sum_{\langle i,j \rangle} \phi_{ij}^2 \right]}} \quad (\text{C.87})$$

$$= \frac{1}{2\beta} \int_0^\beta d\tau \sum_{\langle i,j \rangle} \left\{ \frac{1}{\mathcal{Z}_0} \int \{ \mathcal{D}\phi \} e^{-\int_0^\beta d\tau \left[\frac{1}{U} \sum_i \left(\frac{\partial\phi_i}{\partial\tau} \right)^2 + \frac{K}{2} \sum_{\langle i,j \rangle} \phi_{ij}^2 \right]} \phi_{ij}^2 \right\} \quad (\text{C.88})$$

$$= \frac{1}{2\beta} \int_0^\beta d\tau \sum_{\langle i,j \rangle} \langle \phi_{ij}^2 \rangle = \frac{1}{2\beta} \int_0^\beta d\tau \sum_{\langle i,j \rangle} D_{ij} \quad (\text{C.89})$$

and

$$\frac{\partial}{\partial K} \left(\frac{1}{\beta} \langle \mathcal{S} - \mathcal{S}_0 \rangle \right) = \frac{1}{\beta} \frac{\partial}{\partial K} \langle \mathcal{S} - \mathcal{S}_0 \rangle \quad (\text{C.90})$$

$$= -\frac{1}{\beta} \frac{\partial}{\partial K} \int_0^\beta d\tau \sum_{\langle i,j \rangle} \left(J e^{-\frac{1}{2} D_{ij}} + J' e^{-2D_{ij}} + \frac{K}{2} D_{ij} \right) \quad (\text{C.91})$$

$$= -\frac{1}{2\beta} \int_0^\beta d\tau \sum_{\langle i,j \rangle} D_{ij}. \quad (\text{C.92})$$

These two terms conveniently cancel out. As for the D_{ij} -dependent derivative,

$$\left(\frac{\partial \tilde{\mathcal{F}}}{\partial D_{ij}} \right)_K = \frac{\partial}{\partial D_{ij}} \left[\mathcal{F}_0 + \frac{1}{\beta} \langle \mathcal{S} - \mathcal{S}_0 \rangle \right]_K \quad (\text{C.93})$$

$$= \frac{\partial}{\partial D_{ij}} [\mathcal{F}_0]_K + \frac{1}{\beta} \frac{\partial}{\partial D_{ij}} [\langle \mathcal{S} - \mathcal{S}_0 \rangle]_K \quad (\text{C.94})$$

$$= 0 + \frac{1}{\beta} \frac{\partial}{\partial D_{ij}} [\langle \mathcal{S} - \mathcal{S}_0 \rangle]_K \quad (\text{C.95})$$

$$= \frac{1}{\beta} \frac{\partial}{\partial D_{ij}} \int_0^\beta d\tau \sum_{\langle i,j \rangle} \left(J e^{-\frac{1}{2} D_{ij}} + J' e^{-2D_{ij}} + \frac{K}{2} D_{ij} \right) \quad (\text{C.96})$$

$$= \frac{1}{\beta} \int_0^\beta d\tau \sum_{\langle i,j \rangle} \frac{\partial}{\partial D_{ij}} \left(J e^{-\frac{1}{2} D_{ij}} + J' e^{-2D_{ij}} + \frac{K}{2} D_{ij} \right) \quad (\text{C.97})$$

$$= \frac{1}{\beta} \int_0^\beta d\tau \sum_{\langle i,j \rangle} \left(\frac{\partial}{\partial D_{ij}} J e^{-\frac{1}{2} D_{ij}} + \frac{\partial}{\partial D_{ij}} J' e^{-2D_{ij}} + \frac{\partial}{\partial D_{ij}} \frac{K}{2} D_{ij} \right) \quad (\text{C.98})$$

$$= \frac{1}{\beta} \int_0^\beta d\tau \sum_{\langle i,j \rangle} \left(-\frac{1}{2} J e^{-\frac{1}{2} D_{ij}} - 2J' e^{-2D_{ij}} + \frac{K}{2} \right) \quad (\text{C.99})$$

$$= -\frac{1}{2\beta} \int_0^\beta d\tau \sum_{\langle i,j \rangle} \left(J e^{-\frac{1}{2} D_{ij}} + 4J' e^{-2D_{ij}} - K \right) \quad (\text{C.100})$$

Our minimisation condition, Eq. (C.84), is therefore

$$-\frac{1}{2\beta} \int_0^\beta d\tau \sum_{\langle i,j \rangle} \left(J e^{-\frac{1}{2}D_{ij}} + 4J' e^{-2D_{ij}} - K \right) \left(\frac{\partial D_{ij}}{\partial K} \right) = 0, \quad (\text{C.101})$$

from which the self-consistent equation emerges:

$$J e^{-\frac{1}{2}D_{ij}} + 4J' e^{-2D_{ij}} - K = 0, \quad (\text{C.102})$$

or, as in Eq. (4.15),

$$K = J e^{-\frac{1}{2}D_{ij}} + 4J' e^{-2D_{ij}}. \quad (\text{C.103})$$

To obtain a numerically solvable equation, we need an explicit form for the trial phase average, D_{ij} .

C.2.1 Calculating the trial phase average

Our average D_{ij} , Eq. (C.77), is

$$D_{ij} = \langle \phi_{ij}^2 \rangle_0 = \frac{1}{\mathcal{Z}_0} \int \{ \mathcal{D}\phi \} e^{-\mathcal{S}_0[\phi]} \phi_{ij}^2 \quad (\text{C.104})$$

$$= \frac{1}{\mathcal{Z}_0} \int \{ \mathcal{D}\phi \} e^{-\mathcal{S}_0[\phi]} [\phi_i(\tau) - \phi_j(\tau)]^2, \quad (\text{C.105})$$

where the trial partition function \mathcal{Z}_0 , Eq. (C.72), is based on the trial effective action \mathcal{S}_0 , Eq. (C.74). We introduce the Fourier transform,

$$\phi_i = \frac{1}{N} \sum_k e^{ikr_i} \phi_k, \quad (\text{C.106})$$

onto the average itself:

$$D_{ij} = \langle \phi_{ij}^2 \rangle = \frac{1}{N^2} \sum_{k,k'} (e^{ikr_i} - e^{ikr_j}) (e^{ik'r_i} - e^{ik'r_j}) \langle \phi_k \phi_{k'} \rangle. \quad (\text{C.107})$$

Because of translational invariance,

$$\langle \phi_k \phi_{k'} \rangle = \langle \phi_k \phi_{-k} \rangle \delta_{k', -k}. \quad (\text{C.108})$$

Therefore,

$$D_{ij} = \frac{1}{N^2} \sum_{k, k'} (e^{ikr_i} - e^{ikr_j}) (e^{ik'r_i} - e^{ik'r_j}) \langle \phi_k \phi_{-k} \rangle \delta_{k', -k} \quad (\text{C.109})$$

$$= \frac{1}{N^2} \sum_k (e^{ikr_i} - e^{ikr_j}) (e^{-ikr_i} - e^{-ikr_j}) \langle \phi_k \phi_{-k} \rangle \quad (\text{C.110})$$

$$= \frac{1}{N^2} \sum_k (e^{ikr_i} e^{-ikr_i} - e^{ikr_i} e^{-ikr_j} - e^{ikr_j} e^{-ikr_i} + e^{ikr_j} e^{-ikr_j}) \langle \phi_k \phi_{-k} \rangle \quad (\text{C.111})$$

$$= \frac{1}{N^2} \sum_k (1 - e^{ik(r_i - r_j)} - e^{-ik(r_i - r_j)} + 1) \langle \phi_k \phi_{-k} \rangle \quad (\text{C.112})$$

$$= \frac{1}{N^2} \sum_k [2 - (e^{ik(r_i - r_j)} + e^{-ik(r_i - r_j)})] \langle \phi_k \phi_{-k} \rangle \quad (\text{C.113})$$

$$= \frac{1}{N^2} \sum_k \{2 - 2 \cos [k(r_i - r_j)]\} \langle \phi_k \phi_{-k} \rangle \quad (\text{C.114})$$

$$= \frac{2}{N^2} \sum_k (1 - \cos kr_{ij}) \langle \phi_k \phi_{-k} \rangle. \quad (\text{C.115})$$

Next is the straightforward in this case Matsubara transform,

$$D_{ij} = \frac{2}{N^2} \sum_{k, m} (1 - \cos kr_{ij}) \langle \phi_{k, m} \phi_{-k, -m} \rangle. \quad (\text{C.116})$$

We also Fourier transform the trial effective action, \mathcal{S}_0 in Eq. (C.74). To that end,

$$\sum_i \phi_{i,m}^2 = \sum_i \frac{1}{N} \sum_k e^{ikr_i} \phi_k \frac{1}{N} \sum_{k'} e^{ik'r_i} \phi_{k'} \quad (\text{C.117})$$

$$= \frac{1}{N} \sum_{k,k'} \phi_k \phi_{k'} \frac{1}{N} \sum_i e^{i(k+k')r_i} \quad (\text{C.118})$$

$$= \frac{1}{N} \sum_{k,k'} \phi_k \phi_{k'} \delta_{k,-k} \quad (\text{C.119})$$

$$= \frac{1}{N} \sum_k \phi_k \phi_{-k}, \quad (\text{C.120})$$

$$\sum_{\langle i,j \rangle} \phi_{ij,m}^2 = \sum_{\langle i,j \rangle} (\phi_{i,m} - \phi_{j,m})^2 = \sum_{\langle i,j \rangle} \phi_{i,m}^2 - \sum_{\langle i,j \rangle} 2\phi_{i,m}\phi_{j,m} + \sum_{\langle i,j \rangle} \phi_{j,m}^2 \quad (\text{C.121})$$

$$= z \sum_i \phi_{i,m}^2 - 2 \sum_i (\phi_{i,m}\phi_{i+1,m} + \phi_{i,m}\phi_{i-1,m}) + z \sum_j \phi_{j,m}^2 \quad (\text{C.122})$$

$$= z \frac{1}{N} \sum_k \phi_k \phi_{-k} - 2 \sum_i \frac{1}{N} \sum_k e^{ikr_i} \phi_k \frac{1}{N} \sum_{k'} e^{ik'(r_i+1)} \phi_{k'} + \\ - 2 \sum_i \frac{1}{N} \sum_k e^{ikr_i} \phi_k \frac{1}{N} \sum_{k'} e^{ik'(r_i-1)} \phi_{k'} + z \frac{1}{N} \sum_k \phi_k \phi_{-k} \quad (\text{C.123})$$

$$= \frac{2z}{N} \sum_k \phi_k \phi_{-k} - 2 \frac{1}{N} \sum_{k,k'} \phi_k \phi_{k'} (e^{ik'} + e^{-ik'}) \frac{1}{N} \sum_i e^{i(k+k')r_i} \quad (\text{C.124})$$

$$= \frac{2z}{N} \sum_k \phi_k \phi_{-k} - 2 \frac{1}{N} \sum_{k,k'} \phi_k \phi_{k'} (e^{ik'} + e^{-ik'}) \delta_{k',-k} \quad (\text{C.125})$$

$$= \frac{2z}{N} \sum_k \phi_k \phi_{-k} - 2 \frac{1}{N} \sum_k \phi_k \phi_{-k} (e^{-ik} + e^{ik}) \quad (\text{C.126})$$

$$= \frac{2z}{N} \sum_k \phi_k \phi_{-k} - \frac{2}{N} \sum_k \phi_k \phi_{-k} 2 \cos k \quad (\text{C.127})$$

$$= \frac{2}{N} \sum_k \phi_k \phi_{-k} (z - 2 \cos k) \quad (\text{C.128})$$

$$= \frac{2}{N} \sum_k \phi_k \phi_{-k} f_k, \quad (\text{C.129})$$

where f_k is the lattice factor,

$$f_k = z - 2 \sum_{j=1}^d \cos(k_j a). \quad (\text{C.130})$$

The transformed trial action is

$$\mathcal{S}_0 = \sum_m \left(\frac{\omega_m^2}{\beta U} \sum_i \phi_{i,m}^2 + \frac{K}{2\beta} \sum_{\langle i,j \rangle} \phi_{ij,m}^2 \right) \quad (\text{C.131})$$

$$= \sum_m \left(\frac{\omega_m^2}{\beta U} \frac{1}{N} \sum_k \phi_{k,m} \phi_{-k,-m} + \frac{K}{2\beta} \frac{2}{N} \sum_k \phi_{k,m} \phi_{-k,-m} f_k \right) \quad (\text{C.132})$$

$$= \frac{1}{\beta N} \sum_{k,m} \left(\frac{\omega_m^2}{U} + K f_k \right) \phi_{k,m} \phi_{-k,-m}. \quad (\text{C.133})$$

The inverse space average in D_{ij} is

$$\langle \phi_{k,m} \phi_{-k,-m} \rangle = \frac{\int \{\mathcal{D}\phi\} \phi_{k,m} \phi_{-k,-m} \exp \left[-\frac{1}{\beta N} \sum_{k,m} \left(\frac{\omega_m^2}{U} + K f_k \right) \phi_{k,m} \phi_{-k,-m} \right]}{\int \{\mathcal{D}\phi\} \exp \left[-\frac{1}{\beta N} \sum_{k,m} \left(\frac{\omega_m^2}{U} + K f_k \right) \phi_{k,m} \phi_{-k,-m} \right]}, \quad (\text{C.134})$$

which is two Gaussian integrals of the form:

$$\frac{\int dx x^2 e^{-ax^2}}{\int dx e^{-ax^2}} = \frac{1}{2a}. \quad (\text{C.135})$$

Therefore,

$$\langle \phi_{k,m} \phi_{-k,-m} \rangle = \frac{1}{2 \frac{\beta}{N} \left(\frac{\omega_m^2}{U} + K f_k \right)} = \frac{N}{2\beta \left(\frac{\omega_m^2}{U} + K f_k \right)} \quad (\text{C.136})$$

and D_{ij} itself takes the form

$$D_{ij} = \frac{2}{N^2} \sum_{k,m} (1 - \cos kr_{ij}) \frac{N}{2\beta \left(\frac{\omega_m^2}{U} + K f_k \right)} \quad (\text{C.137})$$

$$= \frac{1}{\beta N} \sum_{k,m} \frac{1 - \cos kr_{ij}}{\frac{\omega_m^2}{U} + K f_k}. \quad (\text{C.138})$$

The bond-averaged version is obtained by summing over nearest neighbours:

$$\bar{D}_{ij} = \frac{1}{z} \sum_j D_{ij} = \frac{1}{\beta N z} \sum_{k,m} \frac{f_k}{\frac{\omega_m^2}{U} + \frac{K}{2} f_k}, \quad (\text{C.139})$$

where an additional factor of $\frac{1}{2}$ has been appended to the K term to compensate for overcounting [64]. After summation over Matsubara frequencies,

$$\bar{D}_{ij} = \frac{1}{N z} \sum_k \sqrt{\frac{f_k U}{2K}} \coth \left(\frac{\beta}{2} \sqrt{\frac{f_k K U}{2}} \right). \quad (\text{C.140})$$

Finally, introducing density of states,

$$\rho(\xi) = \frac{1}{N} \sum_k \delta(\xi - \xi_k), \quad (\text{C.141})$$

into the lattice factor f_k , Eq. (C.130), we obtain Eq. (4.16):

$$\bar{D}_{ij} = \frac{1}{z} \int d\xi \rho(\xi) \sqrt{\frac{(z - \xi) U}{2K}} \coth \left(\frac{\beta}{2} \sqrt{\frac{(z - \xi) K U}{2}} \right). \quad (\text{C.142})$$

Finally, the full form of the self-consistent equation for stiffness K , Eq. (C.103), normalised over U , is

$$\begin{aligned}
\frac{K}{U} = & 2\frac{t}{U} \left(z\frac{t}{U} + \frac{\mu}{U} + \frac{1}{2} \right) \exp \left[-\frac{1}{2z} \int d\xi \rho(\xi) \sqrt{\frac{z-\xi}{2\frac{K}{U}}} \coth \left(\frac{\sqrt{\frac{1}{2}\frac{K}{U}}(z-\xi)}{2\frac{T}{U}} \right) \right] + \\
& + 4 \left(\frac{t}{U} \right)^2 \left[\frac{z}{2 \sinh^2 \left(\frac{\frac{\mu}{U} + \frac{1}{2}}{2\frac{T}{U}} \right)} + 2 \left(z\frac{t}{U} + \frac{\mu}{U} + \frac{1}{2} \right) \right] \\
& \times \exp \left[-\frac{2}{z} \int d\xi \rho(\xi) \sqrt{\frac{(z-\xi)}{2\frac{K}{U}}} \coth \left(\frac{\sqrt{\frac{1}{2}\frac{K}{U}}(z-\xi)}{2\frac{T}{U}} \right) \right] \tag{C.143}
\end{aligned}$$

The order parameters in the SCHA are defined as in Eqs. (1.37-1.39),

$$\Psi_1 = \langle \cos \phi_i \rangle = e^{-\frac{1}{2}\langle \phi_i^2 \rangle}, \tag{C.144}$$

$$\Psi_2 = \langle \cos 2\phi_i \rangle = e^{-2\langle \phi_i^2 \rangle}, \tag{C.145}$$

By analogy to the trial phase average D_{ij} , the single average can be rewritten using the Fourier transform,

$$\langle \phi_i^2 \rangle = \frac{1}{N} \sum_k \langle \phi_k^2 \rangle, \tag{C.146}$$

which leads to Eq. (4.20),

$$\langle \phi_i^2 \rangle = \frac{2}{N^2} \sum_{k,m} \langle \phi_{k,m} \phi_{-k,-m} \rangle \quad (\text{C.147})$$

$$= \frac{2}{N^2} \sum_{k,m} \frac{N}{2\beta \left(\frac{\omega_m^2}{U} + K f_k \right)} \quad (\text{C.148})$$

$$= \frac{1}{\beta N} \sum_{k,m} \frac{1}{\frac{\omega_m^2}{U} + K f_k} \quad (\text{C.149})$$

$$= \frac{1}{\beta N} \sum_k \frac{\beta}{2} \sqrt{\frac{U}{K f_k}} \coth \left(\frac{\beta}{2} \sqrt{f_k K U} \right) \quad (\text{C.150})$$

$$= \frac{1}{2N} \sum_k \sqrt{\frac{U}{K f_k}} \coth \left(\frac{\beta}{2} \sqrt{f_k K U} \right) \quad (\text{C.151})$$

$$= \frac{1}{2} \int d\xi \rho(\xi) \sqrt{\frac{U}{K(z-\xi)}} \coth \left(\frac{\beta}{2} \sqrt{(z-\xi) K U} \right). \quad (\text{C.152})$$

Entropy can also be calculated from the free energy \mathcal{F}_0 ,

$$S = \beta^2 \frac{\partial \mathcal{F}_0}{\partial \beta}, \quad (\text{C.153})$$

as can any other thermodynamic function, based on temperature derivatives.

Appendix D

Magnetic density of states: analytical formulas

The density of states on a square lattice with no orbital magnetic effects present is

$$\rho^{\square}(\xi) = \frac{K\left(1 - \left(\frac{x}{4}\right)^2\right) \theta\left(1 - \left|\frac{x}{4}\right|\right)}{\pi^2}, \quad (\text{D.1})$$

where $K(m)$ is the complete elliptic integral of the first kind and $\theta(x)$ is the unit step function.

The derivation of analytical formulas for density of states functions in various magnetic fields is complex and can be found in [47]. Below are listed explicit formulas used in numerics, at different values of the rotation frustration parameter f . All magnetic effects modify the original square lattice density of states, ρ^{\square} .

D.1 $f = 1/2$

$$\rho_{1/2}^{\square}(\xi) = \frac{1}{2} |x| \rho^{\square}\left(\frac{1}{2}(x^2 - 4)\right). \quad (\text{D.2})$$

D.2 $f = 1/3$

$$\begin{aligned}
\rho_{1/3}^{\square}(\xi) = & \frac{1}{4\sqrt{2}} \left\{ \sqrt{8 - \xi^2} |\xi^2 - 2| \rho^{\square} \left(\frac{1}{2} \xi (6 - \xi^2) \right) \right. \\
& \times \left[\left(\theta(-\xi^2 + 2\sqrt{3} + 4) - \theta(6 - \xi^2) \right) \left| \sec \left(\varphi + \frac{\pi}{2} \right) \right| + \right. \\
& + \left(-\theta(\xi + 2) + \theta(\xi) - \theta(\xi - \sqrt{3} + 1) + \theta(\xi + \sqrt{6}) \right) \sec \left(\varphi + \frac{\pi}{6} \right) + \\
& \left. \left. + \left(\theta(\xi - 2) - \theta(\xi) + \theta(\xi + \sqrt{3} - 1) - \theta(\xi - \sqrt{6}) \right) \sec \left(\varphi - \frac{\pi}{6} \right) \right] \right\}, \tag{D.3}
\end{aligned}$$

where

$$\varphi = \frac{1}{3} \tan^{-1} \left(\frac{\sqrt{32 - \xi^2} (\xi^2 - 6)^2}{\xi (\xi^2 - 6)} \right). \tag{D.4}$$

D.3 $f = 1/4$

$$\begin{aligned}
\rho_{1/4}^{\square}(\xi) = & \frac{1}{2} |\xi^2 - 4| \rho^{\square} \left(\frac{\xi^4}{2} - 4\xi^2 + 2 \right) \left[\sqrt{4 - |\xi^2 - 4|} \theta(-\xi^2 - 2\sqrt{2} + 4) + \right. \\
& \left. + \sqrt{|\xi^2 - 4| + 4} \left(\theta(8 - \xi^2) - \theta((2\sqrt{2} + 4) - \xi^2) \right) \right]. \tag{D.5}
\end{aligned}$$

D.4 $f = 1/6$

$$\begin{aligned}
\rho_{1/6}^{\square}(\xi) &= \frac{1}{4 \cdot 2^{1/4}} \sqrt{-\xi^4 + 8\xi^2 + 16} |\xi^4 - 8\xi^2 + 8| \rho^{\square} \left(\frac{\xi^6}{2} - 6\xi^4 + 12\xi^2 - 2 \right) \\
&\times \left\{ \left(\theta \left((6 - 2\sqrt{3}) - \xi^2 \right) - \theta \left(2 - \xi^2 \right) \right) \right. \\
&\times \sqrt[4]{-\frac{1}{2} \cos \left(2\varphi - \frac{\pi}{3} \right) - \sqrt{2} \cos \left(\varphi + \frac{\pi}{3} \right) + 1} \sec \left(\varphi - \frac{\pi}{6} \right) + \\
&+ \theta \left(-\text{erg}^2 - \sqrt{21} + 5 \right) \tag{D.6}
\end{aligned}$$

$$\begin{aligned}
&\times \left| \sqrt[4]{-\frac{1}{2} \cos \left(2\varphi + \frac{\pi}{3} \right) - \sqrt{2} \cos \left(\varphi - \frac{\pi}{3} \right) + 1} \right| \sec \left(\varphi + \frac{\pi}{6} \right) + \\
&+ \sqrt{2} \left(\theta \left((\sqrt{21} + 5) - \xi^2 \right) - \theta \left(2(\sqrt{3} + 3) - \xi^2 \right) \right) \\
&\times \left. \sqrt{\cos \left(\frac{1}{2} \left(\varphi + \frac{\pi}{4} \right) \right) \cos \left(\frac{1}{2} \left(-\frac{\pi}{4} \right) \right) \sec \left(\varphi - \frac{\pi}{2} \right)} \right\}, \tag{D.7}
\end{aligned}$$

where

$$\varphi = \frac{1}{3} \tan^{-1} \left(\frac{\sqrt{-\xi^4 + 8\xi^2 + 16} |\xi^4 - 8\xi^2 + 8|}{\xi^6 - 12\xi^4 + 24\xi^2 + 32} \right). \tag{D.8}$$

Appendix E

Related publications

1. A. Krzywicka, T. P. Polak, Coexistence of two kinds of superfluidity at finite temperatures in optical lattices, *Annals of Physics* 443:168973, 2022.
2. A. Krzywicka, T. P. Polak, Entropy of pair condensed bosons at finite temperatures in optical lattices with bond-charge interaction, *Journal of Magnetism and Magnetic Materials* 542:168589, 2022.
3. A. Krzywicka, T. P. Polak, Pairing mechanism at finite temperatures in bosonic systems, *Acta Phys. Pol. A* 143:157, 2023.
4. A. Krzywicka, T. P. Polak, Reentrant phase behavior in systems with density-induced tunneling, 2023, under review, arxiv: <https://arxiv.org/abs/2308.16423>.
5. A. Krzywicka, T. P. Polak, Differentiating between interaction-based and correlation-based bosonic pairing mechanisms, 2023, under review.

Bibliography

- [1] C. Ates, B. Olmos, W. Li, and I. Lesanovsky. Dissipative binding of lattice bosons through distance-selective pair loss. *Phys. Rev. Lett.*, 109:233003, Dec 2012.
- [2] A. Beige, S. Bose, D. Braun, S. F. Huelga, P. L. Knight, M. B. Plenio, and V. Vedral. Entangling atoms and ions in dissipative environments. *Journal of Modern Optics*, 47(14-15):2583–2598, 2000.
- [3] Immanuel Bloch, Jean Dalibard, and Sylvain Nascimbène. Quantum simulations with ultracold quantum gases. *Nat. Phys.*, 8(4):267–276, April 2012.
- [4] Immanuel Bloch, Jean Dalibard, and Wilhelm Zwerger. Many-body physics with ultracold gases. *Rev. Mod. Phys.*, 80:885–964, Jul 2008.
- [5] Lars Bonnes and Stefan Wessel. Pair superfluidity of three-body constrained bosons in two dimensions. *Phys. Rev. Lett.*, 106:185302, May 2011.
- [6] A. O. Caldeira and A. J. Leggett. Influence of dissipation on quantum tunneling in macroscopic systems. *Phys. Rev. Lett.*, 46:211–214, Jan 1981.
- [7] B Capogrosso-Sansone, N V Prokof'ev, and B. V. Svistunov. Phase diagram and thermodynamics of the three-dimensional Bose-Hubbard model. *Phys. Rev. B*, 75(13):134302, 2007.
- [8] Yinan Chen and Carlos Navarrete-Benlloch. Collectively pair-driven-dissipative bosonic arrays: exotic and self-oscillatory condensates. 2021.

- [9] D Clément, N Fabbri, L Fallani, C Fort, and M Inguscio. Multi-band spectroscopy of inhomogeneous mott-insulator states of ultracold bosons. *New Journal of Physics*, 11(10):103030, oct 2009.
- [10] A. J. Daley, J. M. Taylor, S. Diehl, M. Baranov, and P. Zoller. Atomic three-body loss as a dynamical three-body interaction. *Phys. Rev. Lett.*, 102:040402, Jan 2009.
- [11] Jacek Dobrzyniecki, Xikun Li, Anne E.B. Nielsen, and Tomasz Sowiński. Effective three-body interactions for bosons in a double-well confinement. *Physical Review A*, 97, 1 2018.
- [12] Jacek Dobrzyniecki and Tomasz Sowiński. Exact dynamics of two ultra-cold bosons confined in a one-dimensional double-well potential. *European Physical Journal D*, 70, 4 2016.
- [13] Eric Duchon, Yen Lee Loh, and Nandini Trivedi. Optical Lattice Emulators: Bose and Fermi Hubbard Models. *arXiv*, page 543, November 2013.
- [14] O. Dutta, M. Gajda, P. Hauke, M. Lewenstein, D.-S. Lühmann, B. A. Malomed, T. Sowiński, and J. Zakrzewski. Non-standard hubbard models in optical lattices: a review. *Reports on Progress in Physics*, 78(6), 2015.
- [15] Francesco Ferri, Rodrigo Rosa-Medina, Fabian Finger, Nishant Dogra, Matteo Soriente, Oded Zilberberg, Tobias Donner, and Tilman Esslinger. Emerging dissipative phases in a superradiant quantum gas with tunable decay. *Phys. Rev. X*, 11:041046, Dec 2021.
- [16] Matthew P A Fisher, Peter B Weichman, G Grinstein, and Daniel S Fisher. Boson localization and the superfluid-insulator transition. *Phys. Rev. B*, B40:546–570, 1989.
- [17] Markus Greiner, Olaf Mandel, Theodor W Hänsch, and Immanuel Bloch. Collapse and revival of the matter wave field of a Bose–Einstein condensate. *Nature*, 419(6902):51, September 2002.

- [18] P Hauke, L Tagliacozzo, and M Lewenstein. Speeding Up Quantum Field Theories. *Science*, 2012.
- [19] J. E. Hirsch. *Physica (Amsterdam)*, 158C:326, 1989.
- [20] Kantaro Honda, Shintaro Taie, Yosuke Takasu, Naoki Nishizawa, Masaya Nakagawa, and Yoshiro Takahashi. Observation of the sign reversal of the magnetic correlation in a driven-dissipative fermi gas in double wells. *Phys. Rev. Lett.*, 130:063001, Feb 2023.
- [21] D. Jaksch, C. Bruder, J. I. Cirac, C. W. Gardiner, and P. Zoller. *Physical Review Letters*, 81:3108, 1998.
- [22] D. Jaksch, C. Bruder, J. I. Cirac, C. W. Gardiner, and P. Zoller. Cold bosonic atoms in optical lattices. *Phys. Rev. Lett.*, 81:3108–3111, Oct 1998.
- [23] D Jaksch and P Zoller. Creation of effective magnetic fields in optical lattices: the hofstadter butterfly for cold neutral atoms. *New Journal of Physics*, 5(1):56, 2003.
- [24] Chaitanya Joshi, Mats Jonson, Patrik Öhberg, and Erika Andersson. Constructive role of dissipation for driven coupled bosonic modes. *Phys. Rev. A*, 87:062304, Jun 2013.
- [25] O. Jürgensen, F. Meinert, M. J. Mark, H.-Ch. Nägerl, and D.-S. Lühmann. *Physical Review Letters*, 113:193003, 2014.
- [26] Hans Kesler, Phatthamon Kongkhambut, Christoph Georges, Ludwig Mathey, Jayson G. Cosme, and Andreas Hemmerich. Observation of a dissipative time crystal. *Phys. Rev. Lett.*, 127:043602, Jul 2021.
- [27] Hans Kessler, Jayson G. Cosme, Christoph Georges, Ludwig Mathey, and Andreas Hemmerich. From a continuous to a discrete time crystal in a dissipative atom-cavity system. *New Journal of Physics*, 22(8):085002, aug 2020.
- [28] Martin Kiffner and Michael J Hartmann. Dissipation-induced correlations in one-dimensional bosonic systems. *New Journal of Physics*, 13(5):053027, may 2011.

- [29] J. Klinder, H. Kessler, M. Reza Bakhtiari, M. Thorwart, and A. Hemmerich. Observation of a superradiant mott insulator in the dicke-hubbard model. *Phys. Rev. Lett.*, 115:230403, Dec 2015.
- [30] T. K. Kopeć. Phase coherence in the Josephson-coupled stack of planar spin-charge separated condensates and the interlayer mechanism of high-T_c superconductivity. *Phys. Rev. B*, 69(5):054504, February 2004.
- [31] Werner Krauth, Michel Caffarel, and Jean-Philippe Bouchaud. Gutzwiller wave function for a model of strongly interacting bosons. *Phys. Rev. B*, 45(6):3137, 1992.
- [32] A. Krzywicka. *Non-standard Bose-Hubbard Models: a variational method approach*. Bachelor's thesis, Adam Mickiewicz University, Poznań, Poland, June 2018.
- [33] A. Krzywicka. *Orbital Magnetic Effects in the Bose-Hubbard Model: a Quantum Rotor Description*. Master's thesis, Adam Mickiewicz University, Poznań, Poland, June 2019.
- [34] A. Krzywicka and T.P. Polak. Coexistence of two kinds of superfluidity at finite temperatures in optical lattices. *Annals of Physics*, 443:168973, 2022.
- [35] Anthony J Leggett. Bose-Einstein condensation in the alkali gases: Some fundamental concepts. *Rev. Mod. Phys.*, 73(2):307, 2001.
- [36] Maciej Lewenstein, Anna Sanpera, Veronica Ahufinger, Bogdan Damski, Aditi Sen De, and Ujjwal Sen. Ultracold atomic gases in optical lattices: mimicking condensed matter physics and beyond. *Adv. Phys.*, 56(2):243–379, 2007.
- [37] Xiangliang Li, Davide Dreon, Philip Zupancic, Alexander Baumgärtner, Andrea Morales, Wei Zheng, Nigel R. Cooper, Tobias Donner, and Tilman Esslinger. First order phase transition between two centro-symmetric superradiant crystals. *Phys. Rev. Res.*, 3:L012024, Mar 2021.
- [38] Y. J. Lin, R. L. Compton, K. Jiménez-García, J. V. Porto, and I. B. Spielman. Synthetic magnetic fields for ultracold neutral atoms. *Nature*, 462(7273):628–632, 2009.

- [39] D.-S. Lühmann, O. Jürgensen, and K. Sengstock. Multi-orbital and density-induced tunneling of bosons in optical lattices. *New Journal of Physics*, 14(3):033021, mar 2012.
- [40] M. J. Mark, S. Flannigan, F. Meinert, J. P. D’Incao, A. J. Daley, and H.-C. Nägerl. Interplay between coherent and dissipative dynamics of bosonic doublons in an optical lattice. *Phys. Rev. Res.*, 2:043050, Oct 2020.
- [41] M. J. Mark, E. Haller, K. Lauber, J. G. Danzl, A. J. Daley, and H.-C. Nägerl. Precision measurements on a tunable mott insulator of ultracold atoms. *Phys. Rev. Lett.*, 107:175301, Oct 2011.
- [42] F Meinert, M J Mark, E Kirilov, K Lauber, P Weinmann, A J Daley, and H C Nägerl. Quantum quench in an atomic one-dimensional Ising chain. *Phys. Rev. Lett.*, 111(5):053003, 2013.
- [43] M. B. Plenio and S. F. Huelga. Entangled light from white noise. *Phys. Rev. Lett.*, 88:197901, Apr 2002.
- [44] M. B. Plenio, S. F. Huelga, A. Beige, and P. L. Knight. Cavity-loss-induced generation of entangled atoms. *Phys. Rev. A*, 59:2468–2475, Mar 1999.
- [45] T. P. Polak. Sign reversal of the boson-boson interaction potential in planar Bose-Fermi mixtures under a synthetic magnetic field. *Phys. Rev. A*, 83(1):11602, January 2011.
- [46] T. P. Polak and T. K. Kopeć. Quantum rotor description of the Mott-insulator transition in the Bose-Hubbard model. *Phys. Rev. B*, 76(9):94503, September 2007.
- [47] T. P. Polak and T. K. Kopeć. Frustration effects in rapidly rotating square and triangular optical lattices. *Phys. Rev. A*, 79(6):063629, 2009.
- [48] Amit Rai, Changhyoup Lee, Changsuk Noh, and Dimitris G Angelakis. Photonic lattice simulation of dissipation-induced correlations in bosonic systems. *Scientific Reports*, 5(1):8438, February 2015.

- [49] Helmut Ritsch, Peter Domokos, Ferdinand Brennecke, and Tilman Esslinger. Cold atoms in cavity-generated dynamical optical potentials. *Rev. Mod. Phys.*, 85:553–601, Apr 2013.
- [50] David Roberts and A. A. Clerk. Competition between two-photon driving, dissipation, and interactions in bosonic lattice models: An exact solution. *Phys. Rev. Lett.*, 130:063601, Feb 2023.
- [51] Tommaso Roscilde. Probing correlated phases of bosons in optical lattices via trap squeezing. *New Journal of Physics*, 11(2):023019, feb 2009.
- [52] Jacob Ross, Piotr Deuar, Dongki Shin, Kieran Thomas, Bryce Henson, Sean Hodgman, and A. Truscott. On the survival of the quantum depletion of a condensate after release from a magnetic trap. *Scientific Reports*, 12, 08 2022.
- [53] Lorenzo Rosso, Alberto Biella, Jacopo De Nardis, and Leonardo Mazza. Dynamical theory for one-dimensional fermions with strong two-body losses: Universal non-hermitian zeno physics and spin-charge separation. *Phys. Rev. A*, 107:013303, Jan 2023.
- [54] Orazio Scarlatella, Rosario Fazio, and Marco Schiró. Emergent finite frequency criticality of driven-dissipative correlated lattice bosons. *Phys. Rev. B*, 99:064511, Feb 2019.
- [55] U. Schneider, L. Hackermüller, S. Will, Th. Best, I. Bloch, T. A. Costi, R. W. Helmes, D. Rasch, and A. Rosch. Metallic and insulating phases of repulsively interacting fermions in a 3d optical lattice. *Science*, 322(5907):1520–1525, 2008.
- [56] Chandan Setty. Glass-induced enhancement of superconducting T_c : Pairing via dissipative mediators. *Phys. Rev. B*, 99:144523, Apr 2019.
- [57] V. S. Shchesnovich and D. S. Mogilevtsev. Three-site bose-hubbard model subject to atom losses: Boson-pair dissipation channel and failure of the mean-field approach. *Phys. Rev. A*, 82:043621, Oct 2010.

- [58] Tomasz Sowiński. One-dimensional bose-hubbard model with pure three-body interactions. *Central European Journal of Physics*, 12:473–479, 2014.
- [59] N. Syassen, D. M. Bauer, M. Lettner, T. Volz, D. Dietze, J. J. García-Ripoll, J. I. Cirac, G. Rempe, and S. Dürr. Strong dissipation inhibits losses and induces correlations in cold molecular gases. *Science*, 320(5881):1329–1331, 2008.
- [60] Antoine Tenart, Gaetan Hecce, Jan Philipp Bureik, Alexandre Dareaux, and David Clement. Observation of pairs of atoms at opposite momenta in an equilibrium interacting bose gas. *Nature Physics*, 17:1364–1368, 12 2021.
- [61] S Trotzky, Y A Chen, A Flesch, I P McCulloch, and et al. Probing the relaxation towards equilibrium in an isolated strongly correlated one-dimensional Bose gas. *Nat. Phys.*, 2012.
- [62] D van Oosten, P van der Straten, and H T C Stoof. Quantum phases in an optical lattice. *Phys. Rev. A*, 63(5):053601, 2001.
- [63] A.-M. Visuri, T. Giamarchi, and C. Kollath. Nonlinear transport in the presence of a local dissipation. *Phys. Rev. Res.*, 5:013195, Mar 2023.
- [64] E. Šimánek. *Inhomogeneous superconductors*. Oxford University Press, 1994.
- [65] P Windpassinger and K Sengstock. Engineering novel optical lattices. *Rep. Prog. Phys.*, 2013.
- [66] K. Xu, Y. Liu, D. E. Miller, J. K. Chin, W. Setiawan, and W. Ketterle. Observation of strong quantum depletion in a gaseous bose-einstein condensate. *Phys. Rev. Lett.*, 96:180405, May 2006.
- [67] T A Zaleski and T K Kopeć. Atom-atom correlations in time-of-flight imaging of ultracold bosons in optical lattices. *Phys. Rev. A*, 84(5):53613, November 2011.
- [68] P. Zupancic, D. Dreon, X. Li, A. Baumgärtner, A. Morales, W. Zheng, N. R. Cooper, T. Esslinger, and T. Donner. *p*-band induced self-organization and dy-

namics with repulsively driven ultracold atoms in an optical cavity. *Phys. Rev. Lett.*, 123:233601, Dec 2019.